UNIVERSITY OF
KWAZULU-NATAL

INYUVESI
YAKWAZULU-NATALI

ARTEMISIA AFRA CRUDE AQUEOUS EXTRACT INDUCES NRF2-MEDIATED ANTIOXIDANT DEFENCE AGAINST OXIDATIVE STRESS AND INHIBITS APOPTOSIS VIA UPREGULATION OF HSP27 AND HSP90 IN A549 LUNG CANCER CELLS

Awande Nkambule

Student number: 212513133

BMedSci Physiology (Wits), BMedSci Hons in Physiology (UKZN),

PG Dip Public Health (MSA)

Submitted in fulfilment of the requirements for the degree of

Master of Medical Science in the Discipline of Medical Biochemistry

School of Laboratory Medicine and Medical Sciences

College of Health Sciences

University of KwaZulu-Natal, Durban, South Africa

2024

TABLE OF CONTENTS

DECLARATION

I **Awande Comfort Monwabisi Nkambule** declare that

1. The research reported in this manuscript, except where otherwise stated, is my original work.
2. The manuscript has not been submitted to UKZN or another institution for the purpose of obtaining a qualification.
3. The research reported in the manuscript was carried out in the Department of Medical Biochemistry and Chemical Pathology, School of Laboratory Medicine and Medical Science, UKZN under the supervision of Dr Khan and Dr Kumalo.

Candidate: [redacted] Date: 8 July 2024

Awande Nkambule

Supervisor: [redacted] Date: 8 July 2024

Dr René Khan

ACKNOWLEDGEMENTS

I would like to thank **Dr Khan.** It would not be possible without her helping hand. She is an experience that I wish upon all budding medical lab scientists. Her knack for precision and love for accuracy together with in-depth knowledge and wisdom inspires. I am equally grateful to **Dr Kumalo.** Having such supervisors has contributed to my personal and professional development. I am fortunate to have gone through such warm but firm hands. I would also like to thank my seniors: **Lebogang** for giving time to help me learn and carrying me though procedures; and **Lu** and **Mthoko** for invaluable assistance; and my fellow colleagues **Ranesh, Mikayla** and **Mayanka** for warmingly welcoming me into the group and helping me get to speed.

DEDICATION

It is said that if you commit your work to **GOD** he will make your plans succeed, therefore my first dedication is to the **Lord**, moreover as a token of gratitude for being a source of strength and granting me the grace to see it through. To my **Mother** and **Father A.T** and **M.A Nkambule** for always seeing the best in me, lifting me up countless times when I am down and for the sacrifices to see me through. I really appreciate it and would like to dedicate this work to you. To my **Aunts** and **Uncles, Brothers** and **Sisters** for the unending support and always assuring me that it can be done. To **KP** for the truly appreciated and cherished love and support through my journey.

~ To **The J man** for being my inspiration to push the boundaries ~

I miss and love you deeply and constantly

You are always in my heart

ABBREVIATIONS

µm	Micrometer
A549	Human non-small cell lung cancer cell line
A.afra	*Artemisia afra*
ADP	Adenine diphosphate
Apaf-1	Apoptotic protease activating factor 1
ATP	Adenosine triphosphate
Bax	Bcl-2-associated X
BCA	Bicinchoninic acid
Bcl2	B-cell lymphoma-2
BH	Bcl-2 homology
BHT	Butylated hydroxytoluene
Bid	BH3 interacting-domain death agonist
BSA	Bovine serum albumin
CCM	Complete culture medium
c-IAP	Cellular inhibitor of apoptosis protein
CoQ	Coenzyme Q
Cu (Cu^{2+})	Copper (Cupric ion)
DMSO	Dimethyl sulphoxide
DNA	Deoxymethylribose nucleic acid
ETC	Electron transport chain
FADD	Fas associated protein with death domain
FasL	Fas ligand
FasR	Fas receptor
FBS	Foetal bovine serum
Gpx	Glutathione peroxidase
GSH	Reduced glutathione
GSSG	Oxidised glutathione
GST	GSH-S-transferase
H_2O_2	Hydrogen peroxide
H_3PO_4	Phosphoric acid
HCl	Hydrochloric acid
HSP	Heat shock protein
HO_2^-	Hydroperoxyl radical

IC_{50}	Half maximum inhibitory concentration
iCAD	Inhibitors of caspase DNase
IKB	Inhibitor of Nuclear factor kappa-light-chain-enhancer of activated B-cells
IKK	Inhibitor of Nuclear factor kappa-light-chain-enhancer of activated B-cells complex
IL	Interleukin
iNOS	Inducible nitric oxide synthase
kDa	Kilodalton
LDH	Lactate dehydrogenase
MDA	Malondialdehyde
MTT	3-(4,5-Dimethyl-2-thiazolyl)-2,5-diphenyl-2H-tetrazolium bromideNAD
(NAD^+)	Nicotinamide adenine dinucleotide
NADH	Nicotinamide adenine dinucleotide + hydrogen (reduced)
NADPH	Nicotinamide adenine dinucleotide phosphate (reduced)
NF-κB	Nuclear factor kappa B
Nrf2	Nuclear factor erythroid 2–related factor 2
MOMP	Mitochondrial outer membrane permeability
$O_2^{\bullet-}$	Superoxide anion radical
OGG1	Oxoguanine glycosylase 1
OD	Optical density
p53	Protein 53
PBS	Phosphate buffered saline
PLK	Polo-like kinase

PUFAs	Polyunsaturated fatty acids
qPCR	Quantitative polymerase chain reaction
RBD	Relative band density
RFU	Relative fluorescence units
RLU	Relative light units
RNS	Reactive nitrogen species
ROS	Reactive oxygen species
Rpm	Revolutions per minute
SDS	Sodium dodecyl sulphate
SDS-PAGE	Sodium dodecyl sulphate - polyacrylamide gel electrophoresis
SEM	Standard error of the mean
TBA	Thiobarbituric acid
TBA/BHT	Thiobarbituric acid/ butylated hydroxytoluene
TBARS	Thiobarbituric acid reactive substances
TCA cycle	Tricarboxylic acid cycle
TEMED	Tetramethylethylenediamine
TNF-α	Tumour necrosis factor alpha
TNFR1	Tumour necrosis factor-receptor 1
TRADD	Tumour necrosis factor –receptor 1 associated protein with death domain
TTBS	Tween 20 - Tris buffered saline
VCl_3	Vanadium (III) chloride
β-actin	Beta-actin

LIST OF FIGURES

CHAPTER 2

CHAPTER 3

CHAPTER 4

APPENDIX

LIST OF TABLES

ABSTRACT

Lung cancer ranks first in mortality rates across all cancer types globally. Currently available treatment options are associated with undesirable outcomes for patients such as treatment related adverse events, low efficacy, and high costs. There have been ongoing efforts in novel drug discovery and development research using medicinal plants as a source for anti-tumour agents that will improve on these aspects. One such promising lead in this space is the South African plant *Artemisia afra*. In this study, the underlying mechanisms associated with the cytotoxicity of *Artemisia. afra* in A549 lung cancer cells were investigated following 48 hours exposure to the plant's crude aqueous extract. Cytotoxicity was assessed using the MTT, ATP and mitochondrial membrane potential (ΔΨm) assays, and CYP3A4 activity was ascertained by luminometry. The free radical production and antioxidant response was determined using the TBARS, nitrates, luminometry and western blotting assays to measure ROS, RNS, GSH and antioxidant protein expression (SOD2, Gpx1, catalase), respectively. The Nrf2, HSP27 and HSP90 protein expression was detected by qPCR or western blotting. Cell death parameters such as caspase activity, phosphatidylserine (apoptosis) and necrosis were quantified by luminometry, and Bcl2 family proteins were ascertained by western blotting. The IC_{50} as per the dose-dependent MTT curve was determined to be at 260 µg/ml. Increased *Artemisia afra* metabolism by CYP3A4 ($p<0.05$) was observed in treated cells compared to the control, but ATP production was decreased ($p<0.05$) despite minimal changes in the ΔΨm. The *Artemisia afra* treatment significantly increased ROS production ($p<0.05$), which was met with a reactive spike in Nrf2 ($p<0.05$) gene expression. Concurrent increase in SOD2, Gpx1 ($p<0.05$) and catalase ($p<0.05$) protein expression, as well as GSH were noted. Little difference was recorded in the levels of nitrates. Pro-apoptotic Bax ($p<0.05$) was upregulated, while anti-apoptotic Bcl2 ($p<0.05$) was reduced. Intriguingly the initiator caspases, caspase 8 ($p>0.05$) and caspase 9 ($p<0.05$) were decreased in treated cells, in accordance with increased potent anti-apoptotic proteins HSP27 ($p<0.05$) and HSP90 ($p<0.05$), positing their role in inhibiting the initiator caspases but xIAP was not changed. Apoptosis was excluded as the major form of cytotoxicity in the treated cells given that the results showed a reduction in execution caspases, caspases 3/7 ($p<0.05$) and reduced PS externalisation ($p<0.05$). Necrosis was also excluded as the mode of cytotoxicity as necrosis, even though LDH levels were increased in the *Artemisia afra* treated A549 cells. The MTT and ATP assay analysis revealed a decline in cell viability after 48 hours of treatment. An antioxidant response was observed, but ROS were increased.

However, cell death by apoptosis was prevented by HSP. Taken together the current study confirmed that the *Artemisa afra* crude aqueous extract mediated cytotoxicity by oxidative stress, but demonstrated anti-apoptotic effects via HSP in A549 cells.

KEYWORDS: Lung cancer, A549 cell line, *Artemisia afra,* oxidative stress, apoptosis, Nrf2, HSP

CHAPTER 1 : INTRODUCTION

1.1 BACKGROUND

Cancer is a debilitating and deadly disease that arises from the unregulated proliferation of cells that, rather than responding to cellular signalling for controlled cell behaviour, grow and divide in an uncontrolled manner (Cooper, 2000; Visser and Joyce, 2023). These cells are able to invade normal surrounding tissues and organs and eventually spread throughout the body (Cooper, 2000; Visser and Joyce, 2023). Generally, the loss of controlled growth and proliferation of cancer cells is the net result of an accumulation of abnormalities in the cell's regulatory systems, as characterised by the hallmarks of cancer (Cooper, 2000; Visser and Joyce, 2023). Cancer remains one of the leading causes of morbidity and mortality worldwide. It is projected that the burden of disease from cancer is likely to grow as population numbers and age increase, and as people adopt many of the lifestyle risk factors associated with the disease (Torre, et al., 2016; Parascandola, et al., 2022). The trend is particularly worrisome considering that low- and middle- income countries bear the brunt of the surge.

The incidence and mortality rates in countries makes it apparent that high-income countries are most likely to experience a reduction or plateauing while in contrast, low- and middle-income countries display a growth in these rates (Torre et al., 2016; Parascandola et al., 2022). These statistics are consequent on the mechanisation of transport and labour, redefinition of the societal roles of women, and globalisation of markets - all characteristic of economic transition (Torre et al., 2016; Lortet-Tieulent et al., 2020). The resultant effect is that low- and middle-income countries adopt cancer-related lifestyle risk factors (tobacco use, reproductive patterns, excess body weight) that are predominantly prevalent in high-income countries (Torre et al., 2016). This causal effect between socioeconomic development and cancer incidence and mortality is, however, not consistent across the different cancer types. It is largely driven by the most prevalent of cancer types; breast, prostate and colorectal cancers, making it easy to neglect other less frequently occurring cancer types that do not conform to the effect and others that may otherwise be unrelated as no plausible correlation can be found (Lortet-Tieulent et al., 2020).

One noteworthy consistency when comparing low- and middle-income countries to high-income countries is the disparity in cancer survival (mortality) rates. For instance, 90% of

individuals diagnosed with breast cancer are likely to survive more than 5 years after diagnosis in the United States as opposed to 40% in South Africa (Cortes et al., 2020). These outcomes are most likely underestimated in low- and middle-income countries because of the quality and completeness of cancer registry data. The disparity is in part due to inequity in access to affordable treatment and cancer care between countries, and in many cases within countries (Cortes et al., 2020; Lortet-Tieulent et al., 2020). It poses as a major challenge in resource-limited settings and emerging economies. South Africa which falls under this category is not immune to this as alluded to with the above statistic on breast cancer 5-year survival.

Lung cancer is described as a tumour located in lung parenchyma or situated within the bronchi (Siddiqui et al., 2022). In the past, prevalence of the disease was extraordinarily rare with only 140 cases reported in medical literature around the year 1898 (Imyanitov et al., 2005). Within decades from then, lung cancer reached epidemic proportions due to the advent of tobacco smoking with concurrent increases in life expectancy around the world (Imyanitov et al., 2005). At present, lung cancer ranks first amongst leading causes of cancer death and second to breast cancer amongst the most common types of tumours (Jones and Baldwin, 2018; Sung, 2021; Bray et al., 2024). In 2020 the Global Cancer Observatory reported a total of 19 292 789 new cancer cases, of which breast and lung cancer accounted for 11.7% and 11.4% respectively (Sung, 2021). Just 2 years later (2022), lung cancer ranked first for incidence and mortality in both sexes, accounting for 12.4% of the 20 million incident cases, and 18.7% of the 9.7 million deaths (Bray et al., 2024). In females, lung cancer is second only to breast cancer, and is the leading cause of cancer-related death in men. Tobacco smoking is the leading risk factor for developing lung cancer, causing about 80-90% of all cases. This is followed by radon in non-smokers, which is believed to be responsible for 3-14% of all lung cancer cases. Mutations in the epidermal growth factor receptor (EGFR), Kirson rat sarcoma viral oncogene (K-ras) and MNNG HOS gene receptor kinase (cMET) are also associated with increased risk for developing the disease (Jones and Baldwin, 2018).

Treatment options for lung cancer are largely dependent on the stage at which the cancer is presented. Currently, options such as thoracic surgery and radiation therapy are indicated in the early stages. Some treatments use a combination of both thoracic surgery, radiation and chemotherapy in those who are deemed medically fit and are at risk for recurrence (Jones and Baldwin, 2018). Advancements in cancer resection treatment such as video assisted surgery and improved radiotherapy have provided less invasive, more precise and accurate removal of

tumorous tissue, and improved survival rates in cancer patients (Jones and Baldwin, 2018). However, the improvement has been limited to early-stage cases of lung cancer. Due to lack of lung cancer awareness/education and the insufficiency of screening programmes, most cancer cases present at a late stage where the success of thoracic surgery and radiation is limited (Jones and Baldwin, 2018).

Other advancements in lung cancer treatment include the recent development of targeted therapy. In this regard, drugs such as Nivolumab have proven to be more effective than standard care chemotherapy in certain driver mutation positive cases. However, these drugs cater for a small subset of cancer cases as these driver mutations have a low prevalence (Muthu et al., 2019). Current chemotherapeutic agents have the disadvantage of non-selectivity, and possess the likelihood of targeting non-cancerous cells in the body. As a result, lung cancer treatment is associated with many unpleasant adverse effects (Muthu, et al., 2019). Furthermore, given that a significant proportion of lung cancer cases present at later stages, the success of current treatment regimens in terms of post-diagnosis survival is low. For instance, small-cell lung carcinoma (SCLC) patients who present at a late stage have a postdiagnosis survival rate of 8 to 13 months (Jones and Baldwin, 2018). In addition, there are inequalities in access to cancer treatment, particularly newer drugs, due to the exorbitant costs of obtaining them. This alludes to the fact that further research towards the development of more effective, less costly and safer drugs needs consideration (Jones and Baldwin, 2018).

In South Africa, a significant number (27 million) of individuals are reliant on traditional medicine, particularly plants, for healthcare, in addition to western medicine or alone (Twilley et al., 2020). In the Eastern Cape alone, approximately 24 plants are routinely used as cancer treatment, and 16 out of the 24 ($1/3^{rd}$) have been scientifically studied and shown to possess anticancer activity (Sagbo and Otang-Mbeng, 2021). The plants are said to be taken concomitantly with western medicine. A significant proportion of people at times prefer medicinal plants over western medicine due to cultural beliefs, perceptions of better efficacy and safety, and lower costs (Sagbo and Otang-Mbeng, 2021). There are potential benefits that could be derived from more knowledge on medicinal plants for complimentary use with western medicine in the treatment of cancer. Aspects of these benefits include advantages in the social, economic and, most importantly, health wellness of people living with the disease. However, in addition to these potential benefits, and more importantly for the current study there has been a growing interest in research on medicinal plants in drug development.

Medicinal plants offer an increasingly appreciated avenue for the development of new, safer and more efficacious drugs (Wanjiru, 2014). The longstanding use of vinca alkaloid drugs (vinblastine and vincristine) as effective treatment of various cancers is exemplary of the importance of novel natural agent discovery in plant species (Wanjiru, 2014). The development of screening methods for extrapolating cytotoxicity - represented by inhibitory concentration (IC_{50}) and the selectivity index – using a variety of independent cancer cell-lines and normal cell lines has been instrumental in the interests in medicinal plants as anticancer agents (Asita et al., 2021). Biological activity screening of medicinal plants harnesses their therapeutic potential. For cancer, cytotoxicity studies are often the first step in evaluating their effectiveness as cancer treatment drugs (Asita et al., 2021).

South Africa has a richly biodiverse botanical heritage that boasts a selection of 350 commonly used medicinal plant species. *Artemisia afra (A. afra)*, popularly known as umhlonyane, is one of the most widely used in the country. *A. afra* has drawn considerable interest for its antitumour activity for the breast, liver, colon and prostate cancer (Spies et al., 2011; Venables et al., 2016; Shelembe et al., 2019; van Loggenberg et al., 2022). Thus far, *A. afra* has been proposed to carry out its cytotoxic effects on cancer cells through the induction of apoptosis via the mitochondrial and caspase dependant pathways (Venables, et al., 2016). Apoptosis is an organised and well-orchestrated mechanism through which cells die in response to stress, cellular signalling or chemotherapy (Venables, 2016). This process occurs through either one of two pathways; the extrinsic pathway, which is death receptor mediated, or the intrinsic pathway, which is mediated by the mitochondria (Venables, et al., 2016). Both pathways are mediated by initiator caspases, and converge for execution by activating caspase 3/7 to effect the consequential program of dismantling the cells and labelling it for cell death.

Shelembe, Mahlangeni and Moodley (2019) showed that gold nanoparticles synthesised with saccharides from *A. afra* were potently cytotoxic for MCF-7 cells and were furthermore selective to the cell strain as opposed to the non-cancerous cell line in their control (Shelembe et al., 2019). They reported the cytotoxicity to be as a result of their compounds effect on the redox status of the MCF-7 cells. Oxidative stress, which contributes to an imbalance to cellular redox state has been shown to be tumorigenic (Shelembe et al., 2019). Endogenous and exogenous sources that contribute to oxidative stress come from the accumulation of reactive oxygen species (ROS) and reactive nitrogen species (RNS). It has been found that cancer cells display a larger proportion of oxidative stress than their normal counterparts (Xing et al., 2022).

These reactive species are kept in balance at physiological levels by non-enzymatic antioxidants and antioxidant enzymes (Xing et al., 2022). In cancerous cells oxidative stress is tightly regulated and is involved in the efficient carrying out of the hallmarks of cancer. It is understood that therapies that increase ROS and RNS production or reduce the production of antioxidants in cancerous cells, disrupt their tightly regulated redox state and leads to ROS mediated cytotoxicity (Xing et al., 2022). van Loggenberg and associates (2022) experimented on the cytotoxic effects of A. *afra* infusions on a lung cancer cell line; however, they only reported on the extent of cytotoxicity leaving the kind of cytotoxicity and mechanisms through which it takes place open to question (van Loggenberg et al., 2022). The present study seeks to further explore the cytotoxicity of *A. afra* aqueous extract and the mechanisms thereof in the A549 cell line.

1.2 PROBLEM STATEMENT / RATIONALE

Lung cancer is the leading cause of mortality from cancer. As populations continue to see growths in life expectancy and the adoption of negative lifestyle risk factors, its burden of disease is projected to rise well into the foreseeable future. The treatment regimens currently available for the disease are associated with a number of undesirable outcomes. They, firstly, have limited efficacy, as shown by low post-diagnosis survival rates amongst a significant proportion of the different types of lung cancer (Ren et al., 2016). Secondly, they may also lead to the development of drug resistance. Lastly, due to factors such as inadequate selectivity for cancerous cells, their use is accompanied by serious adverse effects (Ren et al., 2016). South Africa, being a developing country, is faced with inequity in access to cancer treatment as compared to other countries. For instance, a regimen for a course of non-Hodgkin lymphoma drugs is worth approximately 5.6 years of the average South African annual wage as compared to 1.1 years of the average annual wages in the United States (Cortes et al., 2020). It is reported that in most cases in this setting the cost of drugs precludes treatment (Cortes et al., 2020). Meaning that without support from the health system many people living with cancer cannot afford treatment, and in the backdrop of a projected significant increase in the incidence of the disease, this could pose as a major challenge in society. A large proportion of the population uses *A. afra* for a variety of ailments (Shelembe et al., 2019). It holds the potential to be an effective antitumour agent, however, little is known about the mechanisms involved in its cytotoxic activity (Shelembe et al., 2019; van Loggenberg et al., 2022). This study seeks to further elucidate the cytotoxic mechanisms of *A. afra* in lung cancer (A549) cells.

1.3 SIGNIFICANCE / IMPLICATIONS

There is mounting evidence for urgency in the development of new cancer treatment drugs. Further exploration of the cytotoxicity of the plant could serve as a contribution to the body of knowledge on the possible effects the use of *A. afra* could have on cancer progression. In a country where the plant is near ubiquitous, indicating use of its derivatives as part of cancer treatment could improve the survival rates of people living with cancer, while reducing the costs of achieving that goal should one or a combination of its phytochemicals be found to be a favourable antitumour agent. A significant number of currently commercialised drugs in the field of cancer have been directly or indirectly obtained from natural resources, including medicinal plants (Nobili et al., 2009). The complex mixture of secondary metabolites in whole plant extracts offer valuable insights about their synergistic/antagonistic apoptogenic and anti-proliferative effects, in some cases, more so than tests on single molecules (Russo, 2007).

1.4 RESEARCH QUESTIONS

- Is the crude aqueous extract of *A. afra* cytotoxic to A549 cell line?
- What are the mechanisms involved in the cytotoxic activity of *A. afra*?
- Will *A. afra* prevent oxidative stress in A549 cells?
- What mechanism of cell death will *A. afra* induce in A549 cells?

1.5 HYPOTHESIS

1. *Artemisia afra* will induce cytotoxic effects on A549 cells mediated by oxidative stress.
2. *Artemisia afra* will induce cell death via apoptosis in A549 cells.

1.6 AIMS

The present study aims to investigate the cytotoxic mechanisms of the crude aqueous extract of *A. afra* on the A549 cell line.

1.7 OBJECTIVES

In this study a crude aqueous leaf extract of A. *afra* will be used to assess cell viability of A549 cells post-treatment using the MTT assay. The 50% inhibitory concentration (IC_{50}) will be compared to the untreated control cells in subsequent assays. The mechanisms by which the crude leaf extract of A. *afra* carries out its cytotoxic effects will also be assessed in A549 cells by.

- quantifying adenosine triphosphate (ATP) concentration and mitochondrial membrane potential (luminometry) to determine mitotoxicity.
- evaluating induction of oxidative stress using
    - TBARS and NOS assays to measure the extent of reactive oxygen species and reactive nitrogen species production, respectively.
    - luminometry to quantify GSH.
    - western blotting and qPCR to detect antioxidant enzymes including SOD2, catalase, Gpx, Nrf2 for their protein and gene expression.
- determining the mode of cell death via
    - quantification of initiator and executor caspase activity (luminometry)
    - elucidation of the mode of cell death (luminometry)
    - detection of proteins associated with apoptosis (Bax, Bcl2, xIAP, heatshock proteins) using the western blot assay.

CHAPTER 2 : LITERATURE REVIEW

2.0 INTRODUCTION

Cancer continues to ravage communities across the glow at a growing pace, with lung cancer leading the group of illnesses as a cause of morbidity and mortality (Sung et al., 2021). The current literature review briefly highlights cancer and its epidemiology and delves into aspects of lung including its prevalence, causes, pathophysiology, current treatment and possible target points with with a focus on cellular machinations around oxidative stress. Given the current research project's investigative efforts into the potential of anticancer activity in the plant *Artemisia afra*, a detailed overview of the plant's phytochemical profile, growth patterns and use in traditional medicine will also be covered.

2.1 CANCER

Unregulated proliferation of cells that does not respond to control mechanisms for normal cell behaviour is the basis for tumour development and cancer. Cancer cells are able to invade normal surrounding tissues and organs via metastatic spread throughout the body (Cooper, 2000). Generally, the loss of controlled growth and proliferation of cancer cells is the net result of an accumulation of abnormalities in the cell's regulatory systems that may be attributed to sources intrinsic or non-intrinsic to human cell biology (Cooper 2000; Wu et al., 2018). The association of smoking with lung cancer, human papillomavirus (HPV) with cervical cancer, viral hepatitis with hepatocellular cancer are examples of non-intrinsic sources of cancer, as would inherited genetic variation and errors in DNA replication be examples of intrinsic sources of tumour genesis (Tomasetti et al., 2017; Wu et al., 2018). Any of the variety of cell types found throughout the body have the potential to give rise to cancer; there are therefore over a hundred distinct types of cancer, varying vastly in behaviour and response to treatment, that have been reported so far (Cooper, 2000).

The pathological classification of cancers begins with distinguishing the organ of origin and predominant cell type in the tumour (Sonnenschein et al., 2014). They are also classified as benign or malignant, where benign tumours are those that remain confined to the tissue of origin without invasion of adjacent tissue and do not metastasise; and malignant tumours which are those capable of adjacent tissue invasion and dissemination throughout the body through the lymphatic and circulatory systems (metastasis) (Cooper, 2000; Sonnenschein et al., 2014).

In literature, the latter is the proper description of cancer, and it is this characteristic of tissue invasion and metastasis that makes cancer a difficult disease to treat (Cooper, 2000). Cancers are categorised into three main groups: carcinoma, sarcoma and leukaemia or lymphoma; carcinomas are malignancies of epithelial tissue that make up approximately 90% of all human cancers (Bade and Cruz, 2020). There are only a few frequently occurring cancers, with colon/rectum, breast, prostate, and lung cancers accounting for more than half of all cases and most deaths from cancer (Sung, 2021; Bray et al., 2024). Lung cancer, which is the focal point of this study, is reported to be the most lethal type of cancer (Cooper, 2000; Bade and Cruz, 2020; Sung, 2021; Bray et al., 2024).

2.2 LUNG CANCER

2.2.1 Epidemiology

Lung cancer ranks first amongst the leading causes of cancer deaths worldwide (Bade and Cruz, 2020; Sung et al., 2021; Bray et al., 2024). According to GLOBOCAN lung cancer estimates for 2020 (Figure 2.1), there were almost 2.2 million new cases and 1.8 million deaths, 11.4% of total cancer cases and 18% of total cancer deaths respectively in both sexes combined (Sung et al., 2021). In 2022, 12.4% incident and 18.7% mortality lung cancer cases were recorded (Bray et al., 2024). These rates were significantly higher than those reported for 2012, 2018 or 2020, showing that the incidence and mortality from the disease is on the rise. Men and women are unequally affected by lung cancer. In men, it is the leading cause of morbidity and mortality, whereas, in women, lung cancer was the second leading cause of the incidence of total cancer cases and second to breast cancer as the leading cause of mortality (Sung et al., 2021; Bray et al., 2024).

The incidence and mortality ratio of lung cancer is 1:2 between females and males respectively. However, in several countries in Europe and Northern America, the incidence rates amongst females are approximating male incidence rates (Sung et al., 2021). Studies further reveal that in successively younger birth cohorts in the United States, Canada, Denmark and Germany, the female-to-male incidence ratios are becoming higher (Jemal et al., 2018; Sung et al., 2021). In the South African context, lung cancer similarly holds the position of being the number one cause of cancer mortality (Koegelengburg, 2019). Its incidence rates amongst females and males as reported in 2014 by the National Institute of Communicable Disease stood at 3.95/100

000 in females and 10.12/100 000 in males (Age-standardised incidence rates) (Koegelenberg, 2019).

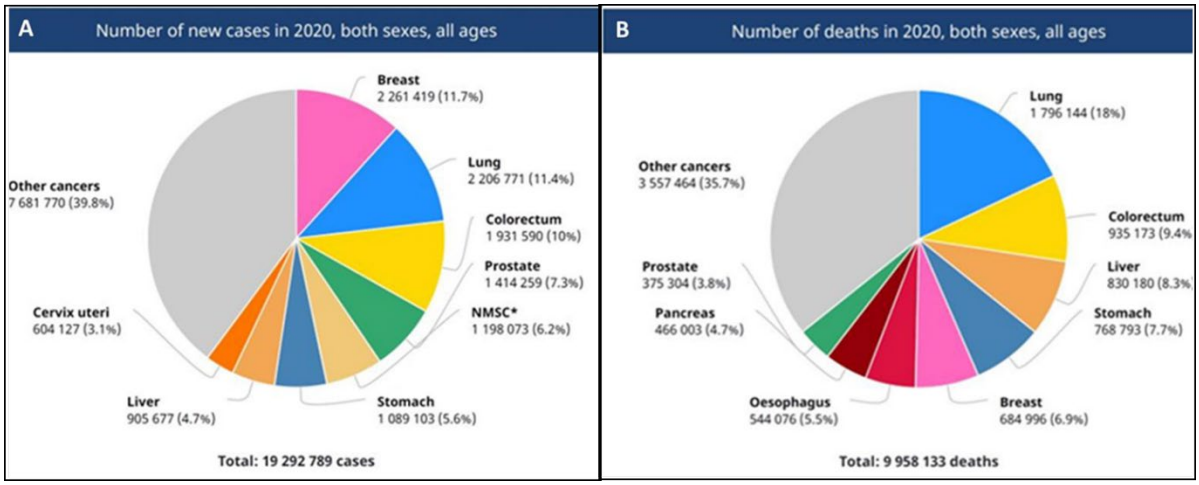

Figure 2.1: Incidence and mortality rates for all cancers worldwide in 2020 (Sung et al., 2021). **(A)** Almost 20 million new cancer cases were diagnosed, with lung cancer ranked second for incidence. **(B)** Nearly 10 million patients succumbed to cancer, and 18% of the mortality was attributed to lung cancer.

2.2.2 Types of lung cancer

Lung cancer is clinically diagnosed as either non-small cell carcinoma (NSCLC) or small cell lung carcinoma (SCLC). They are divided into the two using histology, with NSCLC having further subdivision into squamous and non-squamous carcinoma (Kim et al., 2022).

2.2.3 Risk factors

The established disparities between female and male incidence and mortality rates and the variation in incidence rates across age cohorts are largely attributed to historic patterns in tobacco smoking – currently the leading risk factor for lung cancer accounting for an estimated 70% - 90% of all deaths from the disease (Bade and Cruz, 2020; Schabath and Cote, 2019). Interestingly, from 2006 to 2008 the incidence rates in a number of European countries were found to be higher in females than in males. This alluded to the probability that, though known to be inextricably correlated, in some instances tobacco smoking and sex differences in tobacco smoking alone may be insufficient in explaining prevalence (Lortet-Tieulent, 2015; Bade and Cruz, 2020). Over several decades strides have been and continue to be made in elucidating the risk factors for cancer (Wu et al., 2018). Risk factors for lung cancer are well described by organising them into intrinsic and non-intrinsic categories (Figure 2.2) (Wu et al., 2018).

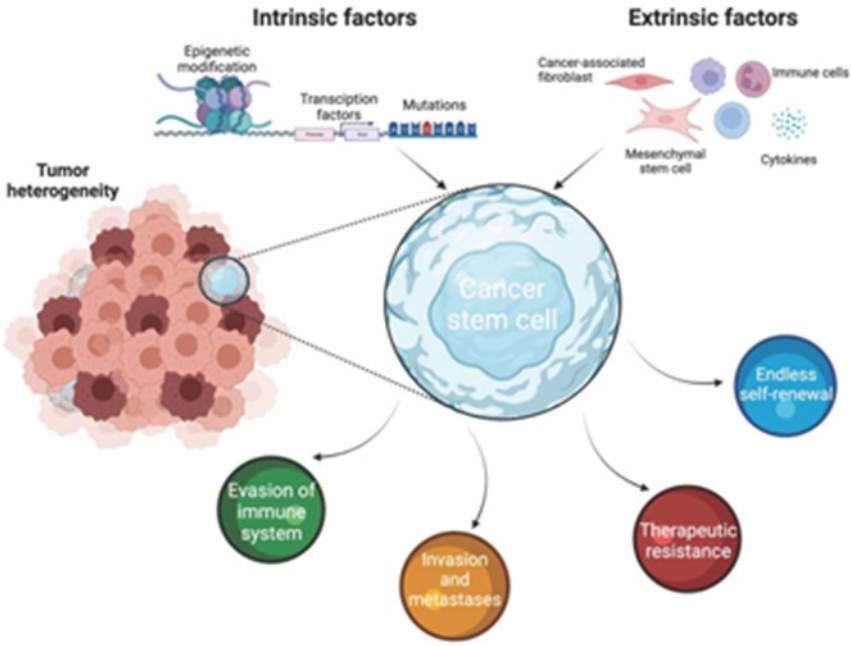

Figure 2.2: Intrinsic and extrinsic risk factors associated with lung cancer. The main intrinsic and extrinsic factors contributing to tumorigenesis (Ponomarev et al., 2022).

2.2.3.1 Intrinsic risk factors

All dividing cells impose an inherent intrinsic risk for cancer development which arises from the basal mutation rate they experience (Wu et al., 2018). This implies that all human beings are exposed to such risk. Single nucleotide errors, insertions and deletions are all examples of randomly acquired mutations that allow for the proliferation and survival of the cancerous cell and its progeny (Wu et al., 2018). These mutations may result in passenger mutations, which are not oncogenic but common in cancer. They may also result in driver mutations which are required for the development of cancer (Wu et al., 2018).

Several cancer registry-based studies have found that a positive family history of lung cancer increases relative risk for developing lung cancer, and recently conducted family aggregation studies have suggested that inheritance of lung cancer predisposition is multifactorial. However, the mechanisms have not been elucidated (Riudavets et al., 2022). High risks were found in a linkage analysis with a major susceptibility locus to chromosome 6q23-25 (Malhotra et al., 2016). A germline mutation in the tumour-suppressor gene protein 53 (p53) known as Li-Fraumeni syndrome has also been reported to be a strong risk factor for lung cancer. Genome-wide association studies report three main lung cancer associated genetic polymorphisms with susceptibility loci in the 15q25, 5p15 and 6p21 regions (Malhotra et al.,

2016). Strong evidence for the association of the susceptibility region in 15q25 with increased risk for lung cancer was reported by three separate GWA studies reporting a nearly precise measure of effect (McKay et al., 2008; Malhotra et al., 2016). This locus has, thus far, been the only one to be replicated in all types of lung cancer (Malhotra et al., 2016). The 15p25 represents a region that codes for nicotinic acetylcholine receptors and includes human telomerase transcriptase gene (TERT) and cleft lip palate and transmembrane-1-gene (CLPTM1L). This has led to linkage of the association with tobacco addiction vulnerability and altered smoking behaviour, a well-established risk factor for lung cancer (Malhotra et al., 2016; Schabath and Cote, 2019; Bade and Cruz, 2020). In addition, telomerase activity has been shown in up to 90% of all human tumours (Malhotra et al., 2016).

Variants in the human leukocyte antigen (HLA-DRD2) gene located in 6p21 have been associated with lung cancer tumorigenesis believed to be of an inflammatory origin (Brenner et al., 2013). It is worth noting that genome wide association (GWA) studies have only explained a proportion of the genetic variance found in lung cancer (Malhotra, et al., 2016). Also, cancer often requires more than one driver mutation to develop. For instance, in 2020 the ICGC/TCGA Pan-Cancer Analysis of Whole Genomes Consortium found that 4 to 5 driver mutations were responsible for the average cancer case under their review and that in approximately 5% of the cases, no driver mutations were recorded in both coding and non-coding DNA (Hirano et al., 2020). Thus, the barrier to tumorigenesis is normally surmounted through the aid of non-intrinsic risk factors (Wu et al., 2018).

2.2.3.2 Non-intrinsic risk factors

Non-intrinsic risk factors include those derived from both endogenous factors such as oxidative stress, inflammation and growth factors, and exogenous factors such as tobacco smoke, radiation and viruses (Malhotra et al., 2016). For lung cancer, the strongest determinant of carcinogenesis known to be associated with all histological types is tobacco smoking. Continuous smokers have an excess risk in the order of 20 – 50 times more of developing lung cancer than those who have never smoked tobacco (Malhotra et al., 2016; Bade and Cruz, 2020; Schabath and Cote, 2019). This risk is reduced with cessation of smoking but persists in long-term quitters relative to never-smokers (Malhotra et al., 2016). The association between tobacco and lung cancer extends beyond cigarette smoking and includes other forms of the product's intake i.e., cigars, hookah and water pipes (Malhotra et al., 2016). Tobacco also

increases the risk for developing lung cancer for those exposed to second hand smoke by an order of 20 – 30% (Malhotra et al., 2016).

Second to tobacco smoking, radon is the main causative agent for lung cancer (main in non-smokers) (Riudavets et al., 2022). Radon is a naturally occurring gas that arises from the decay of the uranium (-238) found in the earth's crust. It diffuses through soil, where it is mostly found, into the air (Riudavets et al., 2022). Radon is also found in the water of both ground and (to an extent) public water systems. The accumulation of radon in the air of confined and poorly ventilated spaces indoors is the main source (up to 50%) of exposure to natural radiation for humans. Studies repot that the radioactive gas is responsible for 3-14% of lung cancer cases (Riudavets et al., 2022). Due to the fact that only 15-25% of all lung cancer cases are from non-smokers, knowledge on other risk factors is relatively less developed. Several other carcinogens such as asbestos, arsenic, air pollutants and diesel have been found to be associated with increased lung cancer risk. Furthermore, localised chronic inflammation and low consumption of fresh fruits and vegetables have also been positively correlated with lung cancer incidence (Riudavets et al., 2022).

2.2.4 Mechanisms

Lung cancer tumours fulfil all the hallmarks of cancer. They sustain proliferation, evade growth suppression, resist cell death, have an immortalised replicative potential, promote angiogenesis, invade and metastasise, reprogramme metabolism and evade the immune system (Imyanitov et al., 2005; Hanahan, 2022). Despite lung cancer being largely heterogenous in the events leading up to tumorigenesis, the pathways underlying such a process are mostly consistent throughout different types. The majority show stimulation through both autocrine and paracrine routes (Imyanitov et al., 2005). For instance, NSCLCs always display autocrine features through overexpression of the epidermal growth factor receptor (EGFR) family of receptor tyrosine kinases (RTKs) and the simultaneous production of the receptor's ligands (Figure 2.3) (Imyanitov et al., 2005). On the other hand, SCLCs show increased expression of KIT receptor leads to increased RTK signalling. In addition, G-protein coupled receptors are also activated through upregulated gastrin-releasing bombesin-like peptide secretion by SCLCs (Imyanitov et al., 2005).

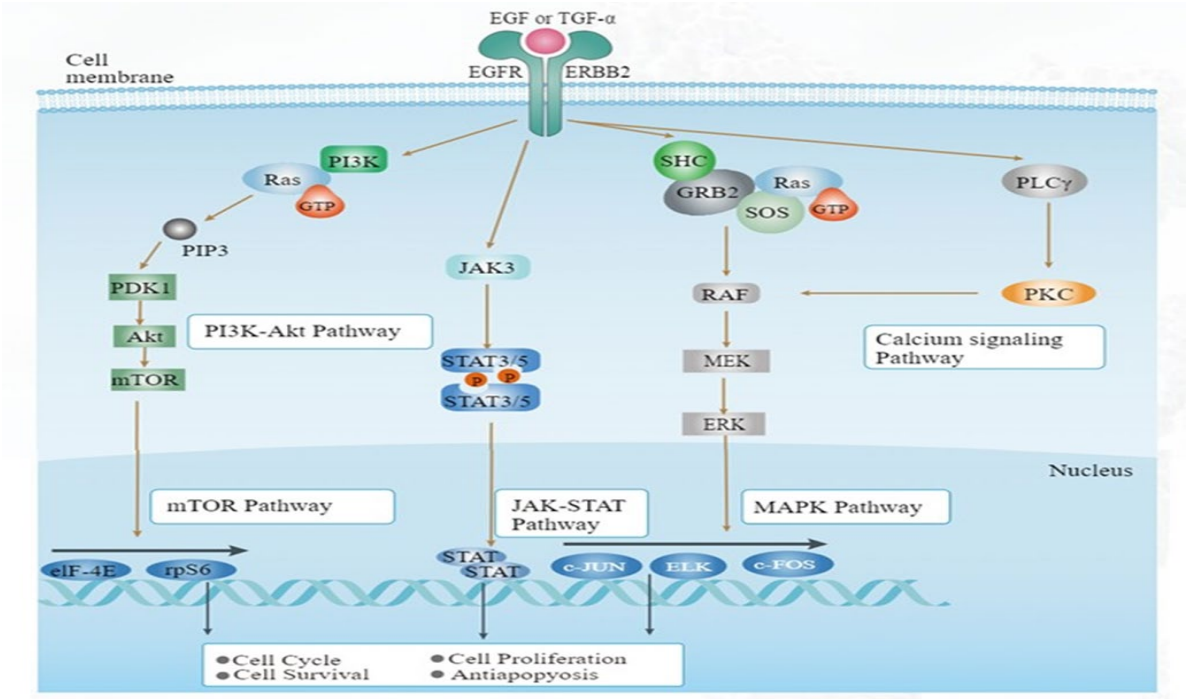

Figure 2.3: Overview of the mechanisms associated with Non-Small Cell Lung Carcinoma. The different signalling pathways in Non-Small Cell Lung Carcinoma linked to cell cycle, survival, proliferation and anti-apoptosis provide attractive targets for treatment (Alamgeer, 2013).

Tumour fibroblasts mediate the paracrine upregulation of the MET signalling cascade by releasing hepatocyte growth factor (HGF) into the tumour microenvironment. Activation of RTKs induces the activation of the P13K/RAS/PLC signalling cascades, of which RAS is the most significant component. Its activation, may through intermediary signalling molecules, activate the Phoshatidylinositol-3 kinase (PI3K) and polo-like kinase (PLK) pathway at different points down their respective cascades (Imyanitov et al., 2005). An activating mutation of K-ras is found in approximately 30% of all lung adenocarcinomas with the exception of SCLC. K-ras is known to mediate the hydrolysis of guanosine triphosphate (GTP) to guanosine diphosphate (GDP). Mutated K-ras loses this capability, and when complexed with GTP it is maintained in a constitutively active state (Imyanitov et al., 2005). In the hypo-phosphorylated state, retinoblastoma (RB) 1 remains functionally active. When activated RB1 releases E2F which augments the expression of s-phase specific genes. This is mediated by CDK4/ or 6 kinase which is the enzyme responsible for inactivation of RB1. CDK/4 or 6 activity is regulated by the cyclin D1 protein. RTK signalling and amplification mutations may lead to increased amounts of cyclin D1 and therefore amplified RB1 activity. In a high proportion of SCLC the RB pathway is always inactivated (Imyanitov et al., 2005). Another regulator of CDK4, the $p16^{INK4a}$ gene is found inactivated in a large proportion of NSCLSs. It is responsible

for the expression of $p16^{INK4a}$ which inactivates CDK4. P53 suppressor gene mutations have also been reported in 50% of NSCLCs and 90% of SCLCs. It is believed that Irregularities in the pathway under the regulation of this gene are responsible for aspects of the deregulated cell cycle and evasive characteristics of cancerous cells within the lung cancer tumour (Imyanitov et al., 2005).

2.2.5 Treatment

The past decade has seen vast advances in the treatment and therefore the survival rate in lung cancer. In England the 1-year survival rate increased from 24.5% to about 37% since the year 1995 (Jones and Baldwin, 2018). Lung cancer treatment options are currently determined by the stage at which it is presented. The staging of lung cancer is as is classified by the International Association for the Study of Lung Cancer's and includes grouping by tumour, nodes and metastases. Thoracic surgery has been to date the mainstay treatment option for early-stage lung cancer in people who are deemed surgically fit (Jones and Baldwin, 2018). Improvements in this form of cancer care such as the advent of video assisted lobectomy has increased the 5-year survival rate of early-stage lung cancer from 66 to 80% in places where this option is more readily available such as in the United Kingdom (Jones and Baldwin, 2018). In early-stage lung cancer patients with comorbidities or who are deemed medically inoperable, radiotherapy is reserved as the first line treatment option.

Since NSCLC is the predominant type of lung cancer, it has received considerable attention in drug development over the years and has therefore seen the development of more targeted and individually tailored drugs when contrasted with SCLC (Jones and Baldwin, 2018). This targeting is based on the detection of driver mutations. Gefitinib is the first example of genetically targeted treatment for NSCLC. It conveys its effects through the inhibition of tyrosine kinase, thus effecting EGFR. The drug had been proven to be effective in EGFR mutation positive NSCLC patients and prompted the development of drugs with a similar mechanism of action including; erlotinib and afatanib (Jones and Baldwin, 2018). For ALK/ROS-1 mutation positive NSCLCs crizotinib, ceritinib, and alectinib are normally the indicated drugs which have been found to be more effective than standard care chemotherapy which includes paclitaxel and carboplatin (Jones and Baldwin, 2018). Another more recent advancement in targeted therapy for NSCLCs is immunotherapy. These are drugs that increase

immune system responsiveness to cancerous cells. Examples of such are the PD-1 inactivating IgG4 monoclonal antibodies Nivolumab and Pembrolizumab (Jones and Baldwin, 2018).

The SCLCs are sensitive to standard care chemotherapy which includes paclitaxel and carboplatin. They, however, have a recurrence rate of 80%, therefore SCLC patients are treated with radiation therapy after completion of 4 to 6 cycles of standard care chemotherapy (Siddiqui et al., 2022). The SCLC patients who present at later stages are treated with platinum-based chemotherapy followed up by radiation therapy. The median survival rate of SCLC presenting at later stages is 8 to 13 months post-diagnosis pointing to a need for innovation in the space of research and development for newer more effective drugs (Siddiqui et al., 2022).

2.3 MEDICINAL PLANTS

The use of natural plants as a source of medicine predates recorded medical literature (Ekor, 2014). The earliest well-known records are documentations of Egyptian medicine (Ebers Papyrus), Chinese medicine (Chinese Materia Medica) and Indian medicine (Ayurveduc system) which date as far back as 1500 BCE, 1100 BCE and 1000 BCE respectively (Cragg and Newman, 2012). Plants have, over years, been used to treat many pathological conditions. Preparations including concoctions, concentrated extracts, chewing of leaves or bark and vapour inhalation from medicinal plants are some of the many methods that have been utilised to administer their healing constituents throughout history worldwide. The WHO reports that due to poverty and lack of access to modern medicine over 60% of the world's population uses medicinal plants as a source for therapy (Allkin, 2017). This is more pronounced in the developing world, such as in Africa and in parts of Asia where approximately 80% of the population are partially or solely reliant on medicinal plants for their healthcare (Ekor, 2014).

The recent past has been met with a tremendous increase in the acceptance, interest and use of medicinal plants as therapy for primary healthcare. This is evident in the present day by their availability not only in pharmacies, but also in supermarkets and at times in retail outlets solely purposed for their sale (Ekor, 2014). Accordingly, medicinal plants have been garnering an ever-growing share of the global drug market over the past two decades (Allkin, 2017). In 2003, the WHO evaluated the annual global market for medicinal plants (traditional medicine) at US$ 17 bill, by 2012 Chinese traditional medicine alone was estimated to be worth US$ 83 bill, signifying considerable growth (Alkin, 2017). Apart from their fair share in the global

drug market, medicinal plants have also proven to be a valuable source for drug development in modern medicine as pharmaceutical agents and as leads for bioactive molecules (Cragg and Newman, 2012).

By the dawn of the 21st century, more than 11% of the drugs considered essential by the WHO were developed from plants. There are numerous examples that demonstrate the benefits that have been derived from the use of medicinal plants in drug development. Examples of such include: morphine, an analgesic isolated from the opium in poppy plant (*Papaver somniferum*) seed pods (Katiyar et al., 2012); artemisinin, the antimalarial discovered in *Artemisia annua* and its equivalent quinine, a crystalline compound found in the bark of *Cinchona spp.*; and chemotherapeutic drugs such as taxol and vinblastine, currently indicated for the treatment of a variety of cancer types are both derived from plant species known to be traditionally used for medicinal purposes (Cragg and Newman, 2012; Thomford et al., 2018). There has been a growing interest in the screening of medicinal plants for their potential antitumor activity. One such medicinal plant that has been of interest is *A. afra*, a member of the *Asteraceae* family of plants (Spies et al., 2011; Venables et al., 2016; Shelembe et al., 2019; van Loggenberg et al., 2022).

2.4 *ARTEMISIA AFRA*

2.4.1 Description

Artemisia afra is a member of the *Asteraceae* family of the *Plantae* kingdom (Patil et al., 2011). It is a medium sized shrub with a leafy ridged stem that grows to an average of 2 meters in height. The bitter tasting leaves grow silver-grey in colour, are oval in shape, soft to the touch and arranged in a fern like fashion (Figure 2.4). Its pale-yellow florets grow racemose in inflorescence, containing the females in the outer most parts and bisexual florets in the inner most parts. When bruised, the plant produces a distinguishable sweet and pungent aroma. Fertilised flowers of *A. afra* are produced between March and July and the seeds between August and November (Patil et al., 2011).

Figure 2.4: The *Artemisia afra* shrub, with its silvery fern-like leaves (Phytoalchemy, 2023).

2.4.2 Distribution

Artemisia afra grows in highland areas in Eastern and Southern Africa including Tanzania, Ethiopia, Kenya, Zaire, Zimbabwe, Angola and South Africa. The plant also grows in parts of North America, Asia and Europe. It is mainly found in volcanic ash, loamy sands and calcareous clay loam soils that are in the 1500 – 3000m altitude range (Patil et al., 2011). In South Africa, *A. afra* can be found growing in all provinces with the exception being the

Northern Cape (Figure 2.5). In these terrains it can be spotted in rocky and mountainous areas as well as in stream banks and alongside forests (Patil et al., 2011).

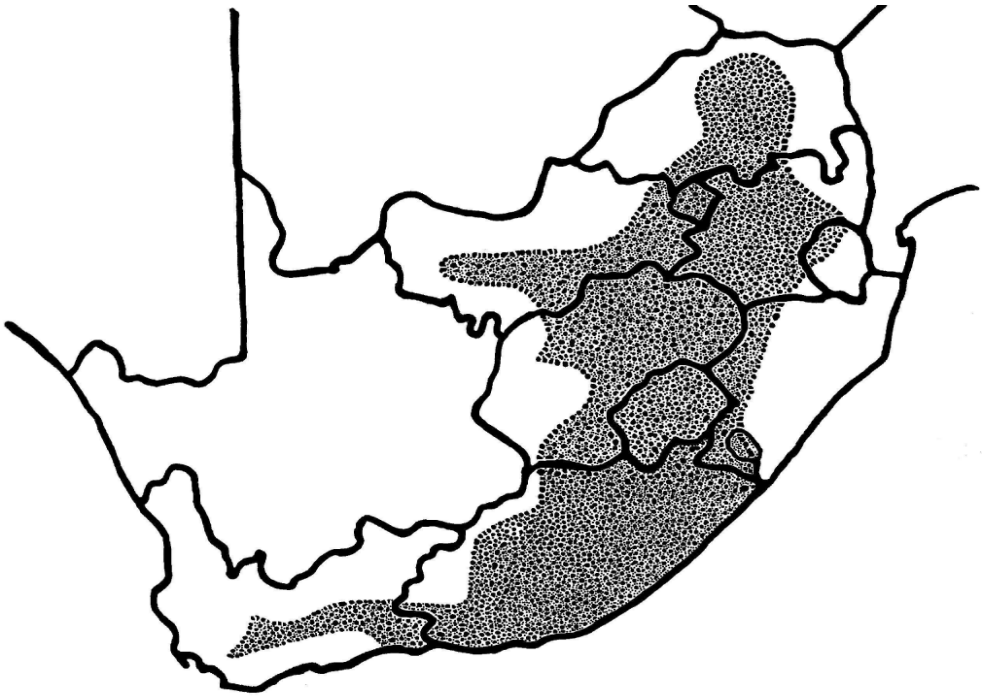

Figure 2.5: Distribution of *Artemisia afra* in all provinces of South Africa excluding the Northern Cape (Scott and Springfield 2004).

2.4.3 Uses

A survey conducted in the southern regions of the Western Cape expressed that amongst respondents, *A. afra* was the most commonly used medicinal plant. The study also reported it to be the most valuable of medicinal plants given that its efficacy spans throughout more illnesses than any other medicinal plant in the region (Dube, 2006). The *A. afra* preparations are routinely used to treat respiratory related ailments such as the common cold, flu, asthma and, in instances, headaches. The vapours from heated leaves are inhaled to alleviate symptoms from these ailments by clearing the respiratory and bronchial airways (Patil et al., 2011). For gastrointestinal disorders such as colic, constipation, indigestion, gastritis and intestinal worms, an orally administered infusion or decoction is prepared from dry leaves. An extract of *A. afra* is topically applied for soothing pain from boils, acne pimples and carbuncles. A hot bath in the decoction of the plant is used to bring out the rashes from chicken pox, measles and mumps. Haemorrhoids, herpes and venereal sores are also bathed in the decoction or infusion (Patil et al., 2011).

Disorders associated with the menstrual cycle are also treated with *A. afra* often by steaming the female genitalia with vapours from the plant's leaves or by orally administering decoctions (Patil et al., 2011). It is also used in the treatment of rheumatism, gout, neurological disorders such as epilepsy and urinary disorders such as haematuria (Patil et al., 2011). Finally, an infusion of two handfuls of *A. afra* leaves is administered as enemas or emetics to treat fevers, in particular the *A. afra* is administered for fevers associated with malarial infections in most parts of Southern Africa where malaria is endemic. In addition, leaves and bulbs from the garlic plant, *Xanthoxylum capensis,* and *A. afra* are mixed in a decoction and administered for the alleviation of fevers.

2.4.4 Traditional preparations

The *Artemisia* plant is widely used as a medicinal plant worldwide, and *A. afra* is no exception in South African traditional medicine. It is utilised amongst a diversity of cultural groups in the country, popularly known as "Mhlonyane'' in isiZulu, "Umhlonyane'' in isiXhosa, "African wormwood'' in English, "Lenyana'' in seSotho, "Wilde als'' in Afrikaans and "Lengana'' in seTswana (Liu et al., 2011). The preparation of a decoction of *A. Afra* involves boiling a quarter cup of fresh leaves in a cupful of water and allowing it to draw for 10 minutes, straining the mixture and then sweetening with honey. The preparation for an infusion follows similar steps where a half a cupful of leaves is added into in 2 litres of boiling water, allowed to draw for 10 minutes and then strained. The decoctions and infusions are normally taken orally or applied topically for the treatment of the above-mentioned ailments (Liu et al., 2011). The complex mixture of these molecules or compounds, including their more physiologically active counterpart – the primary metabolites, in *A. afra* is what the plant owes its success in therapeutic application to (Gakuba, 2009).

2.4.5 Phytochemicals

Secondary metabolites are a class of low molecular mass phytochemical molecules synthesised by plants. These molecules, being non-essential for growth or development, are rather more specified for improving the probability of a plant's survival as it interacts with the external environment (Taleghani et al., 2019). Secondary metabolites are classified into three groups based on their biosynthetic origin, namely terpenes that almost entirely comprise of carbon and hydrogen, nitrogen-containing compounds which have the most diversity in their structure and phenols which comprise of simple sugars containing benzene rings, hydrogen and oxygen

(Taleghani et al., 2019). Some texts may group them into nitrogen-containing and non-nitrogen containing compounds (Wink, 2010). Other texts describe four groups: the alkaloids, terpenoids, phenolics and sulphated amino acids.

A wide range of bioactive phytochemical compounds have been identified in *A. Afra* and reported on in literature (Dube, 2006; Taleghani et al., 2019). These include metabolites such as flavonoids, terpenoids, tannins, cardiac glycosides, alkaloids and saponins (Haile and Jiru, 2022). A few chemical analysis studies have been conducted over the years and have described compounds in the plant that include: 3,3,6-trimethylhepta-1,5-dien-4-one an artemisia ketone detected by Garnero in a chemical investigation that also yielded an artemisia alcohol known as ‘’yomogi’’ (Garnero, 1977; Gakuba, 2009). Silbernagel isolated nanocosane and ceryl cerotinate. Monoterpenes such as β- (1.5) and α- thujone, and sesquiterpenes with glaucolide and guaianolide skeletons have previously been described by researchers (Silbernagel et al., 1990; Gakuba, 2009). Jakupovich *et al.* identified eudesmaafraglaucolide, a eudesmanolide derivative, in the plant. Camphor, borneol and 1,8-cineol are amongst other compounds that have also been described in literature (Jakupovich et al. 1991). A GC and GC-MS analysis of the essential oil of A. *afra* was conducted by Moody and associates. They described 21 components in the oil, where the main constituents were found to be: artemisia ketone (11.7%); tricosane (14%); 1,8-cineol (17.5%); and cis-2,7-dimethyl;-4-octene-2,7-diol (19%) (Gakuba, 2009). It is noteworthy that a number of studies have investigated variations in the expression of secondary metabolites in A. *afra*. It was found on several accounts that factors such as location, seasonality and the age of the plant were associated with variations in the composition of the plant’s essential oils (Gakuba, 2009).

Secondary metabolites that have been identified in *A. afra* in the past decade are listed in Table 2.1 (du Toit and van der Kooy, 2019). This list of secondary metabolites and those mentioned above are not exhaustive of the 131 compounds identified in *A. afra*, but include some that have been investigated and shown to have a potential usefulness as therapeutic agents or templates thereof.

Table 2.1: Secondary metabolites identified in *A. afra* in the past decade (adapted from du Toit and van der Kooy, 2019).

Compound name	Structure	Classification
α-amyrin	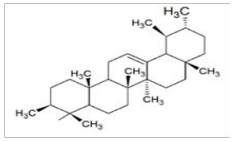	Pentacyclic triterpene
1α,4α-dihydroxybishopsolicepolide	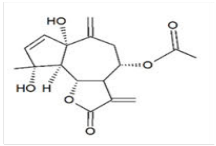	Guaianolide sesquiterpene lactone
12α,4αdihydroxybishopsolicepolide	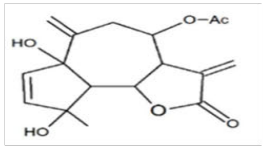	Sesquiterpene
3,5-dicaffeoyl quinic acid	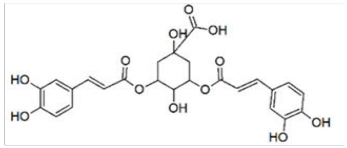	Phenylpropanoid
Acacetin	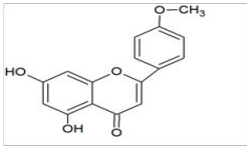	Flavone
Caffeic acid	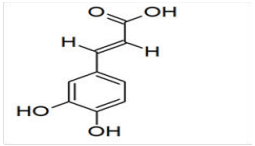	Phenylpropanoid

Compound name	Structure	Classification
Chlorogenic acid	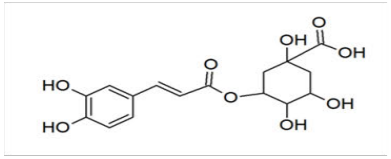	Pheylpropanoid
Isoalantolactone	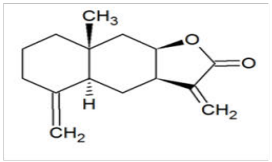	Sesquiterpene
Phytol	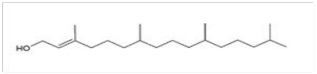	Diterpene
Scopoletin	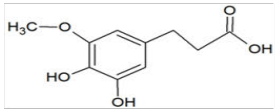	Coumarin
Yomogiartemin	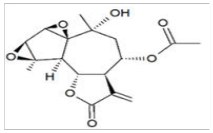	Guaianolide sesquiterpene lactone

A study conducted by Venables *et al.* (2015) singled out isoalantolactone, a class of terpenoids, as one of the main compounds responsible for the cytotoxic effects of *A. afra* on HeLa cells (Venables et al., 2015). It had been previously demonstrated in prior studies that chemical moieties present in the compound such as α-methylene-γ-lactone groups mediate the cytotoxicity it exhibits (Venables et al., 2015). Isoalantalactone is a bioactive sesquiterpene lactone of the eudesmanolide group that occurs naturally in many condiments, vegetables and medicinal plants (Yao et al., 2016). *Artemisia* is known to contain one of the highest proportion of sesquiterpenoids, measuring up to 3% of total dry mass of a plant in members across the genus (Chadwick et al., 2013). This phytochemical, which was isolated from *A. afra* by Venables and associates (2015), has been of particular interest in cancer research as it has been shown to possess antiproliferative and apoptotic effects (Venables et al., 2015). Increasing evidence, from studies conducted within the past decade, suggests its desirability, effectiveness and safety as a chemotherapeutic agent (Rasul et al., 2013; Cia et al., 2014; Di et al., 2014). A number of mechanisms of action of isoalantolactone induced cell death have been posited for different cancer models so far. However, an overarching mechanism which has generated a lot of consensus involves increased apoptosis mediated by the augmentation of reactive oxygen species (ROS) production (Khan et al., 2012; Venables et al., 2015; Chen et al., 2018; Lu et al., 2018; Wu et al., 2022). Taken together this proposes that isoalantolactone has an apoptotic effect through both the intrinsic and extrinsic pathways, mediated by increased levels of ROS (Di et al., 2014; Lu et al., 2018; Khan et al., 2012).

As will be further explored in the section below, ROS are reactive forms of oxygen that pose a threat to the integrity of the cell and its constituents when produced in excess intracellularly (Brieger et al., 2012). It has been established that the cancerous cell maintains high basal levels of ROS and equally expresses increased levels of antioxidants, which suggests it maintains a tightly balanced redox status albeit showing higher concentrations of ROS than the normal cell (Liou and Storz, 2014). The high levels of ROS seen in cancer cells may be as a result of mitochondrial dysfunction, increased receptor signalling, high levels of metabolic activity and increased oxidase activity. Signalling pathways that are ROS-sensitive are persistently activated in cancer. This in part contributes to the exhibition of the characteristic hallmarks of cancer such as proliferation, altered metabolism, increased survival and differentiation (Liou and Storz, 2014).

The signalling pathways affected by ROS include; mitogen activated protein kinase (MAPK)/ Erk, IκB kinase (IKK)/Nuclear factor kappa B (NF-κB) and phosphoinositide-3-kinase (PI3K)/Akt – regulated cascades (Liou and Storz, 2014). Isoalantolactone is reported to increase cytoplasmic ROS concentrations and thus cause ROS-mediated apoptosis in cancerous cells (Khan et al., 2012). Khan and associates (2012) first demonstrated this with pancreatic cancer (PANC-1) cells. They stated that the increased ROS act as secondary messengers that activate the MAPK family member – p38, upregulate the expression of Bcl-2-associated X (BAX) and inhibit the anti-apoptotic B-cell lymphoma-2 (BCL-2) in addition to causing the conventional oxidative damage to the cell leading to apoptosis (Khan et al., 2012). Lu and associates (2018) demonstrated that isoalantalactone mediated increases in ROS, caused a ROS mediated upregulation in death receptor 5 (DR5) in oesophageal cancer cells (Lu et al., 2018). Di and associates (2014) are believed to be the first to demonstrate the upregulation of DR5 in osteosarcoma cells suggesting a role for ROS mediated apoptosis regulated through the extrinsic pathway. They further demonstrated the inhibitory effects that ROS has on NF-κBp65 (Di et al., 2014).

2.5 OXIDATIVE STRESS

All aerobic organisms rely on oxygen as an essential component of life. Approximately 90% of 0_2 absorbed into the human body is consumed during oxidative phosphorylation which yields adenosine-5-triphosphate (ATP) and 10% is consumed by enzymes that use the 0_2 for oxygenation reactions and hydroxylation. Approximately 1% of the 0_2 is converted into reactive forms of oxygen known as reactive oxygen species (ROS) (Burton and Jauniaux, 2011). The ROS are known to be important substrates in metabolism. For instance, hydrogen peroxide (H_2O_2) is a ROS that acts as a second messenger in insulin signalling and in a number of growth factor activated signalling cascades (Sies, 2014). However, ROS is also capable of causing acute and chronic damage to tissue or cellular biomolecules such as proteins, lipids and DNA (Burton and Jauniaux, 2011). The body is equipped with a complex system of antioxidant defences geared towards protection from the oxidative damage caused by ROS. The inability of the body to defend itself from damage due to the defence system being overwhelmed by excess ROS production is known as oxidative stress. Oxidative stress has been implicated as a common denominator in the pathology of several diseases including cancer, cardiovascular disease and neurological disorders (Brieger *et al.,* 2012).

2.5.1 Oxidants

The ROS are by-products produced from the partial reduction of oxygen into its reactive derivatives. Oxygen is highly reactive due to its susceptibility to bond formation. This is because of the biradical configuration of its electrons (Brieger et al., 2012). The reduction of oxygen follows a sequential transition mainly initiating with superoxide ($O_2^{\bullet-}$), the first reactive radical, predominantly produced by complexes I and III of the mitochondrial electron transport chain (Figure 2.6) (Chen et al., 2009). Several other cellular enzymes including nitric oxide synthase (NOS), xanthine oxidase and nicotinamide adenine dinucleotide phosphate (reduced) (NADPH) oxidase are also responsible for $O_2^{\bullet-}$ formation. This radical has a short half-life, is local in effect and does not readily cross membranes. The $O_2^{\bullet-}$ is partitioned by superoxide dismutases (SOD) into molecular oxygen and H_2O_2 (Figure 2.6, 2.7). Ferrous iron and the copper ion catalyses the homolysis of H_2O_2 into hydroxyl radicals ($^{\bullet}OH$) and protons in the Fenton reaction. The $^{\bullet}OH$ is one of the most potent of radicals due to the wide range of biomolecules it can react with. Alternatively, H_2O_2 may be converted to H_2O by glutathione peroxidase (Gpx) (Chen, Azad and Gibson, 2009). The $O_2^{\bullet-}$ also reacts with nitric oxide (NO), forming the highly reactive radical, peroxynitrite ($ONOO^-$) (Figure 2.6, 2.7). Other species include hypochlorous acid (HOCl) and singlet oxygen ($^1O_2$) which are generated from H_2O_2 by peroxidases (Figure 2.6) (Brieger et al., 2012). While most texts on ROS place a focus on their deleterious effects, ROS do have beneficial roles to play as well. For example, the radical H_2O_2 is central in the iodination of the thyroid hormone by haem-peroxidases, and NO plays a regulatory function and serves as a blood pressure regulator. The ROS is also involved in the bactericidal function of macrophages (Brieger et al., 2012).

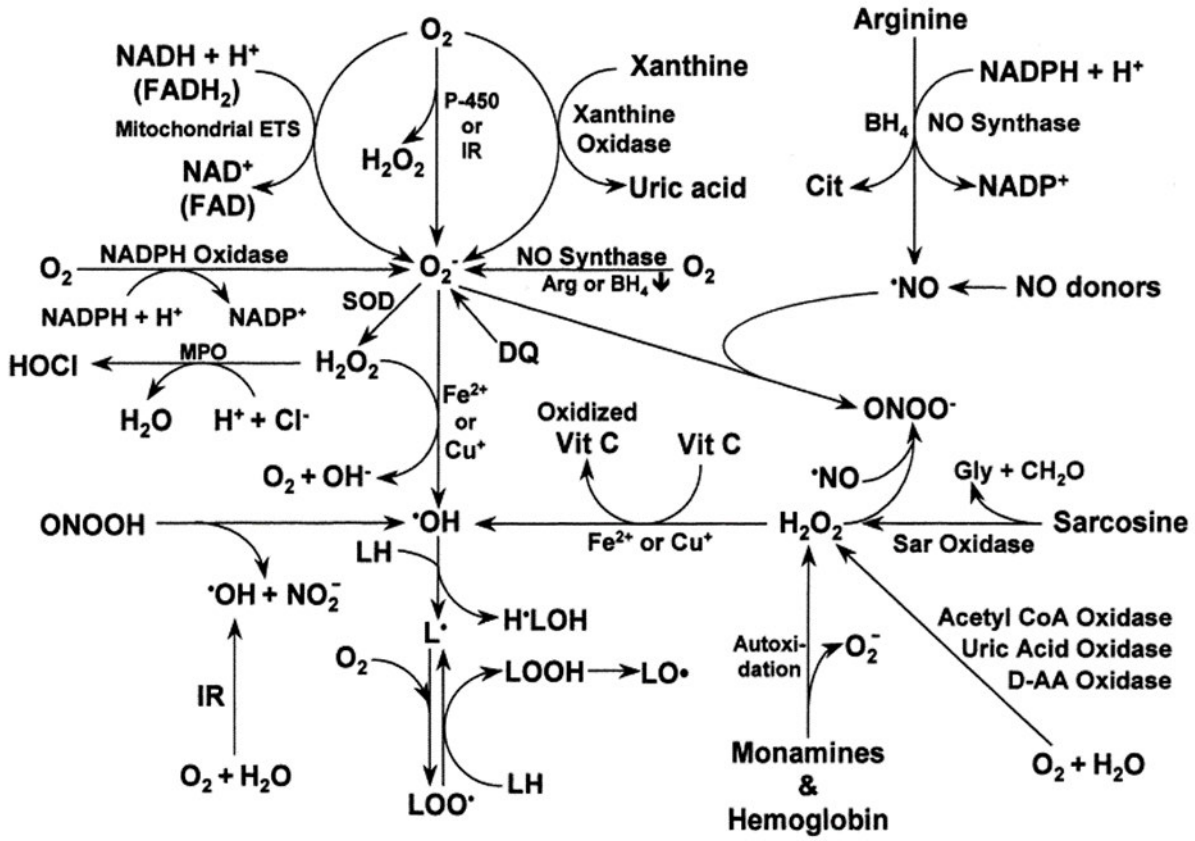

Figure 2.6: Overview of the pathways producing free radicals and the antioxidant defence (Fang, 2002).

2.5.2 Antioxidants

Antioxidants are inhibitors of oxidation that form part of the body's defence systems against oxidants. They may be sourced exogenously or are endogenous (Aziz et al., 2019). Several endogenous antioxidants are responsible for maintaining prevention of the harmful effects of oxidative stress. The first line of defence from oxidative damage are the endogenous chelators. These include transition metal binding proteins that sequester inactive copper and iron (Figure 2.6), such as ferritin and transferrin (Aziz et al., 2019). Ferritin derives its antioxidant activity from its consumption of Fe^{2+} and O_2 (Theil, 2010). Interestingly, it was found that some transition metal binding antioxidants with chelating properties were found to increase ROS concentrations, increasing the potential of carcinogenesis (Timoshnikov et al., 2022). Heme, the lipid soluble form of iron, catalyses the formation of ROS in lipid environments. Plasma hemopexin binds heme and delivers it to the liver for catabolism, thus reducing the net

formation of ROS, while albumin sequesters copper, effectively inhibiting its ability to form ROS (Aziz et al., 2019).

Given the continuous formation of ROS catalysed by spontaneous metal-catalysed reactions and as products of enzyme function throughout the body, the multiple chelator systems that exist are insufficient to maintain physiological ROS levels or redox state (Yang and Lee, 2015). In such a case there are several antioxidant enzymes that have been described and investigated *in vitro* and in animal models (Yang and Lee, 2015). A number of these enzymes are expressed as an adaptive cellular response to oxidative stress. This cellular response is regulated through transcriptional regulatory elements called the antioxidant response elements (AREs). Several transcription factors orchestrate the expression of cytoprotective genes through interacting with the AREs, however the most notable for ARE regulation amongst them is nuclear factor (erythroid-derived 2)-like 2 (Nrf2) (Raghunath, *et al.,* 2018). It is normally bound to its cytoplasmic inhibitor Keap1 and is maintained at very low levels within the cytoplasm. Oxidative stress causes conformational changes in Keap1 that lead to the detachment of Nrf2; Keap1 is also conformationally changed by electrophilic carcinogens that alkylate DNA and products of electrophilic lipid peroxidation. Nrf2 also dissociates from Keap1 upon reaction with an electrophile. All the factors that foster the dissociation of Nrf2 from Keap1 allow Nrf2 to translocate into the nucleus where it forms heterodimers and binds to AREs, thus activating the ARE dependant genes (Raghunath, *et al.,* 2018). Interestingly, there has been growing evidence suggesting that the constitutive activation of Nrf2 in a variety of cancers was associated with the induction of pro-survival genes and promoted cell proliferation through reprogramming metabolism. It was also found that Nrf2 may repress apoptosis and enhance the cell renewal capacity of stem cells (Wu, Lu and Bai, 2019).

The ARE dependant genes code for the expression of enzymes such as SODs, catalase, Gpx (Figure 2.7) and others including hepatic glutathione S-transferase. Superoxide dismutases are a family of metalloenzymes. The major forms include copper-zinc superoxide dismutase (SOD1), an enzyme that is ubiquitous in the cytoplasm and manganese superoxide dismutase (SOD2), which is concentrated in the mitochondria. In partitioning or dismutation, alternate oxidation-reduction of the metal ion containing SOD active sites takes place, thus facilitating the conversion of $O_2^{\bullet-}$ into H_2O_2 and O_2 (Raghunath, *et al.,* 2018; Younus, 2018; Chen, Azad

and Gibson, 2009). An isoform of SOD1 located extracellularly, binds to proteoglycans in vascular walls and is believed to be protective from $O_2^{\bullet-}$ and $ONOO^-$ induced vascular damage.

Catalase is responsible for the degradation of H_2O_2 into water and oxygen (Figure 2.7). There are several diseases known to be associated with a deficiency of catalase or a mutation in the gene coding for its expression (Wu, Lu and Bai, 2019). Glutathione peroxidase is mainly concentrated in the mitochondria, but may at times be located in trace amounts within the cytosol. Its function is the reduction of H_2O_2 into water and the degradation of lipid peroxides into their corresponding alcohols using reduced glutathione (GSH) as a co-factor (Figure 2.7). Thus, GSH holds an important role in the redox status of a cell due to its ability to scavenge ROS and RNS. Nrf2 signalling plays a central role in the regulation of the levels of GSH intracellularly through promoting the expression of enzymes such as glutamate-cysteine ligase (GLC) (Wu, Lu and Bai, 2019).

Vitamins A, C and E are also well known for their antioxidant properties. They form the last line of an exogenous defence against oxidative stress (Figure 2.7). Vitamins C and E in their aqueous and lipid phases respectively act as hydrogen atom donors thus reducing oxidants (Aziz et al., 2019). The radicals that they subsequently form are highly unreactive, stabilised and are enzymatically degraded. In addition to reducing radicals, Vitamin C is also responsible for the reduction and recycling of oxidised Vitamin E. In concert Vitamin C and E prevent lipid peroxidation of plasma lipoproteins and membranes (Aziz et al., 2019). Vitamin A is a potent antioxidant that protects the skin and retina from UV radiation damage (Aziz et al., 2019).

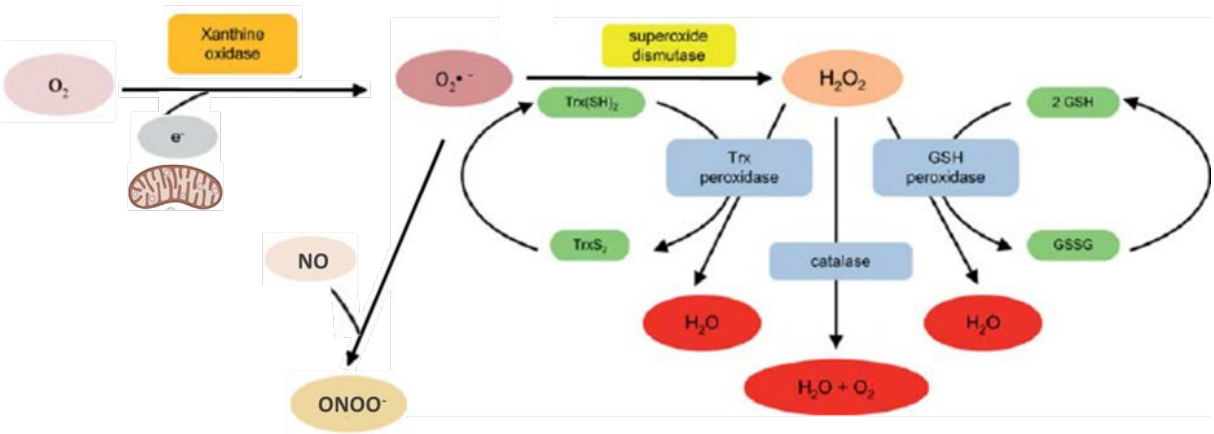

Figure 2.7: The role of antioxidants in the defence against free radicals (Celerado et al., 2011).

2.5.3 Effects of oxidative stress

Since ROS are an important component in the killing of bacteria and viruses, it is important to note that from an evolutionary perspective, it was beneficial for people to maintain high levels of ROS in order to fight of pathogens in the era of epidemics of infectious disease centuries ago (Firuzi et al., 2011).However, the accumulation of ROS is accompanied by harm to cellular biomolecules such as proteins, lipids and DNA through oxidation, a process involving the loss of an electron or the gain of oxygen (Pizzino et al., 2017). This puts ROS under the spotlight as a contributor to the pathogenesis and/or progression of several diseased states (Pizzino et al., 2017). Several biomolecular structures are affected by ROS culminating in different outcomes. Protein oxidation results in the modification of amino acids, peptide chain fragmentation, cross-linked product aggregation. Although oxidised proteins are more likely to be proteolysed, an increase in oxidated proteins results in the loss of their physiological functionality and biochemical roles (Aziz et al., 2019). It is believed that protein oxidation may be central in the pathogenesis of cataracts and may be the cause of aging. The DNA in the nucleus and mitochondria is also constantly exposed to oxidative stress and is highly prone to oxidative damage by ROS. Apart from $^{\bullet}OH$, which poses the most detriment to the integrity of DNA, $O_2^{\bullet-}$, RNS and photochemical pathways have been implicated in the disruption of DNA stability (Dumont and Monari, 2015). These entities attack the sugar and base moieties of DNA through oxidation leading to degradation, single-strand breakages and protein cross linkage amongst other lesions involving epigenetic proteins. As is well known, these lesions may be carcinogenic and are also, again, associated with accelerated aging (Aziz et al., 2019).

Since a high number of lipids (polyunsaturated fats) are found as the structural building blocks of bio-cellular membranes, cell membranes are highly susceptible to oxidation by ROS through a chain reaction process called lipid peroxidation (Pizzino, *et al.,* 2017). In this process, ROS oxidise one lipid molecule after the other in a chain reaction format producing lipid peroxidation products such as ketones, acids, lipid hydroperoxides, oxysterols and aldehydes. The interplay between inflammation and oxidative stress which consequently results in high levels of lipid peroxidation products has been implicated in life threatening illnesses such as severe sepsis, acute kidney injury and cardiac injury (Pizzino et al., 2017). Lipid peroxidation also plays an important role in programmed cell death (Figure 2.8) (Sroda-Pomianek et al., 2018). They are believed to be able to interact with both the intrinsic and extrinsic pathways, this will be further explored in a later section (Su et al., 2019).

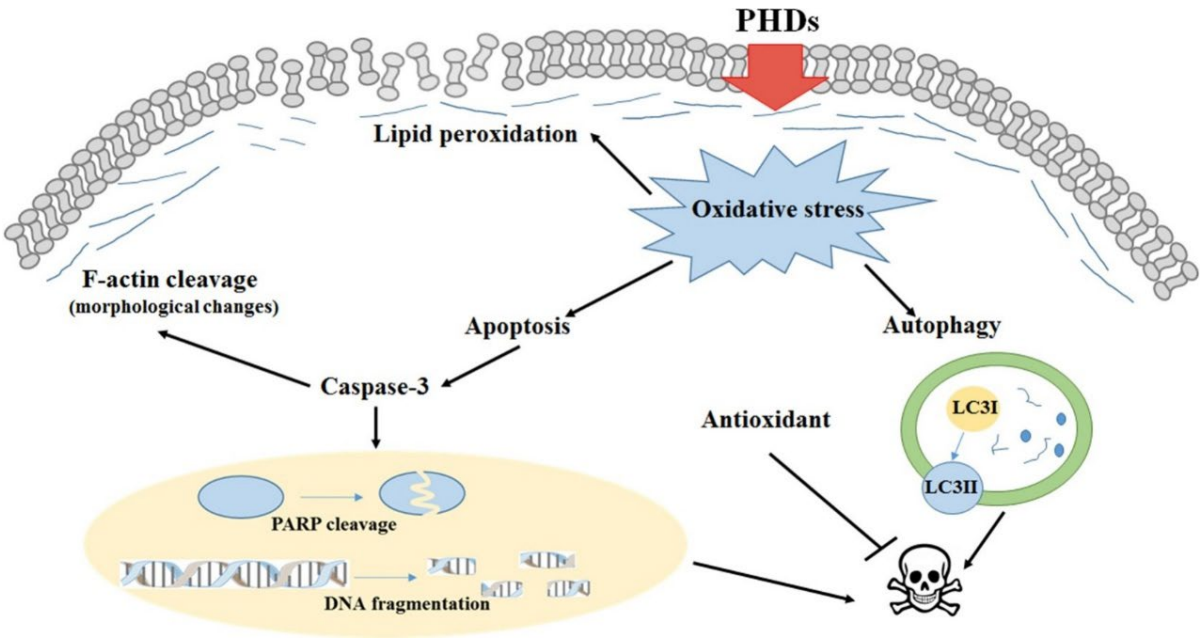

Figure 2.8: Programmed cell death as a result of lipid peroxidation product accumulation Sroda-Pomianek et al., 2018).

2.6 APOPTOSIS

At some point in a cell's lifetime, it has to demise. Two distinct mechanisms exist for such an end; necrosis and apoptosis (D'Arcy, 2019). However, several other pathways of cell death including autophagy have been described in recent years (D'Arcy, 2019). Necrosis is an energy dependant form of unregulated or uncontrolled cell death normally induced by external injuries such as physical or chemical insults. Cells undergoing necrosis swell, lose membrane integrity and spill out their cytosolic content into the extracellular space. This tends to result in an inflammatory response, which more than often poses a threat to the health of surrounding cells (D'Arcy, 2019). On the other hand, apoptosis is a more organised form of cell death that involves controlled lysing of proteins and the formation of apoptotic bodies that soon are phagocytosed by macrophages. Apoptosis forms part of the homeostatic mechanisms regulating tissue cell population that underly normal development and aging (Elmore, 2007). It also takes place during immune reactions or in cells sub-lethally damaged by pathogens or noxious stimuli. It is often difficult to distinguish necrosis from apoptosis. One of the distinguishing properties between apoptosis and necrosis of note is that apoptosis normally does not result in an inflammatory response. Interestingly, there exists a form of apoptosis that does result in inflammation termed pyroptosis (D'Arcy, 2019). Aberrations in the extent of apoptosis in tissue has been implicated in several diseases including neurodegenerative disorders, autoimmune disease, ischaemic damage and cancer (Elmore, 2007). Apoptosis

follows two complex mechanisms of activation, which too are energy dependant; the intrinsic (mitochondrial) pathway and the extrinsic (death receptor) pathway (Elmore, 2007).

2.6.1 Intrinsic pathway

The intrinsic pathway is a mitochondrial-initiated event that involves non-receptor-mediated intracellular signalling in the induction of apoptosis (Salens *et al.,* 2004; Wang and Younse, 2009). Two forms of intracellular signalling leading to apoptosis via the intrinsic pathway are described. The first involves the loss of suppression of apoptosis through the failure of the suppression of death programs; this normally occurs as a result of decreased levels of a number of growth factors, cytokines and hormones (Elmore, 2007). The second significant pathway is under the regulation of the B-cell lymphoma 2 (Bcl2) proapoptotic (Bax, Bak and Bok) and anti-apoptotic (Bcl_{XL}, Bcl-W and MCL-1) family of proteins (Salens et al., 2004; Wang and Younse, 2009). The latter may be activated following insults from stimuli including radiation, DNA damage, pathogenic infection, toxins or hypoxia. Proapoptotic and antiapoptotic proteins tightly regulate mitochondrial outer membrane permeabilisation (MOMP), a process involving the opening of the mitochondrial transition pores leading to the release of cytochrome c from the mitochondria into the cytoplasm (Riley et al., 2019; Suh et al., 2013). Following insults by the above-mentioned stimuli, the Bcl2 family members Bax and Bal are activated, oligomerised on the mitochondrial outer membrane and its permeabilization ensues (Figure 2.9) (Riley et al., 2019). The MOMP marks an important part of the intrinsic apoptotic pathway as cells rarely survive after this process begins, it is therefore considered 'the point of no return (Riley et al., 2019). Both Bax and Bak are crucial components of the intrinsic pathway; their central role was alluded to by Wei and associates when they demonstrated that $Bax^{-/-}$ $Bak^{-/-}$ double knock out cells significantly resisted apoptosis in response to a variety of apoptotic stimuli (Wang and Youle, 2009). In addition, Bcl2, Bcl_{XL} and MCL-1 inhibit the activity of Bax and Bak and therefore an imbalance between the two may influence the release of cytochrome *c* and therefore apoptosis (Wang and Youle, 2009).

Cytochrome *c* is a water soluble protein that plays a central role in ATP generation within the mitochondria (Brentnall et al*.,* 2013; Elmore, 2007). Upon its release into the cytoplasm following MOMP, cytochrome *c* facilitates caspase-3 activation through the assembly of the apoptosome (Figure 2.9). The apoptosome is a large complex formed by caspase-9 and Apoptotic protease activating factor 1 (Apaf-1) in the presence of cytochrome *c*, and is known

as the platform of activation of caspase-9 (Brentnall et al., 2013; Elmore, 2007). Active caspase-9 is an initiator caspase in the intrinsic apoptotic pathway which directly activates caspases -7 and -3. Activated caspase-7 is a prerequisite for apoptotic cell detachment. Caspase-3 forms part of the caspases known to play a role in the final pathway of apoptosis termed the execution pathway (Brentnall et al., 2013; Elmore, 2007).

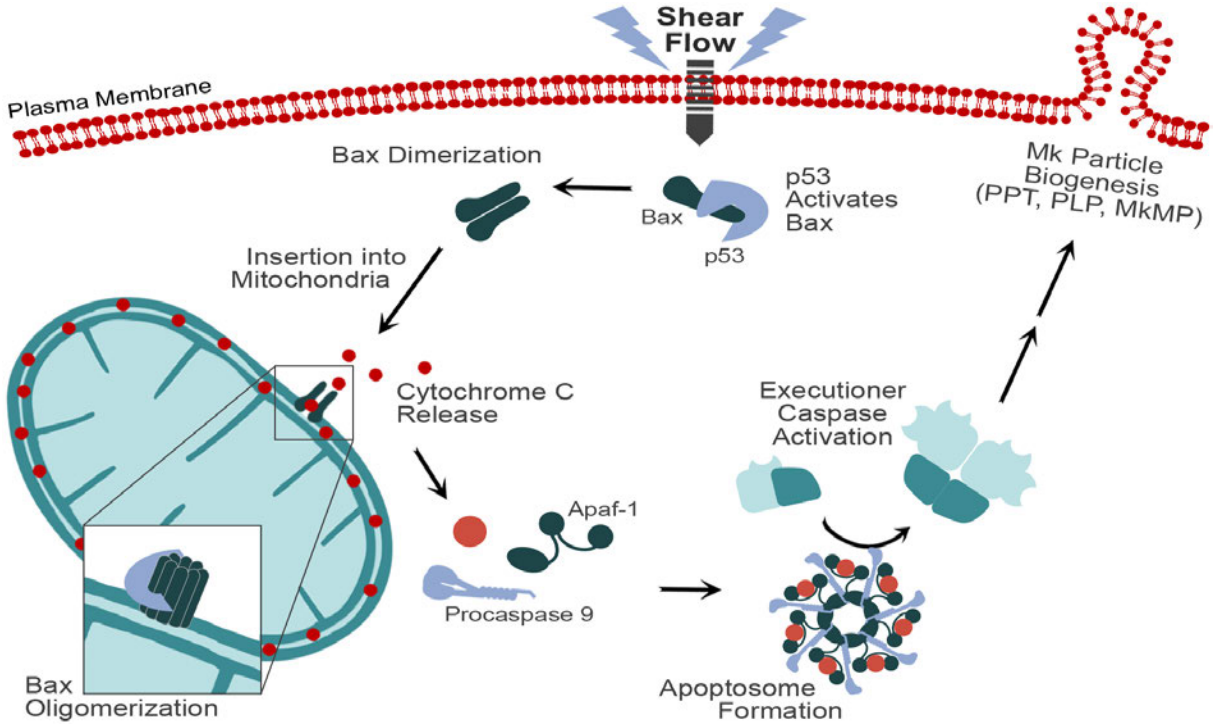

Figure 2.9: Apoptosome formation from the union of Apaf-1, procaspase-9 and cytochrome c (Luff et al., 2018).

2.6.2 Extrinsic pathway

The extrinsic apoptotic pathway involves transmembrane receptor-mediated signalling in the initiation of apoptosis. Upon stimulation by their respective ligands, the transmembrane receptors termed the tumour necrosis factor (TNF) receptor family transmit their death signals intracellularly through cytoplasmic ‘’death domains’’ (Elmore, 2007). The death ligands are a group of cytokines secreted by active lymphocytes. A number of death ligands and their corresponding transmembrane receptors have been described to date, including; TNF-α/TNFR, FASL/FASR and APO3L/DR3 (Elmore, 2007). The TNF-α/TNFR and FAS/FASL are one of the more well-known models in which the sequence of events that define the extrinsic phase of the pathway have been best characterised. The TNF family of receptors death domain is an ~80

amino acid long highly conserved region. It was shown that key residue mutations within the region inhibited ligand induced cytotoxicity (Hughes et al., 2009).

The FAS/FASL engagement results in aggregation of the receptor and recruitment of the adaptor protein Fas associated protein with death domain (FADD) to the intracellular domain of FAS (Figure 2.10). This process occurs through death domain to death domain homophilic interactions (Hughes, *et al.,* 2009). The TNF-α/TNFR interaction results in the recruitment of Tumour necrosis factor –receptor 1 associated protein with death domain (TRADD) together with FADD and RIP (Elmore, 2007). This occurs before the final step of the death-inducing signalling complex (DISC) formation which is completed by the recruitment of the initiator caspase, procaspase-8 through its interaction with FADD (Figure 2.10) (Hughes, *et al.,* 2009). This process can be inhibited by a protein called c-FLIP which is binds caspase-8 and FADD, causing them to be ineffective. However in the absence of c-FLIP, through auto catalysis in the DISC, procaspase-8 is cleaved into its active form caspase-8 which marks the beginning of the execution phase (Elmore, 2007).

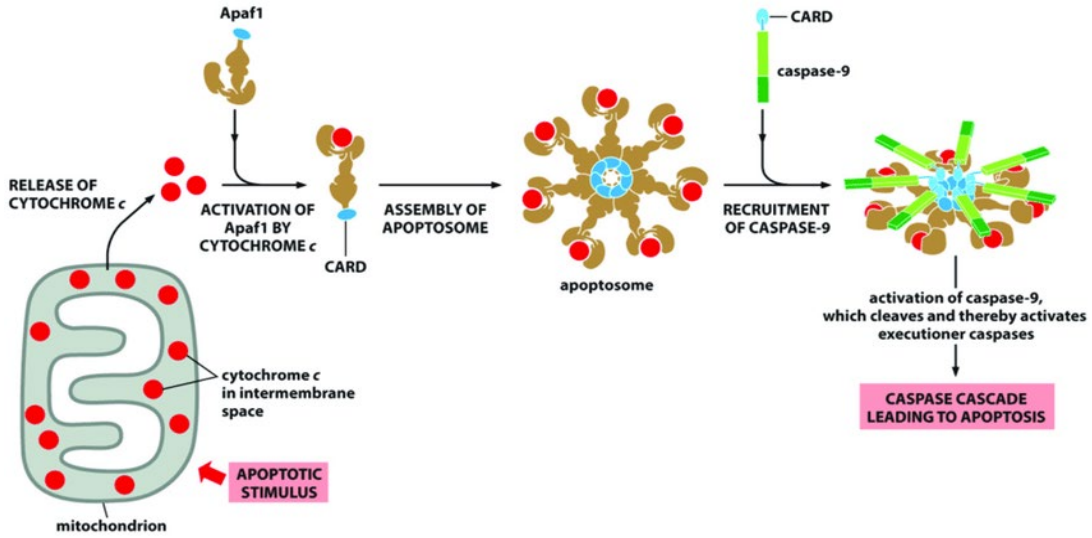

Figure 2.10: The extrinsic pathway of apoptosis. Formation of the apoptosome and recruitment of caspase 9 leading to activation of executor caspases (Gharibi, 2019).

2.6.3 Execution phase

The execution phase of apoptosis is the end point at which the intrinsic and extrinsic pathways independently intersect. Caspases-3, -6, and -7 are considered as the effector caspases responsible for the morphological and biochemical changes seen in apoptotic cells; the most significant of these caspases is caspase-3/7 (Elmore, 2007). Notable cellular changes in the

terminal phase of apoptosis include; nuclear material degradation, cytoskeletal degradation, protein degradation, protein crosslinking and ultimately phagocytic recognition (Figure 2.11). The caspase-activated DNase (CAD) is an endonuclease responsible for the degradation of DNA and condensation of chromatin within the nuclei, but under normal physiological conditions is bound to its inhibitor the Inhibitors of caspase DNase (ICAD). Activated caspase-3 cleaves ICAD causing the dissociation and thus activation of CAD. Caspase-3 is also responsible for the reorganisation of the cytoskeleton and the disintegration of the cell into apoptotic bodies which are then recognised and phagocytosed by macrophages (Figure 2.11) (Elmore, 2007). The phagocytic recognition of apoptotic bodies is another function regulated by caspase-3. Recognition of apoptotic bodies as targets for phagocytosis is the last step in apoptosis and requires externalisation of phosphatidylserine (Figure 2.11) and cellular fragments on the surface of apoptotic cells. Evidence suggests that this process is under the regulation of caspases -3 and -8 (Elmore, 2009). Externalisation of phosphatidylserine is what gives apoptosis its non-inflammatory property as it facilitates early recognition, uptake and disposal (Elmore, 2007).

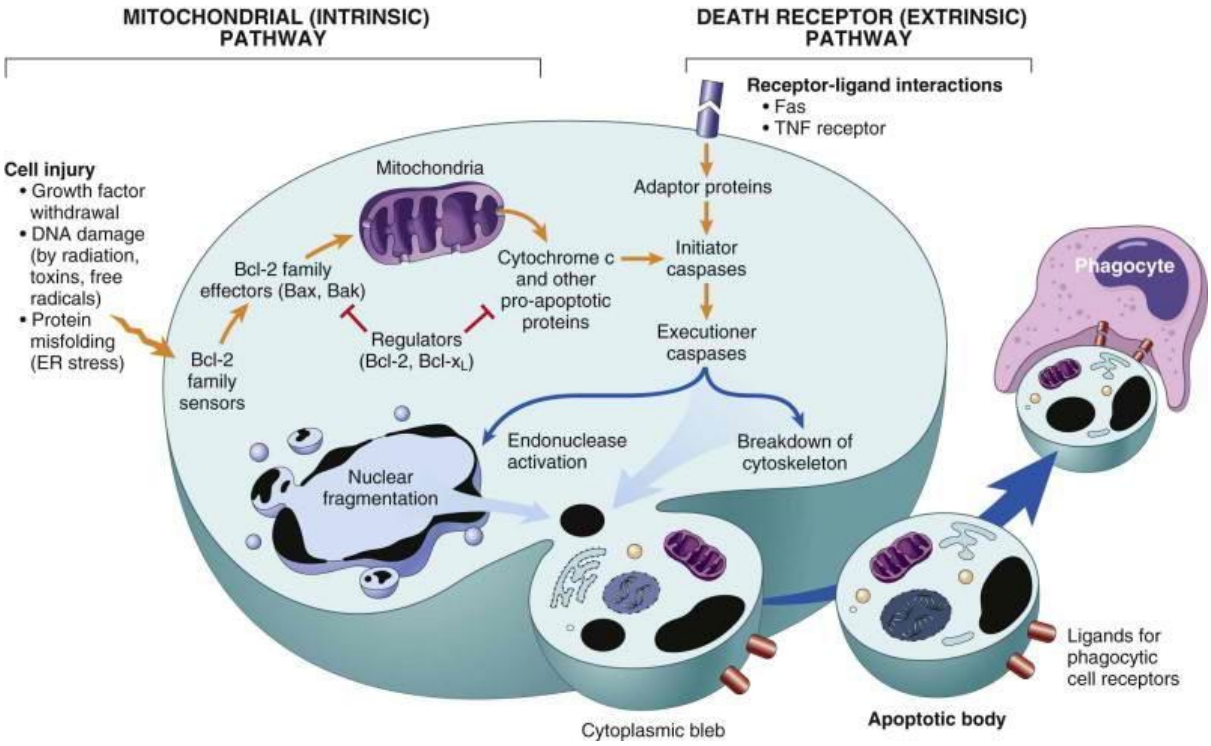

Figure 2.11: Execution phase of apoptosis, depicting nuclear fragmentation, the breakdown of the cytoskeleton, the formation of apoptotic bodies and their phagocytosis by phagocytic cells, mostly macrophages (Saunders, 2010).

2.7 INTERSECTION BETWEEN OXIDATIVE STRESS, APOPTOSIS AND CANCER

Literature provides evidence that ROS are the inciting agents in several cancer cases (Mates et al., 2012; Guo et al., 2018; Hayes et al., 2020). This notion is supported by the observation that pharmacological suppression of ROS with apocynin inhibited the development of lung adenocarcinoma in oncogenic K-RAS^{G12D}-driven mouse model (Hayes et al., 2020). Their ability to induce DNA changes in the form of deletions, rearrangements, mutations and gene amplification put them at the forefront as the insult leading to tumorigenesis (Mates et al., 2012). Due to their high metabolic activity and poor oxygenation, cancer cells are prone to the production of ROS in higher amounts as compared to normal cells especially during periods of hyperproliferation (Arfin et al., 2021; Hayes et al., 2020). As aforementioned, increased levels of ROS augments their secondary messenger functions, gene expression regulation and deleterious effects on the cell. ROS, therefore, play an important role in the presentation of the hallmarks seen in cancer, which is a paradoxical feat (Arfin et al., 2021). The proposed mechanism for this is interprotein and interprotein bridge formation that is a result of cysteine and/or tyrosine residue redox-reactions that change protein function and generate an array of cellular responses (Perillo et al., 2020).

Normally, cells with such DNA damage are destined for death through apoptosis. Cancerous cells evade apoptosis mediated by ROS by regulating them to tolerable and functional levels through the Warburg effect. This is a process that results from the alteration of the last steps of glycolysis where lactate is preferentially produced irrespective of the concentrations of oxygen and the availability of functional mitochondria. The subsequent result of this is increased levels of NADPH, the cofactor essential in GSH production, therefore avoiding ROS levels that would trigger senescence or apoptosis (Liberti and Locasale, 2016; Arfin et al., 2021). As mentioned before Nrf2 is inactive when bound to Keap1. However, when Keap1 is oxidised, Nrf2 translocates to the nucleus where it promotes the expression of glutamate-cysteine ligase thus increasing intracellular GSH concentrations conferring the same effect as mentioned above (Perillo et al., 2020). Nrf2 normally plays the role of a tumor suppressor. Instead under conditions where it is hyperactivated, it creates a microenvironment that favours proliferation and survival against oxidative stress. One way which it achieves this is through its propensity to transcriptionally upregulate the heat shock factor 1 (HSF) promoter under oxidative stress (Soumyadip et al., 2018). HSF 1 in concert with Nrf2 are in turn responsible for the production of heat shock proteins (HSPs) which are a family of molecular chaperones that play an integral

part in proteostasis (Soumyadip et al., 2018). HSPs have been shown to interfere with the activation of caspases necessary for apoptosis (Soumyadip et al., 2018).

Cancer cells also tightly regulate their redox status through the transcription factor p53, which has a controversial role as it may promote the expression of both antioxidant and oxidant genes. Exceedingly high levels of ROS may promote p53 expression, while moderate amounts inhibit it (Perillo et al., 2020). Active p53 has multiple roles including directing cells to either senescence, cell cycle arrest or apoptosis (Figure 2.11). When p53 is over-expressed, it activates pro-oxidant genes including Bax, Puma and Pox. These genes code for proteins that are capable of inducing the uncoupling of mitochondria, thus leading to apoptosis (Lu et al., 2008).

The nuclear factor kappa B (NF-κB) pathway is more than often found altered in cancerous cells in a fashion that promotes survival and proliferation (Morgan and Liu, 2010). Interestingly, NF-κB also shares a bidirectional relation with ROS; NF-κB may promote the transcription of pro- and anti-oxidant enzymes, while ROS stimulate cytoplasmic NF-κB activity but inhibits it in the nucleus (Morgan and Liu, 2010). Interestingly Nrf2 promotes the NFkB translocation to the nucleus activating survival genes through suppressing both apoptosis and necrosis (Rubio et al., 2018). The inhibition of the NF-κB pathway was found by Xia and group (2018) to reduce proliferation, and angiogenesis in addition to inducing apoptosis in human fibroblast-like synovial cells (Xia et al., 2018). Further research has shown that NF-κB may also be activated by mitogen-activated protein kinases (MAPKs) (Xia et al., 2018). The MAPKs play a major role in transduction of growth factor related signals from the cell surface to the nucleus. MAPKs regulate a variety of cellular events including cell survival and cell death (Xia et al., 2018). A number of intracellular and extracellular stimuli have been shown to activate MAPK pathways including ROS (Son et al., 2011). The mechanisms through which ROS activate MAPKs are illusive however, it was shown that with the prevention of ROS accumulation with antioxidants, MAPK activation was lowered (Son et al., 2011).

2.8 CONCLUSION

Lung cancer, its epidemiology, aetiology, treatment and its inner workings have been coverd. Along side profiling *A. afra* from a botanics, phytochemical and medicinal perspective. It is

clear that oxidative stress, apoptosis and cancer are complexly correlated in a tightly regulated fashion. Thus, an agent such as *A. afra* that can selectively disrupt this correlation to reduce growth, proliferation and induce death warrants further investigation as is in the current study.

CHAPTER 3 : METHODOLOGY

3.1 MATERIALS

The A549 cells were purchased from Cellonex (Separations, Johannesburg, South Africa (SA). All cell culture media including foetal bovine serum (FBS) were procured from Thermo Fisher Scientific (Waltham, Massachusetts, United States (USA)), and plasticware was acquired from Lasec (Johannesburg, SA). The Promega (Madison, Wisconsin, USA) luminometry reagents and Cell Signalling Technology (CST, Danvers, Massachusetts, USA) antibodies were obtained from Anatech (Johannesburg, SA). The phosphate buffer saline (PBS) tablets, methylthiazol tetrazolium (MTT) salt, bicinchoninic acid (BCA) assay kit, β-actin and acrylamide were purchased from Merck (Johannesburg, SA). The Bio-Rad (Hercules, California, USA) western blot reagents were procured from Lasec (Johannesburg, SA). Unless stated otherwise, all other reagents were acquired from Merck (Johannesburg, SA).

3.2 CELL CULTURE

The A549 cells were grown in 25 cm^2 culture flasks in complete culture medium (CCM) consisting of Dulbecco's minimum essential medium supplemented with 1% penicillin-streptomycin, 1% L-glutamine and 10% FBS. The cells were incubated at 37°C with 5% carbon dioxide overnight supply. Cell growth was consistently monitored and the medium replaced every two days or when deemed necessary. When cells were approximately 80% confluent, the spent CCM was decanted and cells were washed three times with PBS before adding 1 ml of trypsin to dislodge the cells. The cells were consistently monitored during the trypsinisation process, and trypsin was discarded when the cells were rounded. The flask was agitated to bring the cells into suspension, and 10ml of fresh CCM was added to the flask. Cell numbers were determined using the trypan blue exclusion method, and adjusted for the various assays.

3.3 *A. AFRA* CRUDE EXTRACT PREPARATION

The *A. afra* leaves were obtained from the Durban Market (Kwa-Zulu Natal, SA) and verified by the University of Kwa-Zulu Natal herbarium. A stock solution (5mg/ml) of *A. afra* was prepared by dissolving 20mg of dried and blended leaves into 4 ml of CCM. The stock solution was filtered through a 0.45µM filter (Millipore), and diluted with CCM to obtain the required treatment concentrations.

3.4 3-(4, 5-DIMETHYLTHIAZOL-2-YL)-2, 5-DIPHENYLTETRAZOLIUM BROMIDE (MTT) ASSAY TO ASSESS CELL VIABILITY

3.4.1 Principle

The MTT assay is used in the determination of cellular metabolic activity, viability and proliferation. It is based on the reduction of the yellow water-soluble MTT salt into purple-blue formazan product in the mitochondria as a marker of these characteristics. The reduction is catalysed by NAD(P)H-dependant mitochondrial enzymes (Figure 3.1) (Ghasemi *et al.,* 2021). A spectrophotometer is used to quantify the formazan at 570nm, which is directly proportional to the number of viable and proliferating cells. The MTT assay is used in the determination of the minimum concentration of a treatment required to reduce a population of cells by 50% (Ghasemi *et al.,* 2021).

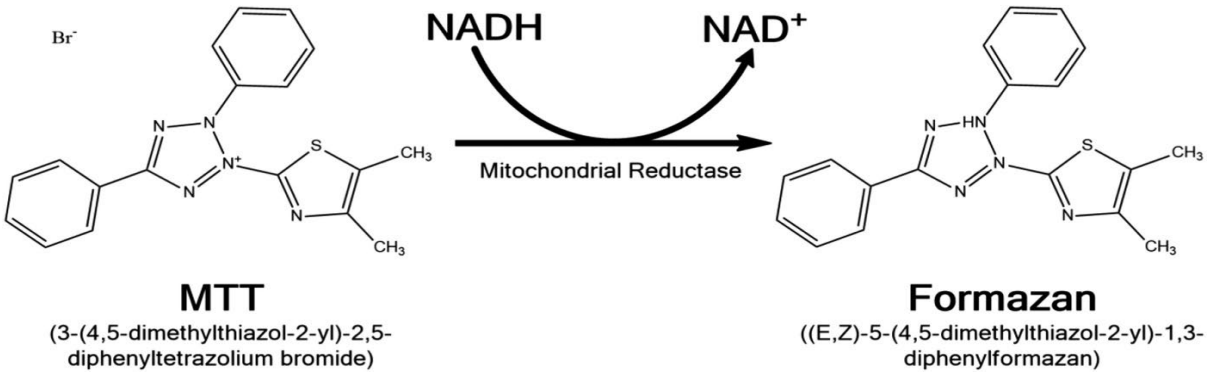

Figure 3.1: Conversion of MTT into formazan by mitochondrial reductase (Kamiloglu *et al.*, 2020).

3.4.2 Protocol

The MTT assay was utilised to determine cytotoxicity and cell viability to obtain the half-maximal inhibitory concentration (IC_{50}) of the extract in A549 cells. A 25 cm^2 flask of A549 cells was trypsinised, the cell suspension was counted and the cells were seeded into a 96 well microtiter plate (20 000 cells/well in 150 µl CCM) in triplicate and allowed to adhere overnight (37°C, 5% CO_2). The cells were then treated with varying concentrations of the extract ranging from 0 – 5 000 µg/ml for 24 hours and 48 hours (37°C, 5% CO_2) respectively. Following incubation, treatment was discarded and replaced with 20 µl of 5 mg/ml MTT salt solution (in 0.1M PBS) and 100µl of CCM per well, then incubated for 4 hours (37°C, 5% CO_2). Afterwards, the MTT solution was discarded and replaced with 100µl of DMSO per well and was incubated for 1 hour (37°C, 5% CO_2) to allow for the solubilisation of the formazan

crystals. Absorbance was then measured utilising the SPECTROstar® Nano microplate reader (BMG LABTECH, Ortenberg, Germany) at 570/690nm. A calculation for cell viability in the treatment group in relation to the untreated group was carried out using absorbance.

$$\text{Cell viability} = \left(\frac{Absorbance\ of\ treated\ cells}{Absorbance\ of\ control\ cells}\right) \times 100$$

GraphPad Prism v5.0 (GraphPad Software Inc. La Jolla, California, USA) was used to construct a concentration-response curve to determine the IC_{50} value. The 48 hour IC_{50} value (260µg/ml) was used in subsequent assays.

3.5 SAMPLE PREPARATION

Two confluent 75cm^2 flasks of A549 cells were selected for treatment, one flask was treated with 260µg/ml *A. Afra* and the other flask served as the control with CCM only. After 48 hours, the treatment medium was removed from the flasks, and retained for the thiobarbituric reactive substances (TBARS) assay, nitrate/nitrite assay and lactate dehydrogenate (LDH) assay. The flask of cells was washed three times with PBS, and the cells were trypsinised and counted for the luminometry assays, as well as western blotting and quantitative polymerase chain reaction (qPCR).

3.6 THE LDH ASSAY TO MEASURE CYTOTOXICITY

3.6.1 Principle

Cytosolic LDH produces NADH and pyruvate during the oxidation of lactate in anaerobic glycolysis (Kumar, Nagarajan and Uchil, 2018). Since LDH is released from damaged cells through the plasma membrane, quantification of extracellular LDH serves as a biomarker of cytotoxicity. The LDH assay comprises of 2 steps; the reduction of NAD^+ to $NADH/H^+$ during the oxidation of lactate to pyruvate by LDH is followed by the transfer of H/H^+ from $NADH/H^+$ to resazurin to yield resorufin in a reaction catalysed by diaphorase (Figure 3.2). The fluorescent product is measured at an excitation of 560nm and emission of 590nm (Kumar, Nagarajan and Uchil, 2018).

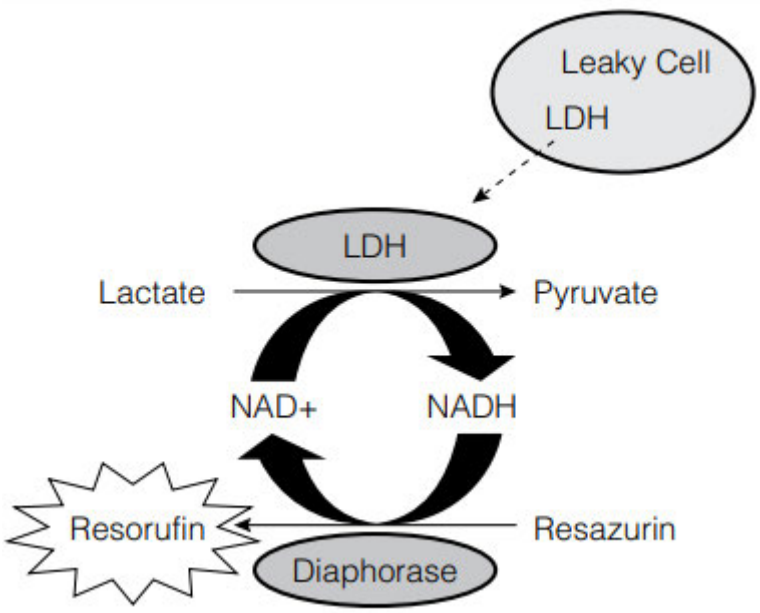

Figure 3.2: Principle of the LDH release assay that produces a red formazan that reflects cellular toxicity Promega (2023).

3.6.2 Protocol

Cell membrane damage was determined by quantifying extracellular LDH utilising the CytoTox-ONE™ membrane integrity assay (Promega, # G7890). The retained treatment CCM (IC_{50} and control) was dispensed into an opaque 96-well microtiter plate in triplicate (50µl per well). The LDH reagent was prepared according to the manufacturer's instruction, then 25µl of the LDH reagent was added into each well and incubated at room temperature (RT) in the dark for 10 minutes. A stop solution was added to each well (12.5µl per well). Thereafter, fluorescence was measured at e ($560nm_{Ex}/590nm_{Em}$) using the Modulus^{TM} microplate luminometer (Winooski, USA). The results obtain are represented as the mean relative fluorescence units (RFU).

3.7 ADENOSINE TRIPHOSPHATE (ATP) ASSAY TO MEASURE MITOCHONDRIAL INTEGRITY

3.7.1 Principle

Cells rely on ATP produced by cells in the mitochondrial electron transport chain (ETC) through oxidative phosphorylation for survival, because it is the main source of energy for cellular activity (Ahmad, 2023). Membrane integrity loss results in the abrupt depletion of ATP from the cell through cellular ATPase consumption. Furthermore, in the presence of mitochondrial dysfunction, the cell effectively loses its ability to produce ATP which may

result in cellular death (Ahmad, 2023). The ATP assay quantifies ATP based on the bioluminescence produced as a result of energy release during the reaction of D-luciferin with luciferase; D-luciferin is a substrate produced in the ATP dependant conversion of inactive luciferin (Riss *et al.,* 2016). In the presence of Mg^{2+}, D-luciferin reacts with luciferase, producing energy which releases a detectable luminescent signal (Figure 3.3). The intensity of the signal is directly proportional to ATP concentrations and therefore cell viability (Riss *et al.,* 2016).

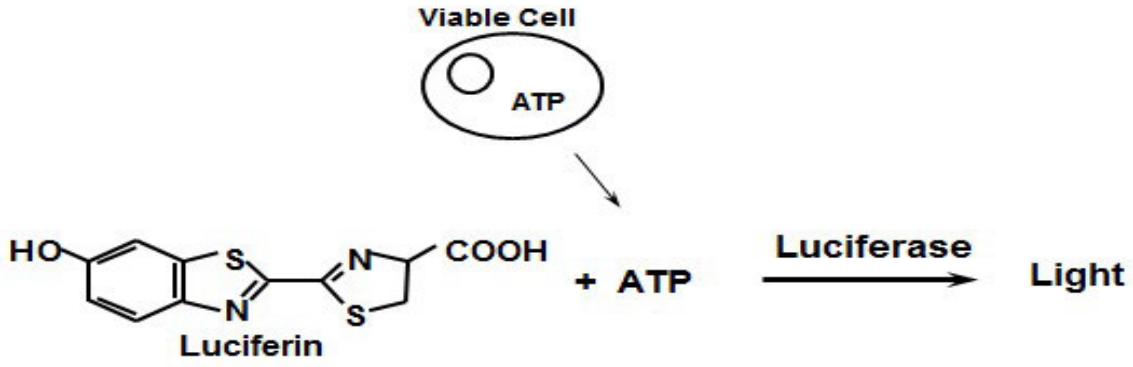

Figure 3.3: Schematic of ATP and luciferin acting as substrates for the reaction of luciferase light generation (Riss *et al*., 2016).

3.7.2 Protocol

The ATP concentration was quantified using the Cell Titer-Glo® assay according to the manufacturer's protocol (Promega, #G7571). After trypsinisation of treated flasks, control and IC_{50} treated A549 cells (20 000 per well in 50µl of 0.1 M PBS) were seeded into an opaque 96-well luminometer plate in triplicate. Thereafter, 25µl of prepared ATP reagent was added to each well and the plate was incubated in the dark for 30 minutes at RT to allow the luciferin-luciferase reaction to proceed. The resultant luminescence was quantified using the Modulus™ microplate luminometer (Winooski, USA) and the results obtained were expressed as relative light units (RLU).

3.8 JC-10 ASSAY TO ASSESS MITOCHONDRIAL MEMBRANE POTENTIAL

3.8.1 Principle

The JC-10 assay is used to for the determination of mitochondrial membrane potential ($\Delta\Psi m$), and is a sensitive indicator of the function of mitochondria and therefore cellular function. JC-10 is a cationic dye that selectively accumulates in the mitochondrial matrix, where it forms red fluorescent aggregates when the mitochondrial membrane is polarised (Figure 3.4). In the

case where cells are apoptotic or necrotic, which would suggest mitochondrial membrane depolarisation and dysfunction, JC-10 diffuses out of the mitochondria and is found as green fluorescent monomers intracellularly (Figure 3.4). Red fluorescent aggregates are therefore formed in healthy cells due to the high mitochondrial membrane potential and green fluorescent aggregates are formed in cells with depolarised mitochondria (Younes *et al.,* 2022). The ratio of red to green fluorescence is used to measure changes in ΔΨm. Changes in the ΔΨm may also suggest an active role for intrinsic apoptosis (Younes *et al.,* 2022).

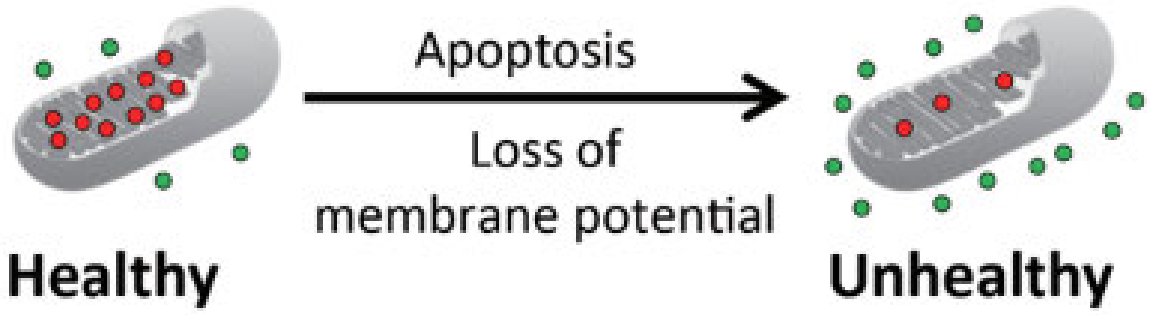

Figure 3.4: Red JC-10 aggregates forming in healthy cells and green aggregates forming in unhealthy depolarised cells (Cmics Bio, 2018).

3.8.2 Protocol

Normal functioning of cellular mitochondria as reflected by the ΔΨM was measured using the JC-10 dye according to the manufacturer's instructions (Merck, #MAK159). After 48 hours of incubation under treatment, 20 000 A549 cells in 50µl of 0.1 M PBS was added to a white microtiter plate in triplicate. After adding 25 µl of JC-10 reagent to each well, the plate was incubated for 30 minutes in the dark at RT. Fluorescence was then measured using the Modulus^{TM} microplate reader (Turner Biosystems, Sunnyvale, USA) at 540nm$_{Ex}$/590nm$_{Em}$ and 490nm$_{Ex}$/525nm$_{Em}$ respectively. The results were obtained as RFU and used to calculate the fluorescence intensity ratio of red JC-10 aggregates and green JC-10 monomers. Data was expressed as this ratio.

3.9 TBARS ASSAY TO MEASURE OXIDATIVE STRESS

3.9.1 Principle

The TBARS assay is a calorimetric assay based on signalling for the presence of products of lipid peroxidation as a marker of ROS levels or oxidative stress. In this assay an endoperoxide resulting from the oxidation of lipid substrates termed malondialdehyde is measured (MDA),

and represents the levels of oxidative stress given that ROS levels are hard to measure directly (De Leon and Borges, 2020). In this assay, MDA reacts with thiobarbituric acid (TBA) to yield MDA-2TBA adducts in the presence of heat and acid (Figure 3.5). The adducts are reddish-pink in colour, thus may be measured using spectrophotometry at 530 - 540 nm (De Leon and Borges, 2020). The intensity of colour produced relates to the extent of lipid peroxidation and thus oxidative stress.

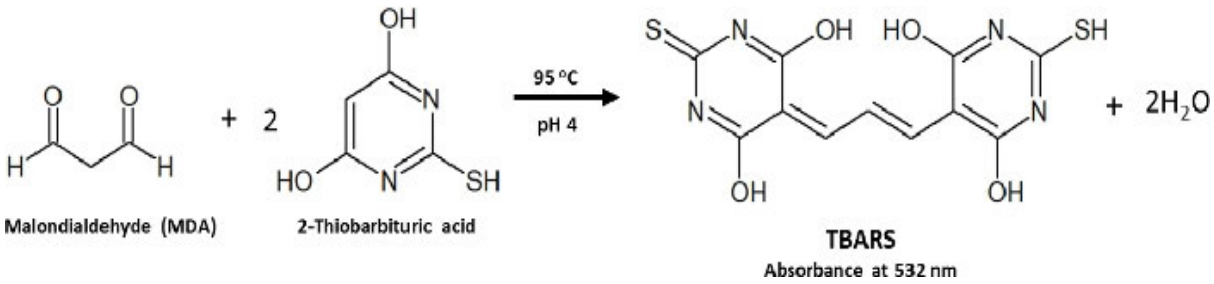

Figure 3.5: Reaction of MDA and TBA under low pH (4) and high temperature (100°C) (De Leon and Borges, 2020).

3. 9.2 Protocol

Oxidative stress was measured indirectly through quantifying lipid peroxidation using the TBARS assay. Four test tubes containing 200µl of treatment medium (control and IC_{50}) and method controls including a positive control (199µl CCM, 1µl MDA) and negative control (200µl CCM). Thereafter, 200µl of 7% phosphoric acid (H_3PO_4) was added into each test tube followed by 200 µl of TBA/BHT to all test tubes excluding the negative control, which was instead supplemented with 200µl of 3Mm hydrochloric acid (HCl). The test tubes were vortexed for 1 minute each and then 200µl of 1 M HCl was added in each. The test tubes were then placed in a 100°C water bath for 15 minutes. After cooling to RT, 1500µl butanol was added to each of the test tubes which were then vortexed for 30 seconds. Samples were allowed to settle for separation of the mixture into two distinct layers. The upper butanol layer was then pipetted into a microcentrifuge tube and 100µl of the sample was pipetted into a 96-well plate in triplicate. The absorbance was measured using a SPECTROstar® Nano microplate reader (BMG LABTECH, Ortenberg Germany) at 532/600 nm, and MDA concentration was calculated using the following equation:

$$[MDA] = \frac{sample\ absorbance}{156\ mM^{-1}} \times 1000$$

Data was presented as MDA concentration in µM.

3.10 NITRATE/NITRITE ASSAY TO MEASURE NITROSATIVE STRESS

3.10.1 Principle

This assay is used to measure the overall presence of reactive nitrogen species (RNS) in a sample. Nitric oxide (NO) is a RNS produced from the enzymatic oxidation of L-arginine by nitric oxide synthases (Antoniou, 2018). However, NO is an unstable free radical with a short half-life. It is rapidly degraded into its more stable metabolite products nitrate (NO_3^-) and nitrite (NO_2^-). Vanadium (III) chloride (VCl_3) is used to catalyse the reduction of NO_3^- to NO_2^- by nitrate reductase (Figure 3.6). This is followed by the Greiss reaction, a two-step reaction where NO_2^- reacts with sulphanilamide yielding a diazonium cation that is coupled with N-(-1-napthyl)ethylenediamine (NEDD) to form a purple azo-derivative which has a strong absorbance at 540-690nm (Figure 3.6) (Antoniou, 2018) .

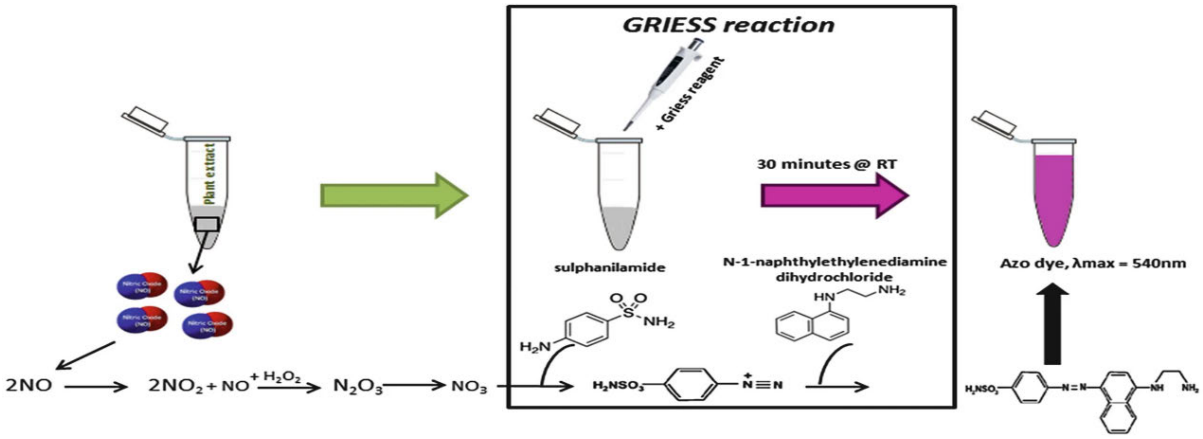

Figure 3.6: Schematic reaction from NOS to representation as azo dye through the Griess reaction (Antoniou, 2018).

3.10.2 Protocol

The concentrations of NO were indirectly measured using the nitrite reduction assay. Standard sodium nitrate solutions (0-200µM) were prepared and 50µl was added into a 96-well microtiter plate in triplicate. In addition, 50µl of each sample (treated CMM from control and IC_{50}) was added into each well. Subsequently, 25 µl of VCl_3, 25µl of sulphanilimide and 50µl of NEDD were added into each well in quick succession and the plate was incubated at 37°C in the dark for 45 minutes. The absorbance was measured at 540/600 nm using the SPECTROstar® Nano microplate reader (BMG LABTECH, Ortenberg Germany). Results were expressed as nitrate concentration in µM from the standard curve prepared.

3.11 GLUTATHIONE ASSAY TO MEASURE RESPONSE TO OXIDATIVE STRESS

3.11.1 Principle

The glutathione system comprises of glutathione reductase, glutathione oxidase and glutathione. This system maintains the concentration of ROS at physiological levels. Therefore, the levels of reduced glutathione (GSH) provide an indication of oxidative stress (Nuhu *et al.*, 2020). The GSH-Glo™ assay (Figure 3.7) is luminescence based assay for quantification of sample GSH levels. It is based on the conversion of a luciferin derivative into luciferin in a reaction catalysed by glutathione-S-transferase in the presence of GSH. A reagent that detects luciferin is coupled to the reaction with luciferase and ATP. This produces a luminescent signal that is directly proportional to the levels of GSH (Yasgar *et al.,* 2010).

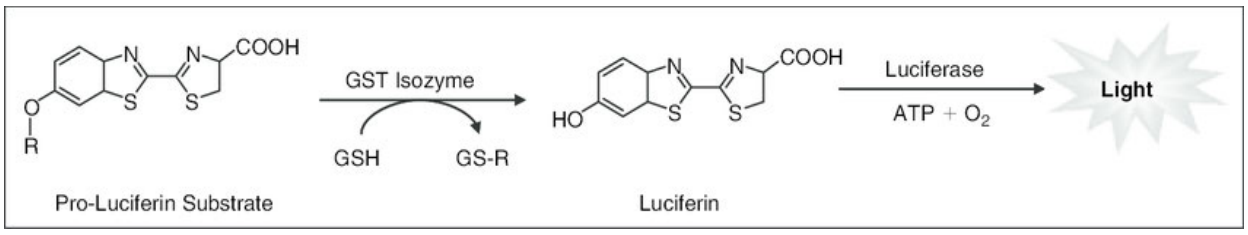

Figure 3.7: Schematic representation of GSH assay reaction (Yasgar *et al.*, 2010).

3.11.2 Protocol

The GSH assay was carried out according to the manufacturer's instructions. After treating A549 cells with *A. afra* for 48 hours, 20 000 control and IC_{50}-treated cells per well (in 50µl of 0.1 M PBS) were seeded into a 96-well luminometer plate in triplicate. Thereafter, 25µl of prepared 2X GSH-Glo reagent was added in each well and mixed on the plate shaker. The plate was incubated at RT in the dark. After 30 minutes incubation, 12.5µl of luciferin detection reagent was added and the plate was incubated a further15 minutes before reading the luminescence on the Modulus™ microplate luminometer (Turner Bio-systems, Sunnyvale, California, USA). The results obtained were expressed as RLU.

3.12 CASPASE ACTIVATION FOR INTRINSIC AND EXTRINSIC APOPTOSIS

3.12.1 Principle

Caspase 3/7, -8 and -9 activity was assessed using Promega caspase-Glo assays for the respective caspases. Caspases are a family of endoproteases that are responsible for maintaining cellular homeostasis by regulating apoptosis and inflammation (Mcllwain, Berger,

and Mak, 2013). During apoptosis, activation of caspases results in the activation or inactivation of substrates that subsequently lead to the ordered disassembly of cell (Mcllwain, Berger, and Mak, 2013). The caspase activity assay (Figure 3.8) consists of a cell lysis and aminoluciferin-DEVD substrate. Substrate lysis exposes the aminoluciferin-DEVD to active caspases which in turn cleave it to release aminoluciferin (Promega Corporation, 2010). The aminoluciferin then reacts with luciferase in the presence of ATP, O_2 and Mg^{2+} and generates light in the process. The light generated is luminometrically quantifiable and is proportional to the activity of caspases in a sample (Promega Corporation, 2010).

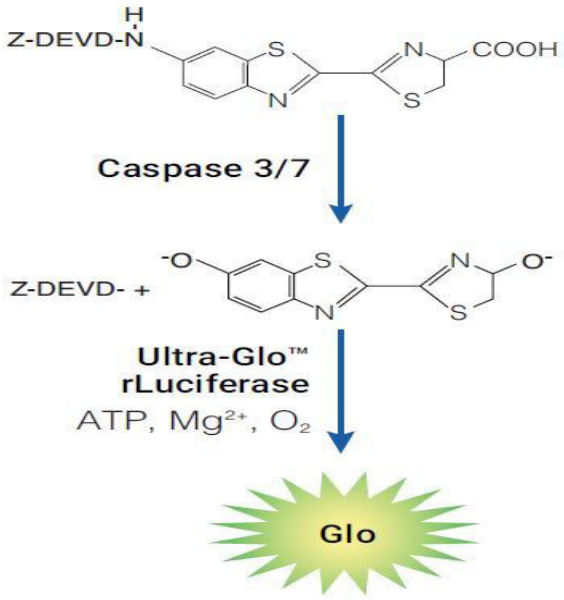

Figure 3.8: Schematic of caspase assay luciferin luciferase reaction (Promega Corporation, 2010).

3.12.2 Protocol

Caspase 3/7, -8 and -9 activity was assessed using the Promega Caspase-Glo® assays. The caspase reagents were prepared according to the manufacturer's instructions, and 25 µl of the respective caspase reagents were added into treatment wells containing 20 000 cells per well in 50µl of 0.1 M PBS in an opaque 96-well luminometer plate. Following the incubation in the dark at RT for 30 minutes, luminescence was measured utilising the Modulus™ microplate luminometer (Winooski, USA). The results were expressed as RLU.

3.13 ANNEXIN V APOPTOSIS AND NECROSIS ASSAY

3.13.1 Principle

The annexin V assay is used to determine the quantity of cells undergoing necrosis vs apoptosis in a cell population. It is based on the principle that cells express phosphatidylserine on the inner surface of the lipid bilayer cell membrane (Lakshmanan and Batra, 2016). During apoptosis, the bilayer inverts and phosphatidylserine becomes exposed on the outer surface of the cell, allowing it to be detected by annexin V; annexin V binds to the charged head groups of phosphatidylserine through a Ca^{2+}-dependant reaction (Figure 3.9). It is differentiated from necrosis due to the leakiness of the cell that is characteristic of this process. In necrosis, the damaged cell membranes allow the dye to enter the cells which have exposed DNA that is detectable with propidium iodide (Figure 3.9) (Lakshmanan and Batra, 2016).

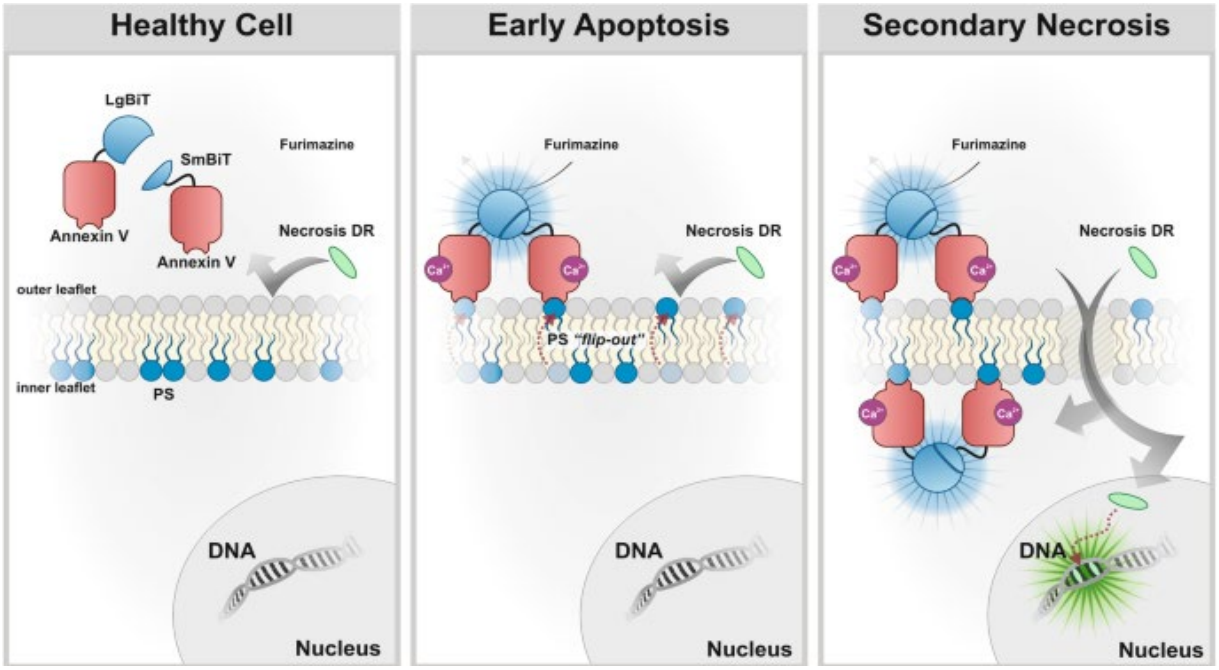

Figure 3.9: Diagrammatic illustration of the principle of annexin V assay differentiating between apoptosis and necrosis (Kupcho *et al*., 2019).

3.13.2 Protocol

Apoptotic vs necrotic activity was assessed using the RealTime-Glo™ Annexin V apoptosis and necrosis Assay (Promega, #JA1011). Treated cells (20 000 cells per well in 50µl of 0.1M PBS) were pipetted into an opaque 96-well luminometer plate in triplicate. The reagent was prepared according to the manufacturer's instructions, then 25µl was added to each well and the plate was incubated at RT in the dark for 30 minutes. Following incubation, the

luminescence and fluorescence (485±20nm excitation and 525±30nm emission) was measured using the Modulus™ microplate luminometer (Turner Bio-systems, Sunnyvale, California, USA) and the results were represented as RLU and RFU respectively.

3.14 WESTERN BLOT

3.14.1 Principle

Western blotting is a technique used to isolate and quantify specific proteins in samples within a complex mixture of proteins (Mahmood and Yang, 2012). The steps (Figure 3.10) involved in the accomplishment of this technique are; 1) separation of proteins by molecular mass and shape through a polyacrylamide gel using an electric current, 2) transfer of the separated proteins onto a high-affinity solid support and, 3) membranes are blocked to reduce non-specific binding and precise marking the target protein with specified primary antibodies; 4) secondary antibodies which can be visualised using chemiluminescence due to their linkage to a label; 5) the band density is measured and normalised against a housekeeping protein applying densitometry software (Mahmood and Yang, 2012).

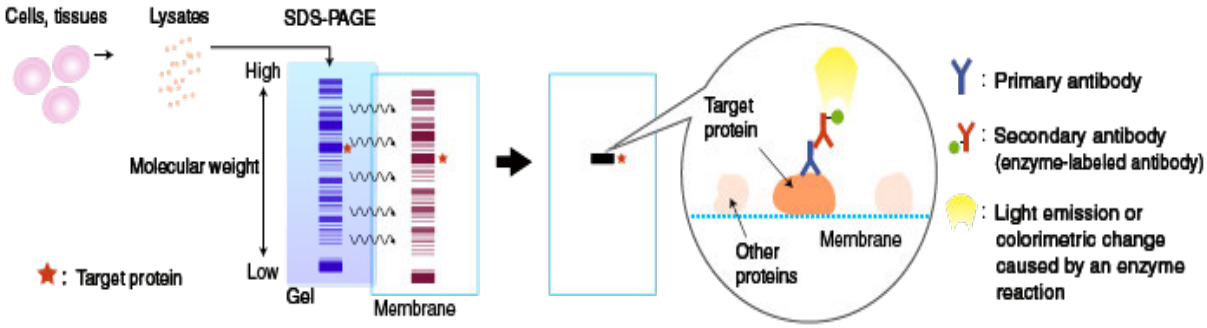

Figure 3.10: Schematic of principles of the western blotting technique (JSR Life Sciences Company 2016).

3.14.2 Protocol

Western blotting was utilised to detect and measure the quantity of the expression of proteins in a homogenous sample. An isolation of crude protein was carried out using Cytobuster™ reagent (Novagen, San Diego, CA, USA) supplemented with protease and phosphatase inhibitor (Roche Germay); 400 µl of the cytobuster reagent was added to the treated and untreated flasks, the flasks were placed on ice for 15 minutes and then scraped. The cell lysate was decanted into a microcentrifuge tube and then cooled in ice for another 10 minutes. Following cooling, the tube was then centrifuged for 5 minutes at 10 000 x g at 4°C.

The crude protein containing supernatants were removed and subsequently quantified using the bicinchoninic acid (BCA) assay; 25µl of crude protein and bovine serum albumin (BSA) - standards (0.2, 0.4, 0.6, 0.8 and 1mg/ml) was added in triplicate to a 96-microtitre plate. A 4 µl $CuSO_4$ and 198 µl BCA solution was prepared and 200µl of the solution was decanted into each sample and standard well. The plate was then incubated at 37℃ for 30 minutes and absorbance was measure at 562nm using a SPECTROstar® Nano microplate reader (BMG LABTECH, Otenberg, Germany). Using the acquired mean absorbance of the standards of proteins a standard curve was constructed and the extrapolated equation used to calculate the concentration protein in each sample. The protein samples were standardised to 1mg/ml, and Laemmli buffer [de-ionised water (dH_2O), 0.5M Tris-HCl (pH 6.8), glycerol, 10% sodium dodecyl sulfate (SDS), ß-mercaptoethanol, 1% bromophenol blue] was added to each sample in a 1:4 ratio. The samples were then boiled at 100℃ for 5 minutes and then cooled at RT. Thereafter they were stored at -80℃ until further use.

The SDS-PAGE gels were prepared, and 25µl of the standardised samples were loaded into the wells. The gels were composed of a lower 10% resolving gel layer and a 4% upper stacking gel layer [10% resolving gel; dH_2O, 1.5M Tris-HCl (pH 8.8) 10% (w/v) SDS, 30% Acrylamide/Bis, 10% ammonium persulfate (APS) and tetramethyl ethylenediamine (TEMED) and 4% stacking gel: dH_2O, 1.5M Tris-HCl (pH 8.8) 10% (w/v) SDS, 30% Acrylamide/Bis, 10% APS and TEMED]. The gels were then submerged into a 1x running (electrode) buffer [dH_2O, glycine (pH 8.3, 4℃) and subjected to a 150V electric field using the Bio-Rad compact power supply for an interval of 90 minutes.

Upon completion of the electrophoresis, the gels were placed into a cold transfer buffer [dH_2O. Tris, glycine, methanol (pH 8.3)] for 10 minutes. The Transblot®Turbo Transfer system (Bio-Rad, California, USA) was then used to transfer the proteins onto a nitrocellulose membrane. Thereafter nitrocellulose membranes were blocked for 2 hours at RT with 2% BSA [TTBSA, 150mM NaCl. KCl, 25mM Tris (pH 7.5) containing 0.5% Tween 20]. The membrane was then probed with primary antibodies [SOD2, catalase, Gpx1, HSP27, HSP90, Bax, Bcl2, and xIAP] for 1 hour on the shaker following the removal of the blocking solution. This was done at 1:1000 dilution in 2% BSA/TTBS. Thereafter the membranes were incubated overnight at 4℃ to allow for antibody binding. On the following day, the membranes were equilibrated to RT for 1 hour, following which TTBS was used to wash primary antibodies off 5 times in 10

minute intervals per wash. After being washed, the membranes were incubated with 5 ml secondary antibody conjugated to horse-radish peroxidase (HRP) [anti-rabbit IgG, (SOD2, catalase, Gpx1, Bax, and xIAP) or anti-mouse IgG (Bcl2, HSP27, and HSP90)]. This was done in a 1:2500 dilution in 2% BSA/TTBS for 2 hours on the shaker and thereafter incubated overnight at 4°C. The secondary antibody was then washed off 5 times in 10 minute intervals with TTBS. The Clarity Wester ECL Substrate (Bio-Rad) was used to view images of the membranes and the Chemidoc™ Imaging system and Bio-Rad imaging system (Bio-Rad, California, USA) were used to for capturing. 5% hydrogen peroxide (H_2O_2) was then used to quench the membranes at 37°C for 30 minutes. They were then rinsed with TTBS 3 times in 10 minute intervals and then blocked with 2% BSA in TTBS for 1 hour and then probed with, the normalising protein, beta (ß)-actin (Sigma) for 1 hour. The membranes were washed with TTBS 3 times over 10 minute intervals. Imaging was done with the Chemidoc™ Imaging system and Bio-Rad imaging system (Bio-Rad, California, USA). Analysis was done by measuring the band intensity of each protein and the bands were normalised against ß-actin. Data was presented as relative band density (RBD).

3.15 QUANTITATIVE POLYMERASE CHAIN REACTION (QPCR) ASSAY

3.15.1 Principle

The qPCR assay (Figure 3.11) is a highly sensitive technique that measures specific nucleic acid sequences. It builds on conventional PCR by combining the process of amplification and detection into a single step where DNA amplification is measured in real time, as the reaction proceeds. To achieve this, a variety of fluorescence chemistries are used to correlate PCR product concentrations with fluorescence intensity, thereby allowing for the measurement of the quantity of specific DNA in a sample (Garibyan and Avashia, 2013). The technique requires: 1) The DNA target sequence that will be amplified; 2) forward and reverse primers complementary to the 3' end of the forward and reverse strands of the target sequence; 3) Taq polymerase; 5) deoxy nucleoside triphosphates (dNTPs) as building blocks of the newly synthesised DNA strands; and 6) $MgCl_2$ that serves as a DNA stabiliser and is necessary for Taq polymerase to function optimally (Garibyan and Avashia, 2013). Given that the PCR reaction is used to amplify DNA, RNA-based PCR requires that RNA is isolated and then reverse transcribed into complementary DNA (cDNA). SYBR green is added into the qPCR reaction (Garibyan and Avashia, 2013). The SYBR emits fluorescence as it binds to the amplified DNA as the PCR cycle progresses. A house keeping gene GAPDH is used as a

control to quantify the amplified target gene against. Computer-generated software is then used to calculate relative gene expression in the qPCR reaction (Garibyan and Avashia, 2013).

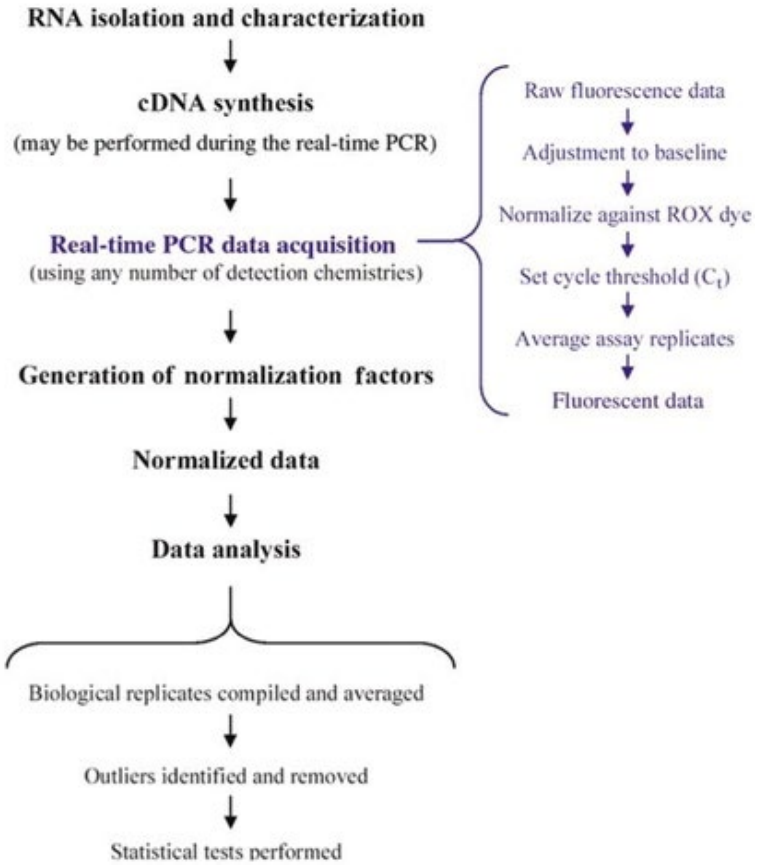

Figure 3.11: Quantitative Polymerase Chain Reaction workflow schematic (Wong and Medrano 2018).

3.15.2 Protocol

RNA was isolated according to the in-house protocol using Trizol. 500 µl of the trizol reagent was added to the treatment and control flasks and incubated for 10 minutes at 4℃ to break down the cells while maintaining the structure of RNA. The cells were then removed from the flasks and transferred to microfuge tubes and stored in trizole at -80℃ overnight. Thereafter 100 µl of chloroform was added to thawed samples and then incubated for 3 minutes at RT. Thereafter, the cell suspensions were centrifuged at 12 000 x g and 4℃ for 15 minutes, following which, the aqueous phase was removed. 250µl of isopropanol was added and the samples were stored at -80 ℃ overnight. The samples were then thawed and centrifuged at 12 000 x g and 4℃ for 15 minutes. The supernatant was discarded and the pallet washed with 75% ethanol and then centrifuged at 7400 x g and 4℃ for 15 minutes. Thereafter the ethanol was removed and the samples were allowed to air dry. The pallets were resuspended in 15µl

nuclease free water and incubated for 3 minutes at RT. The RNA quantity was then measured using the Nanodrop 2000 spectrometer (Thermo-Fisher Scientific) and RNA integrity was measured using the $A_{260/}$ A_{280} ratio. RNA concentration was standardised to 1 000ng/ µl and then used to prepare cDNA. The iScript cDNA synthesis Kit® (Bio-Rad, Hercules, California, USA) was used to synthesise cDNA as per the manufacturers instructions. Gene expression was quantified using the iScript cDNA synthesis Kit® (Bio-Rad, Hercules, California, USA). The method described by Livak and Schmittgen (2001) was used to determine the changes in relative mRNA expression. 2-ΔΔCt represented the fold change in mRNA expression (Garibyan and Avashia, 2013).

Table 3.1: Target genes, sequences and annealing temperatures.

Gene	**Primer**	**Sequence**	Annealing temperature
Nrf2	Forward Reverse	5' -AGTGGATCGTGCCAACTACTC -3' 5'-CATCTACAAACGGAATGTCTG-3'	52.6℃
Catalase	Forward Reverse	5'-TAAGACTGACCAGGGCATC-3' 5'-CAACCTTGGTGAGATCGAA-3'	60℃
GAPDH	Forward Reverse	5'-TCCCTGAGCTCTAGCCTCCAC-3' 5'-GGAGGAGTGGGTGTCGCTGT-3'	61.4℃

3.16 STATISTICAL ANALYSIS

GraphPad Prism V5.0 software (GraphPad Software Inc. La Jolla, California, USA) was utilised to analyse the obtained data. All the assays were performed in triplicate and repeated to verify reproducibility and accuracy. The data was expressed as mean ± standard deviation. One-way analysis of variance (one-way ANOVA) and an unpaired students *t*-test with Welch's correction was utilised to determine statistical differences between treatment and control groups. Only *p* values less than 0.05 were considered significant.

3.17 Ethical consideration

Given that the study was carried out in vitro on prestored immortalised cell lines, ethical clearance was therefore not sought after.

CHAPTER 4 : RESULTS

4.1 CELL VIABILITY AND METABOLIC ACTIVITY

4.1.1 Cell viability

The 48 hour toxicity of the 0 - 5 000µg/ml crude aqueous leaf extract of *A. afra* towards A549 lung cancer cells was measured using the MTT assay. There was an evident decrease in cell viability with increasing concentration of *A. afra* as shown by the dose-response curve (Figure 4.1). Cell viability in control cells was 100%, and was maintained above 80% for the treatments up to 100µg/ml. The 200µg/ml *A. afra* treatment decreased cell viability to 58%, while further increases in concentration yielded cell viabilities below 50%. The lowest cell viability of 4% was evident for the 2000 – 5000µg/ml treatments, and the inhibitory concentration that caused a 50% reduction in A549 cell viablity (IC_{50}) was recorded to be 260µg/ml; the IC_{50} was used for treatment in subsequent assays, with untreated control cells receiving CCM only.

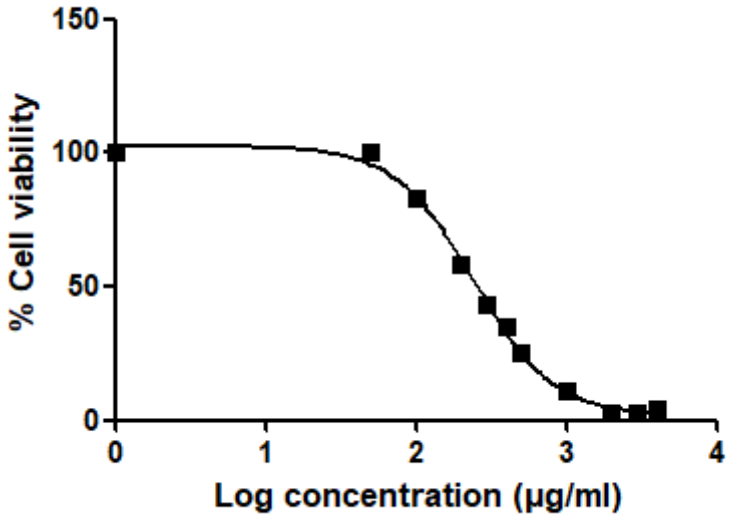

Figure 4.1: Dose-response curve showing a reduction in A549 cell viability following 48 hours of *A. afra* crude extract treatments in concentrations of 0 -5 000 µg/ml. The IC_{50} level for the treatment was determined to be at 260µg/ml.

4.1.2 CYP3A4

The metabolism of *A. afra* by CYP3A4 in A549 cells was increased from 375.007±9.899 RLU in the control to 412.008±15.875 RLU in the IC_{50}-treated cells ($p = 0.0494$).

.

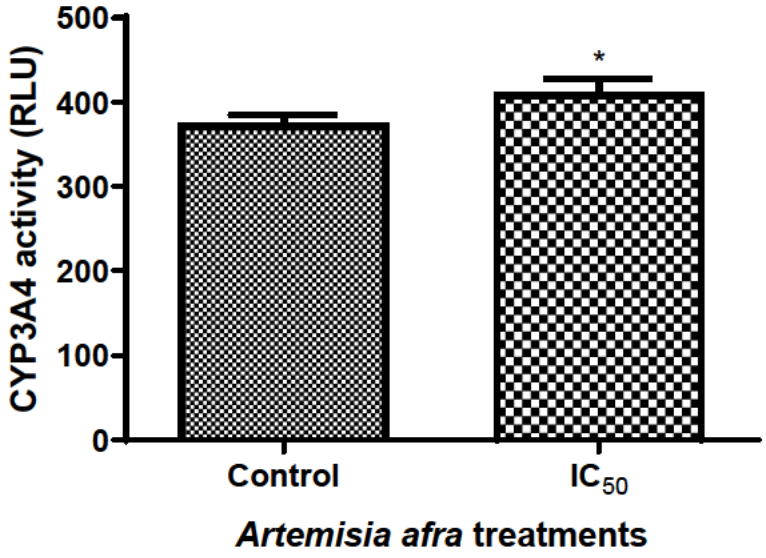

Figure 4.2: *Artemisia afra* increased CYP3A4 activity in A549 lung cancer cells (*$p \leq 0.05$; unpaired students t-test with Welch's correction).

4.1.3 Mitochondrial integrity

The luminometric CellTitre-Glo® was used to quantify ATP concentrations in the treated and untreated A549 cell samples as a measure of mitochondrial integrity. The *A. afra* treatment decreased the concentration of ATP by 41.4% in the IC_{50}-treated A549 cells (11130000±202800 RLU; $p = 0.0033$) relative to the control (19000000±404100 RLU) as shown in Figure 4.3A. Changes in the A549 cellular $\Delta\Psi m$ were detected using the JC-10 dye. The IC_{50} *A. afra* treatment did not affect the $\Delta\Psi m$ (3.779±0.008579) compared to the control (3.804±0.03720) as shown by the red/green fluorescence (Figure 4.3B).

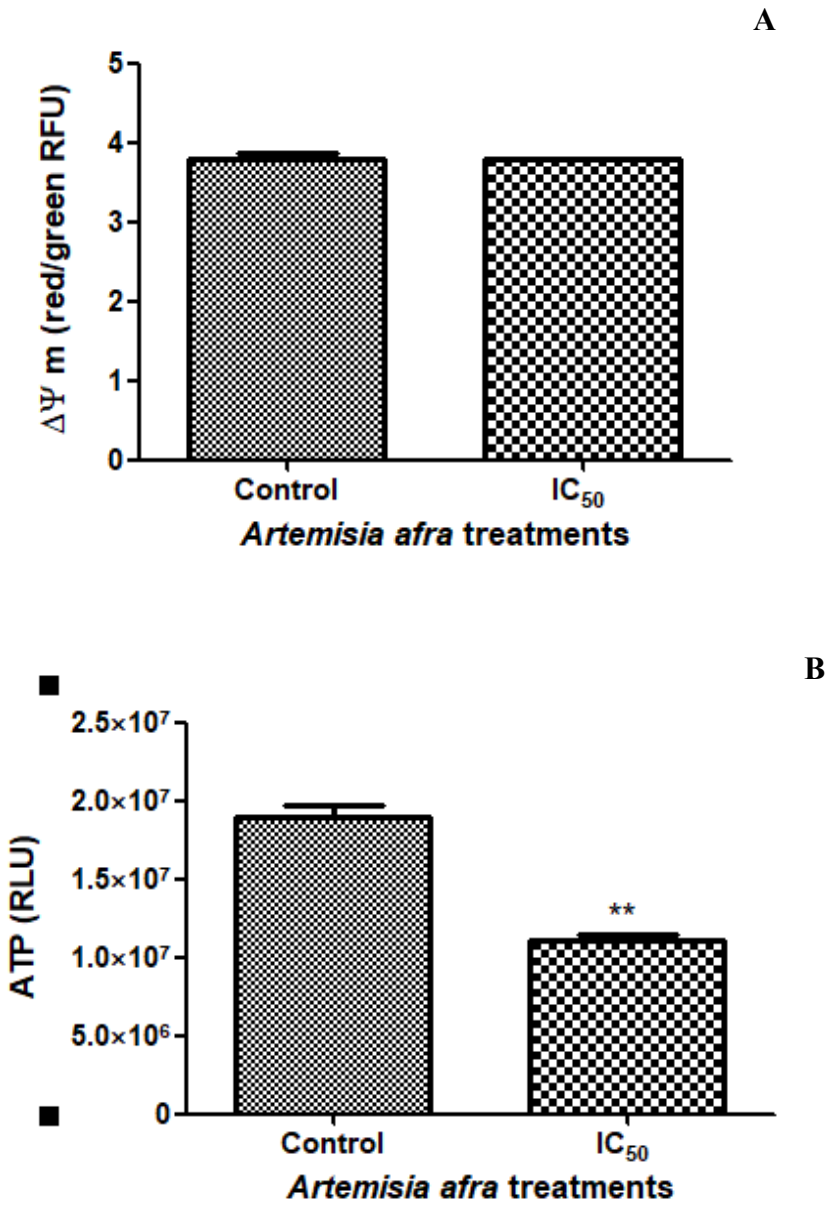

Figure 4.3: Effect of *A. afra* on mitochondrial integrity in treated and control A549 cells. (A) The concentration was significantly reduced in treated cells relative to the control. **(B)** The IC_{50} treatment maintained minimal impact on the ΔΨm of treated A549 cells, yielding a value similar to that of the control. (**$p \leq 0.05$; unpaired students t-test with Welch's correction).

4.2 FREE RADICAL PRODUCTION AND ANTIOXIDANT RESPONSE

4.2.1 Malondialdehyde (MDA) concentration as a measure of ROS

The MDA concentration was measured to quantify products of lipid peroxidation as an indicator of ROS levels using the TBARS assay. The *A. afra* crude extract increased ROS by 67.5% from 0.008333±0.0003701µM in the control to 0.02564±0.001480µM; $p = 0.005$) for the treated group (Figure 4.4).

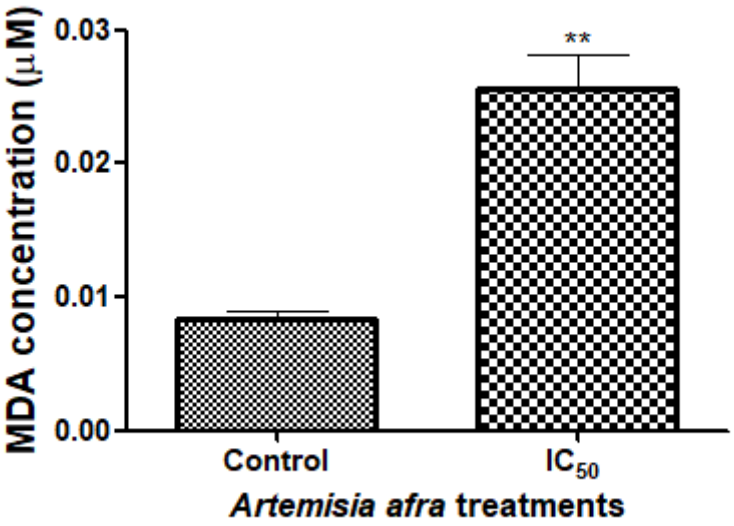

Figure 4.4: MDA concentration in treated A549 cells with a significantly higher value than the control ($p \leq 0.05$; unpaired students *t*-test with Welch's correction).**

4.2.2 Nitrate/nitrites concentration for RNA detection

The RNS levels were quantified using the nitrate/nitrite assay. The IC_{50} *A. afra* treated A549 cells (3.300±0.1528µM; $p = 0.602$) displayed a non-significant change in the levels of nitrite/nitrates as compared to the control (3.400±0.05774µM) as shown in Figure 4.5.

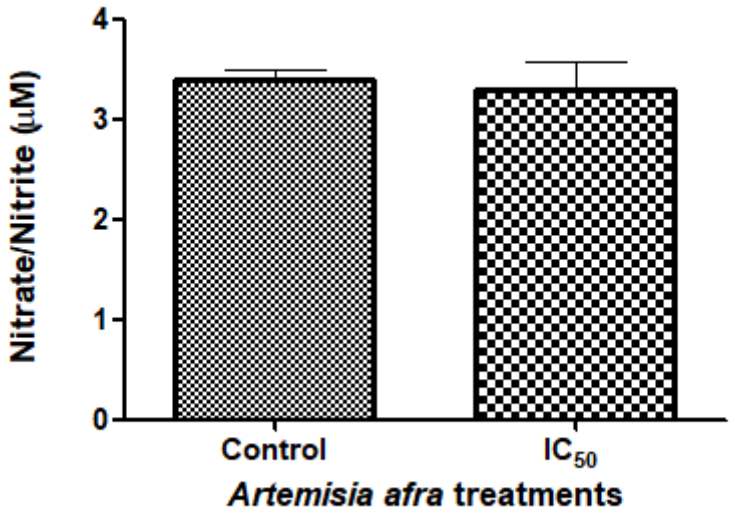

Figure 4.5: No significant difference between the nitrate/nitrite levels of the *A. afra* treated group (3.300±0.1528µM) as compared to the control (3.400±0.05774µM) (p = 0.602, unpaired students *t*-test with Welch's correction).

4.2.3 Antioxidant response

The antioxidant response was determined by western blotting for SOD2, catalase and Gpx1, luminometric quantification of GSH, and gene expression of catalase and Nrf2. The SOD2 protein expression (Figure 4.6A) was slightly increased by the *A. afra* treatment from 2.593±0.03957 RBD in the control to 2.699±0.01453 RBD for the IC_{50}-treated cells (p = 0.2377), while Gpx1 protein expression (Figure 4.6B) increased to 0.8319±0.03049 RBD (p = 0.0015) in the treated cells, compared to the untreated control cells (0.05414±0.001436 RBD). The GSH concentration (Figure 4.6C) was increased by approximately 10% from 943400±28690 RLU in the control to 1038000±35640 RLU (p = 0.1301) in *A. Afra* treated A549 cells. Gene expression of catalase (Figure 4.6D) was increased by 227.3% to 3.273±0.2917 fold change (p = 0.0813), and corresponded with the increase in catalase protein expression from 0.3767±0.003562 RBD in the control to 0.7289±0.01066 RBD in the IC_{50}-treated cells (p = 0.0010) (Figure 4.6E). Furthermore, Nrf2 gene expression (Figure 4.6F) increased to 2.594±0.2469 fold change (p = 0.0232) in accordance with the increased antioxidant expression.

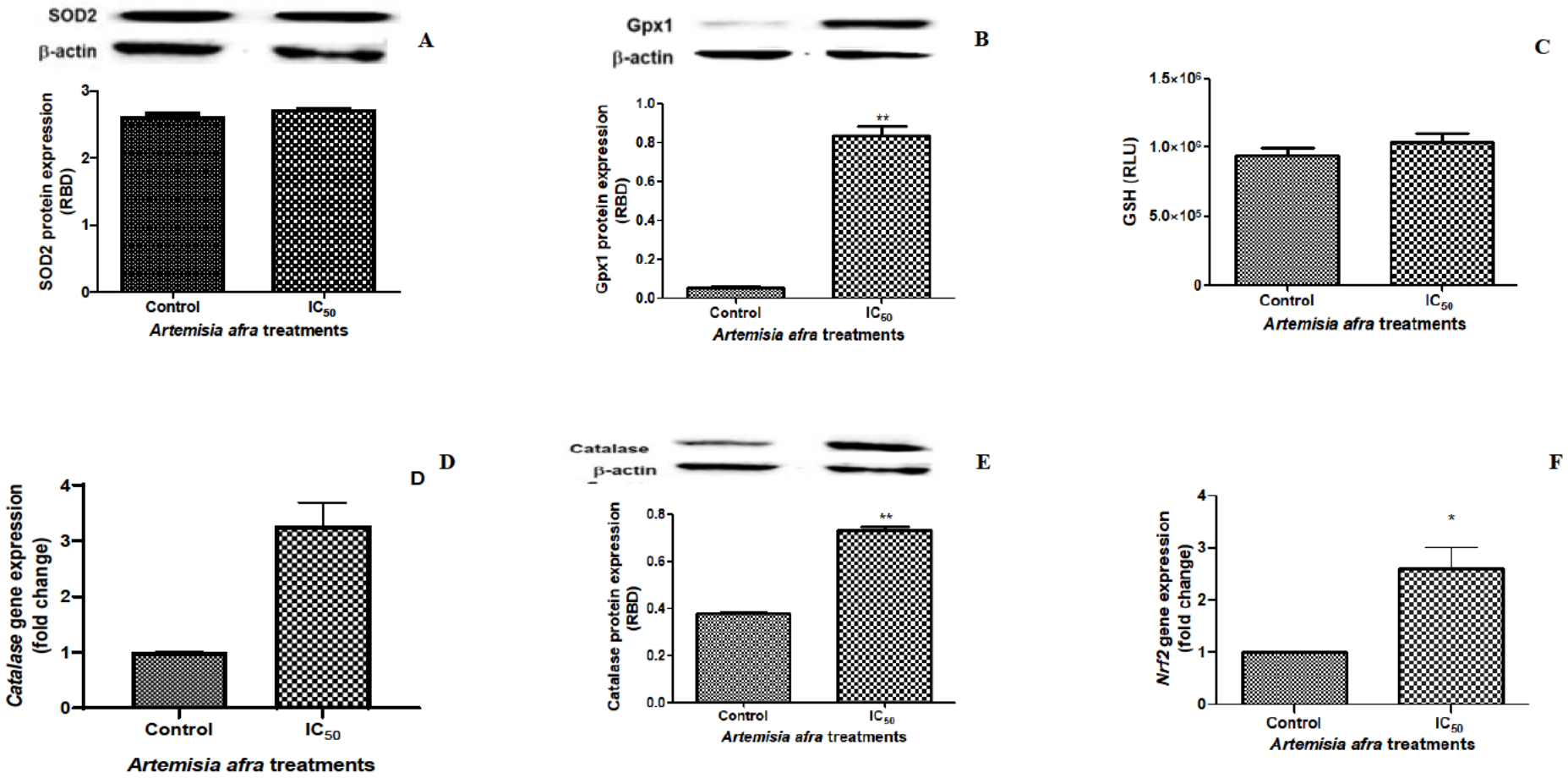

Figure 4.6: Antioxidant response for A549 cells treated with *A. afra* for 48 hours. (A) The SOD2 protein expression was not significantly increased relative to the control. **(B)** Protein expression of Gpx1 was significantly increased compared to the control. **(C)** Intracellular GSH was non-significantly increased by the crude *A. afra* extract relative to the control. **(D)** Gene expression of catalase was not significantly increased as compared to the control. **(E)** Catalase protein expression was significantly increased in the treatment group compared to the control. **(F)** The Nrf2 gene expression was significantly increased compared to the control. (*$p \leq 0.05$; unpaired student's *t*-test with Welch's correction).

4.3 CELL DEATH

4.3.1 Initiation of apoptosis

The initiator caspases, as well as pro- and anti-apoptotic Bcl-2 family were quantified to determine if apoptosis was initiated by the extrinsic or intrinsic pathway. The *A. afra* treatment decreased caspase 8 (Figure 4.7A) from 1987000±12490 RLU in the control to 1508000±7988RLU (p = 0.5803) in the treated cells. Similarly, caspase 9 (Figure 4.7B) was decreased to 2829000±33550 RLU (p = 0.0065) in the IC_{50}-treated cells compared to the control (783000±69540 RLU). Interestingly, proapoptotic Bcl-2 family protein - Bax (Figure 4.7C) increased by 76.92% in the *A. afra* treated A549 cells (1.030±0.01874 RBD; p=0.0009), compared to the control (0.5822 ± 0.02832 RBD). Of equal interest, antiapoptotic Bcl-2 protein expression was reduced by 20.1 % in the treatment group to 1.138±0.006747 RBD compared to the control group (1.424±0.004865 RBD) (p< 0.0001) (Figure 4.7D). xIAP was similar in the control (0.08581±0.001175 RBD) and treatment group (0.08966±0.0002302 RBD, p = 0.0844) (Figure 4.7E).

4.3.2 Execution of apoptosis

Initiation of apoptosis does not mean that apoptosis will be executed. In this study, the decreased activity of initiators was verified by the failure to activate caspase 3/7. The caspase 3/7 activity (Figure 4.8A) decreased by 21.85% in the *A. afra* IC_{50}-treated A549 cells (1405000±17930 RLU) compared to the untreated cells (1798000±33320 RLU) (p = 0.0019). In accordance with decreased caspase 3/7, phosphatidylserine was not externalised (Figure 4.8B), and was decreased from 565400±9619 RLU in the control to 695800±13540 RLU (p = 0.0043). Interestingly, in accordance with caspase inhibition both HSP 90 (Figure 4.8D) and HSP 27 (Figure 4.8C) expression was significantly increased in the treatment group from 0.00003669±0.000004432 RBD to 0.0001640±0.00002215 RBD (p = 0.0301) in the control group and from 0.01494±0.002536 RBD to 0.01494±0.002536 RBD (p = 0.0069) in the control group respectively.

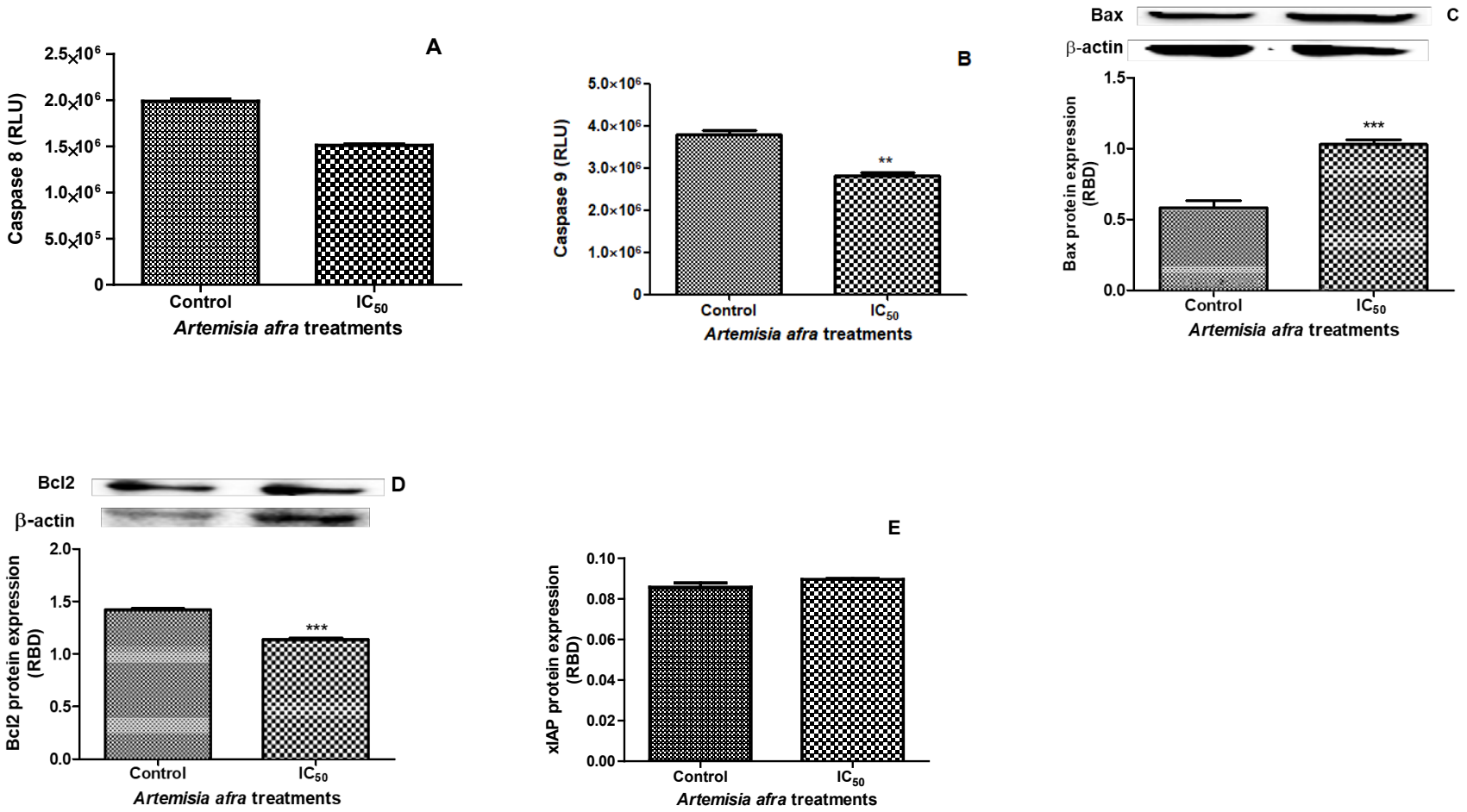

Figure 4.7: Initiation of apoptosis. (A) Caspase 8 levels were non-significantly decreased in the treatment group compared to control. **(B)** Caspase 9 levels were significantly reduced in the treatment group compared to the control. **(C)** Bax levels were siginificantly increased in the treatment group compared to the control. **(D)** Bcl-2 expression was significantly decreased in the *A. afra* treatment group compared to the control. **(E)** xIAP was non-significantly increased in the treated group compared to the control. (*$p \leq 0.05$; unpaired student's *t*-test with Welch's correction).

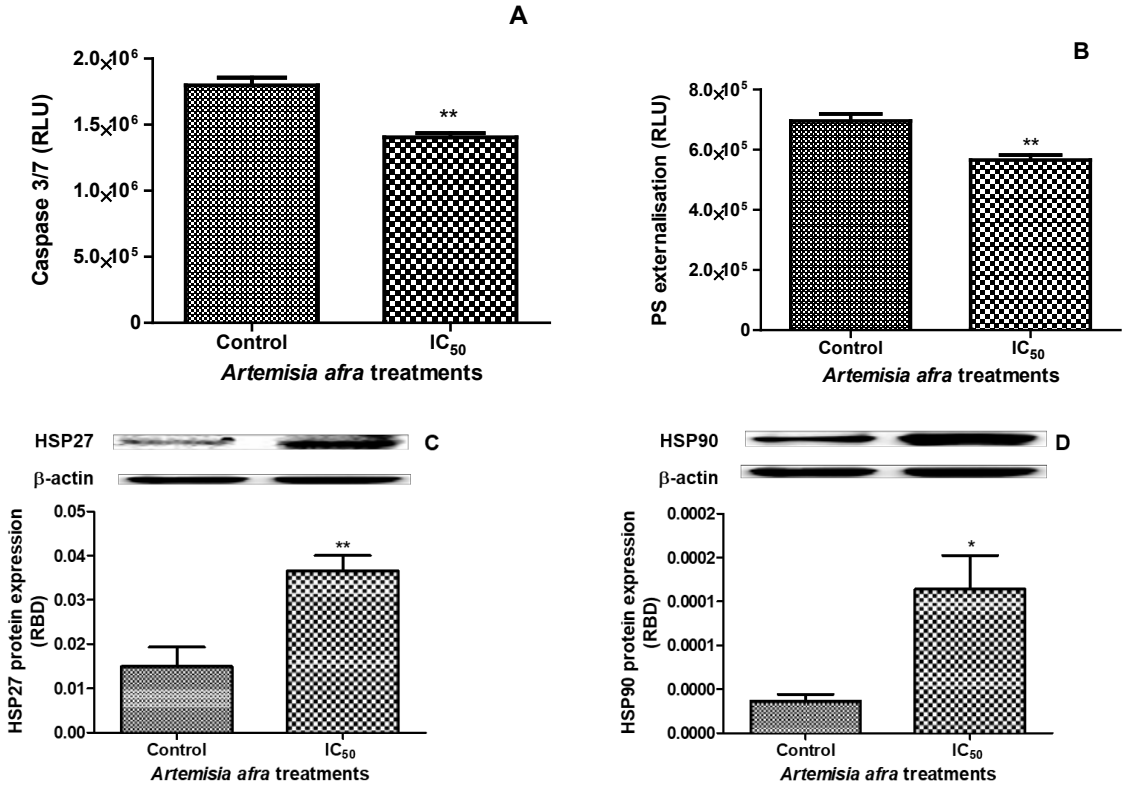

Figure 4.8: Execution of apoptosis. (A) Caspase 3/7 activation was significantly reduced in the treatment group compared to the control. **(B)** PS externalisation was significantly decreased in the treatment group compared to the control. (C) HSP 27 levels were significantly increased in the treatment group compared to the control. (D) HSP 90 levels were significantly increased in the treatment group compared to the control. (*$p \leq 0.05$; unpaired student's *t*-test with Welch's correction).

4.3.3 Necrosis as the mode of cell death

The annexin V and LDH assays were used to determine whether cytotoxicity was occurring as a result of necrosis. The IC_{50} *A. afra* treated cells (412100±8004 RFU; $p = 0.1916$) showed no significant increase in the levels of necrosis compared to the no treatment group (396600±4615 RFU) (Figure 4.9A). Similarly, the LDH levels in the treatment group (336000±1023 RLU; $p = 0.1020$) also showed no significant increases compared to the no treatment group (312700±7999 RLU) (Figure 4.9B).

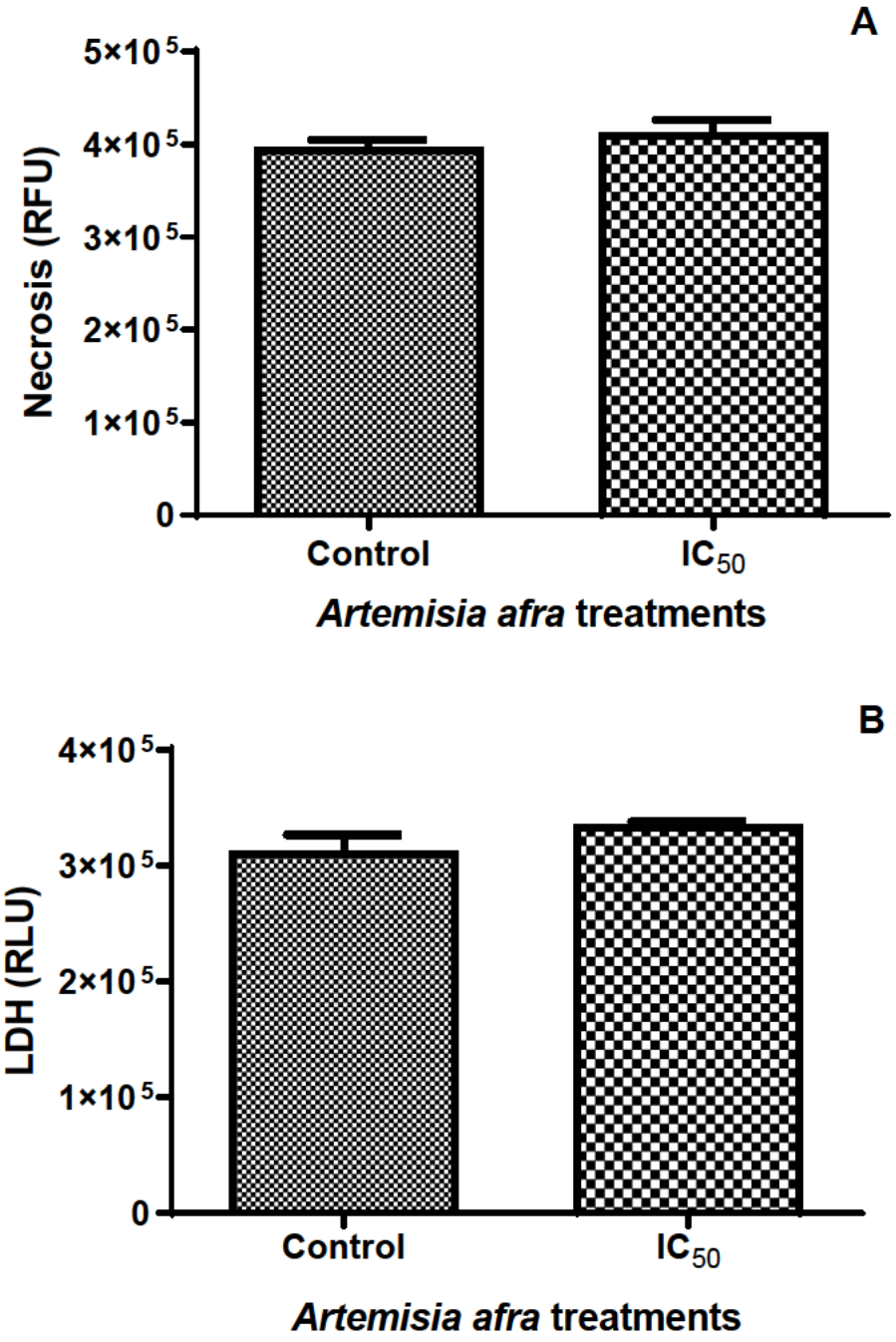

Figure 4.9: Necrosis as a mode of cell death. (A) Annexin V showed no significant increases in necrosis levels in the treatment group (412100±8004 RFU) compared to the control (396600±4615 RFU; $p = 0.1916$). **(B)** LDH levels were non-significantly increased in the treatment group (336000±1023 RLU) compared to the control (312700±7999 RLU; $p = 0.1020$). (*$p \leq 0.05$; unpaired student's *t*-test with Welch's correction).

CHAPTER 5: DISCUSSION

The burden of disease from cancer is growing at a pace that is equal to improvements in life expectancy and the modernisation of lifestyles across the world (Parascandola et al., 2022). While colorectal, breast, lung and prostate cancer account for more than half of all global cancer cases, lung cancer stands out as a major contributor to morbidity and mortality, causing the most cancer-related deaths worldwide (Sung, 2021). Currently available curative or therapeutic options for the affected are associated with a plethora of undesirable outcomes including exorbitant pricing, limited efficacy and serious adverse effects (Ren et al., 2016). In the case of lung cancer, for example, late-stage SCLC patients at present are unlikely to survive for more than a year post diagnosis. In addition, Wang e*t al*. (2019) confirmed that there is an increase in risk of adverse effects such as myelosuppression and increases in mortality rates amongst aged and frail Chinese ethnicities who received their first course of chemotherapy (Jones and Baldwin, 2018; Wang et al., 2019). Advancements within the chemotherapeutics space have been astounding, with innovations such as targeted therapy, immunoengineering and nanotechnology for drug delivery paving the way to futuristic management of the disease and proposing the promise of the possibility to completely eradicate lesions and significantly reduce morbidity and mortality (Personalised Medicine coalition, 2017; Krzyszczyk *et al.,* 2018). However, these advancements are for many reasons found lacking and will be found lacking into the foreseeable future without further investigations that will narrow down on more effective, safer and low cost alternatives to complement and/or improve on what is currently available (Personalised Medicine coalition, 2017). As it stands, any class of chemotherapy is ineffective in 75% of patients who are then often bound to suffer unnecessary drug related adverse events and economic burden (Personalised Medicine coalition, 2017). Taken together, this places an importance on studies that explore which materials elicit favourable responses regarding preventing carcinogenesis and inducing cytotoxicity in cancerous cells, and the nature (mechanisms) of said response (Asita et al., 2021). One kind of such investigations in pursuit of novel discovery of such materials is research on medicinal plants for the purposes of the development of more efficacious, affordable and safer drugs, of which the traditional medicinal herb *A. afra* is no exception (van Loggenberg et al, 2022). It has drawn considerable attention for its potential antitumour activity (Spies, *et al*., 2011; van Loggenberg et al, 2022; Venables et al, 2016; Shelembe et al, 2019). van Loggenberg and associates have reported on the cytotoxicity of the plant towards the lung cancer cell line. However, they did not report on

the mechanism thereof. Therefore, the current study is the first to report on the cytotoxic activity of the crude aqueous extract of the plant on the lung cancer A549 cell line and the underlying molecular mechanisms through which the cytotoxicity is carried out after 48 hours of treatment (van Loggenberg, 2022).

In order to exert a cytotoxic mechanism in cell, an applied xenobiotic must gain entry to the cells where it encounters the cytochrome P450 family of enzymes, which are important in drug metabolism. Cytochrome P450 3A4 is primarily associated with bioactivation or detoxification of drugs. In this study CYP3A4 was increased by *A. afra* (Figure 4.2), implying that the enzyme was induced and that subsequent effects may be attributed to either the parent or biotransformed compounds in the extract. The function of bioactivation of compounds in the extract to their cytotoxic constituents carried out by the enzyme CYP3A4 increased as concentrations of the enzyme increased. This is alluded to by the dose-dependant reduction in cell viability as per the MTT assay results. A shortfall of the study's investigative approach, is the lack of exploration into a direct correlation between CYP3A4 function and cell viability, it is rather inferred through assessment of the MTT curve, as well as the exact phytochemicals which undergo biotransformation under the helm of this enzyme. Cytotoxic mechanisms are usually associated with interference with metabolic activity within exposed cells, particularly resulting in effects on the mitochondria. The *A. afra* treatment was associated with a dose-dependent decline in the number of viable cells (Figure 4.1) indicating cytotoxicity, likely through disruption of succinate dehydrogenase (SDH) function, which was consistent with prior studies using extracts of the plant on different cell lines (Venables, *et al*., 2016; Shelembe, Mahlangeni, and Moodley, 2019; van Loggenberg, *et al*., 2022). The SDH is an integral component of the ETC that transfers electrons from $FADH_2$ to complex III while serving as a catalyst for the oxidation of succinate to fumarate (Ahmad, 2023). Cellular dysfunction owed to the disruption of SHD function is an early sign of declining cell viability and is normally shortly associated with a reduction in ATP production (Ahmad, 2023).

Cellular viability disruption via mitochondrial dysfunction is associated with reduced ATP production and a reduced $\Delta\Psi m$ (Younes et al., 2022). Significant reduction in the levels of ATP (Figure 4.3A) imply that *A. afra* disrupted normal cellular activity in the A549 cells. A decline in ATP production in the treated cells signals the uncoupling of oxidative phosphorylation. Indeed, Narasinhan *et al*. (1988) noted that sesquiterpene lactones, one of the

bioactive compounds found in A. *afra*, possess alkylating sites that could disrupt oxidative phosphorylation via alkylating enzymes in the ETC such as SDH or ATP synthase and/or alkylation of cytochromes or iron-sulfur proteins in the ETC. The alkylation of these key proteins interferes with electron transfer reactions in the ETC and prevent ATP formation (Narasinhan *et al*., 1988; Venables *et al*., 2016; Ferreira *et al.,* 2018). This is the mechanism by which the first effective non-hormonal chemotherapeutic drugs carried out their function (Ferreira *et al.,* 2018). It is not only ATP production that will be affected; it is possible that disruption of the ETC complexes will also interfere with ΔΨm, since ΔΨm is driven by proton pumps within the complexes, and is integral for ATP production (Younes et al, 2022). Interestingly, despite the sharp decline in ATP production, *A. afra* treated cells showed no difference of note in the ΔΨm compared to the control group (Figure 4.3B). This indicated that although there was a disruption in the ETC, there was, however, little to no depolarisation of the mitochondrial membrane (Younes et al., 2022). Continued respiration in the absence of ATP synthesis may be explained by uncoupling of the return of protons into the mitochondrial matrix down their electrochemical gradient, forming of a membrane potential, and the production of ATP by synthases (Cadenas, 2018). This is possible as some protons return into the mitochondrial matrix through pathways that are independent of ATP synthases in a process called a proton leak, accounting for the maintained ΔΨm in the face of reduced ATP production (Cadenas, 2018).

However, interference with electron transfer in the mitochondria could culminate in increased ROS production and A. *afra* may be associated with ROS formation as a by-product of incomplete electron transfer in the ETC likely induced by disrupted SDH function, as some electrons may be transferred directly to O_2 to form ROS (Zhao et al., 2019). The results in this study suggests that the *A. afra* IC_{50} treatment augments ROS production, given that the MDA levels were significantly elevated upon treatment (Figure 4.4). Since negligible change in ΔΨm was observed, ROS production may be associated with complex II which is also related to SDH. Under physiological conditions, complex II ROS generation is negligible; however, it was shown that in complex II mutation related disease ROS levels were produced to a greater extent from this complex than any other, being only third to complex I and complex III out of the 11 sites in the ETC where $O_2^{\bullet-}$ is sourced (Zhao et al., 2019). One of the fates of $O_2^{\bullet-}$ generated under these conditions is the formation of RNS after reacting with NO. It is therefore expected that with increases in $O_2^{\bullet-}$ production, concentrations of RNS should also be increased

(Thuy le et al., 2017). In this study, the levels of RNS were relatively unchanged in the treated group compared to the control. Three different nitric oxide synthases (NOS) are responsible for NO generation; inducible NOS (iNOS) being the most relevant in this case, and is well known to be under the regulation of MAPK and JNK/STAT (Adams et al., 2015). The findings point to an inhibitory effect that the IC_{50} treatment could have on iNOS that would lead to a reduced production of NO in turn reducing the levels of substrate for RNS production (Adams et al., 2015). This is in correlation with the findings of Jeong and associates (2018), where they found that *Artemisia* extracts reduced the production of NO through repressing MAPK pathways (Jeong et al., 2018). Alternately, the dismutation of $O_2^{\bullet-}$ to H_2O_2 by SOD, and subsequent antioxidant activity, would decrease the substrate necessary for RNS production (Zhao, 2020). Similar to ROS, RNS possess proapoptotic properties (Wang, *et. al.,* 2021). Meaning that increased levels would result in the activation of apoptosis. Given that RNS has been shown to affect mitochondrial membrane enzyme activity, it therefore acts synergistically with ROS to activate intrinsic apoptosis. The study's findings are a reduced activity of intrinsic apoptosis (Wang, *et. al.,* 2021). This would mean that without the inhibitory effects treatment has on nitrite/nitrate production, increased levels thereof would lead to nitrosative stress that, in hand with ROS, would bring the cells past a threshold of intrinsic apoptosis activation that would supersede any inhibition (Wang, *et. al.,* 2021). However, nitrite/nitrate levels were relatively unchanged and this correlates with the low levels of intrinsic apoptosis seen in the treated cells.

The antioxidant response is vital to the removal of harmful ROS associated with lipid peroxidation in this study (Figure 4.4), and is reliant on Nrf2, a critical transcription factor that governs the expression of genes coding for antioxidant enzymes and facilitates the production of GSH (Glorieux et al., 2024). This transcription factor is known to exhibit a dual role in cancer. It may, depending on the context, promote tumour progression, have a cytoprotective effect, and/or play a role in metastasis (Glorieux et al., 2024). It is regulated by KEAP1, which is a redox-sensitive ubiquitin ligase substrate adaptor. During periods of oxidative stress KEAP1 is conformationally modified by ROS, resulting in its dissociation from Nrf2; Nrf2 then undergoes stabilisation, accumulation and nuclear translocation, where it then induces the induction of genes for enzymes such as SOD2 and Gpx1 (Glorieux et al., 2024). Nrf2 also regulates *de novo* synthesis of GSH through maintaining levels of glutathione reductase – the

enzyme responsible for reducing GSSG to GSH; and through regulating GCL (Harvey et al., 2008). Indeed, the elevated ROS levels in the treatment group correlated with a significant reactionary rise in the gene expression of Nrf2 (Figure 4.6F), which was associated with increases in the protein expression of SOD2 (Figure 4.6A), Gpx1 (Figure 4.6B) and GSH (Figure 4.6C). It is well established that SOD2 works by converting O_2^- into H_2O_2, while Gpx1 uses GSH as a substrate to reduce H_2O_2 to H_2O. The Gpx1/GSH also degrades lipid peroxide and peroxynitrite (Zhao, 2020). In the process, GSH is converted to GSSG (Nuhu et al., 2020).

Catalase is another antioxidant enzyme that converts H_2O_2 to H_2O and O_2, and is also regulated by Nrf2. This study found that *A. afra* upregulated catalase gene expression but at non-significant levels followed by significant increases in its protein expression. The disparity seen in protein and mRNA expression is likely due to posttranscriptional regulation (Glorieux et al., 2015). It is well established that during periods of heightened oxidative stress Nrf2 activates ARE dependant genes that mount an antioxidant response, and the current study's findings are consistent with such (Chen et al., 2009; Younus, 2018). Flavonoids are known to be activators of Nrf2/ARE gene activation at low concentrations, thus the flavonoids in the *A. afra* crude extract may be a contributing factor to the increases in Nrf2 expression and subsequent antioxidant response seen in the treatment group (du Toit and van der Kooy, 2019; Suraweera *et al.,* 2020). However, despite the favourable antioxidant response, lipid peroxidation was still evident indicating that oxidative stress prevailed, which may lead to the cell death associated with decreased cell viability.

Cell death is mediated via several pathways, including apoptosis and necrosis. Cellular membranes are normally intact during apoptosis, thus propidium iodide is useful in differentiating between necrotic and apoptotic cytotoxicity (Lakshmanan and Batra, 2016). In this study, necrosis was not the mode of cell death induced by the *A. afra* treatment (Figure 4.4A), and is corroborated by the LDH levels that were relatively unchanged (Figure 4.9B). LDH is a stable cytoplasmic enzyme that leaks out of the cell into the extracellular space during loss of membrane integrity such as in cells undergoing necrosis (Kumar et al., 2018). This finding is interesting since it suggests an intact plasma membrane despite the observed lipid peroxidation (Figure 4.4); it also excludes necrosis as the mechanism of cytotoxicity and implies that the mode of cell death may be apoptosis. ROS are known have the ability to produce toxic protein aggregates that tend to lead to necrosis through the formation of nonspecific membrane pores (Lee, *et. al.*, 2018). The strength of oxidative stress has been

reported to be a determinant in the decision of a cell to undergo apoptosis or necrosis, where under circumstances of weak oxidative stress, apoptosis is favoured over necrosis, and vice versa in circumstances of strong oxidative stress (Nishida, *et. al.,* 2022). Given that the annexin V and LDH assay show little to no necrosis in the treated cells, it should be that the levels of oxidative stress are below the threshold necessary to incite necrosis (Nishida, *et. al.,* 2022). Similarly with ATP concentrations, they are required to be close to, if not completely, exhausted in order for necrosis to take place (Nishida, *et. al.,* 2022). Some availability of ATP is necessary for apoptosis. It is a possibility that the levels of ATP in the treated cells are not low enough to incite necrosis (Nishida, *et. al.,* 2022).

Intrinsic apoptosis is controlled by the Bcl2 family, where anti-apoptotic Bcl2 prevents pro-apoptotic Bax from forming pores in the outer mitochondrial membrane (MOMP), Bcl2 inhibits apoptosis by forming a heterodimer with Bax, and promotes survival through Ca^{2+} regulation and its antioxidant effect (Qian et al*.,* 2022). The Bax protein expression was significantly higher in the *A. afra*-treated cells (Figure 4.7C), while Bcl2 protein expression was significantly reduced (Figure 4.7D). These are the conditions necessary for the initiation of the intrinsic pathway of apoptosis and the findings therefore confirm the pro-apoptotic properties of *A. afra.* (Qian, *et al.,* 2022). The resulting MOMP allows pro-apoptotic proteins to leak through the pores and activate a caspase cascade that leads to programmed cell death. Interestingly, caspase 9 that is associated with the intrinsic pathway of apoptosis was decreased (Figure 4.7B); this suggests a role of an inhibitory factor that acts on caspase 9 post MOMP formation so that intrinsic apoptosis was prevented. Neither was apoptosis initiated via the extrinsic pathway, since caspase 8 activity was also decreased (Figure 4.7A).

Usually, the initiator caspases cleave and activate the downstream executors of apoptosis, caspase 3/7, which are responsible for the morphological and biochemical changes that occur in apoptotic cells (Elmore, 2007). Since both of the initiator caspases (8 and 9) were decreased, the reduction in the activation of the execution caspases (Figure 4.8A) was not surprising. Failure to activate caspase 3/7 means that apoptosis was not executed, and is supported by the decreased PS externalisation (Figure 4.8B). These findings are not in keeping with those of Ali and associates where they described a ROS-dependant activation of Bax/Bcl2 and subsequent activation of the caspase 3 pathway leading to apoptosis in human keratinocyte cells (Ali et al., 2018). However, it does suggest that inhibitors of apoptosis were likely to play a role in the inhibition of caspase activity.

The inhibitor of apoptosis (IAP) proteins are known to block apoptosis by binding to activated caspases. In particular, xIAP is a potent inhibitor of caspase 3/7 and caspase 9 activity (Eckelman et al., 2006; Yabal et al., 2014). In this study, protein expression of xIAP remained unchanged (Figure 4.7E), and xIAP was not responsible for the observed inhibition. Heatshock proteins (HSPs) are primarily expressed in the cellular stress response such as during high levels of oxidative stress (Soumyadip et al., 2018; Szyller and Bil-Lula, 2021). Oxidative stress has an effect on the expression of HSPs though Nrf2 and HSF1. It was therefore expected that increased expression of Nrf2 (Figure 4.7F) and raised ROS levels (Figure 4.4) should be met with an upregulation of the HSPs. Indeed, the results show a steep increase in both HSP27 (Figure 4.8C) and HSP90 (Figure 4.8 D) protein expression. The HSPs primary functions are the prevention of protein misfolding and aggregation, and protection against apoptosis (Soumyadip et al., 2018; Szyller, and Bil-Lula, 2021; Peng 2022). HSP 27 is a small HSP that has the ability to inhibit apoptosis at multiple levels including caspase 3, and at the level of cytochrome c after its release from the mitochondria where it prevents apoptosome formation (Wang et al., 2014). This feature explains lower levels of caspase 3 activation (Figure 4.8A) and poses to be the reason why intrinsic apoptosis would be initiated by Bax/Bcl2 (Figures 4.7C, D) without subsequent increases in activated caspase 9 (Figure 4.7B). The mechanisms through which HSP90 conveys its anti-apoptotic function remain elusive. However, it is well known that highly expressed HSP90 is correlated with inhibition of apoptosis (Peng, 2022). Emerging evidence posit a number pathways through which HSP90 inhibits apoptosis. It is believed that HSP90 upregulates Bcl2 thereby inhibiting cytochrome c release from the mitochondria (Peng, 2022). This proposed mechanism, however, does not correlate with the current study's findings of a reduced Bcl2 protein expression (Figure 4.7D) in the face of raised levels of HSP 90 (Figure 4.8D). Another proposed mechanism is that HSP 90 inhibits Apaf-1 thereby restricting the formation of the apoptosome which is necessary for cleaving pro-caspase 9 to its active form (Peng, 2022). This mechanism corresponds with the findings of this study where lowered caspase 9 activation was observed (Figure 4.7B). Nonetheless, studies point to HSP90s anti-apoptotic effect in cancers (colorectal, lung and gliomas) through a reduction in cell viability of HSP90 knockdown cells and in cells where the protein was inhibited (Peng, 2022). This further supports the notion that HSP90 is indeed anti-apoptotic and that raised levels as seen in the results are rightly correlated with reduced apoptosis.

CHAPTER 6: CONCLUSION

The suboptimal performance of currently available cancer treatments warrants the need for ongoing efforts to find more effective, safer and affordable alternatives. Medicinal plants have a long-standing history of being an invaluable source in the space of drug development towards these ends. *Artemesia afra*, a popular South African medicinal plant, has garnered attention for its antitumour activity. The current study sought to contribute to the body of knowledge on *A. afra*'s cytotoxic effect and the underlying mechanisms in A549 lung cancer cells.

The A549 cells were treated with *A. afra*'s crude extract for 48 hours, following which they showed a reduction in cell viability as shown by the MTT and ATP assays, and was associated with increases in cellular ROS production. This was attributed to *A. afra*'s sesquiterpene lactone content which is known to cause uncoupling of the ETC and increase mitochondrial superoxide output (Venables *et al.,* 2016). There was a concomitant upregulation of antioxidants including Gpx1 and catalase in response to increased oxidative stress. Levels of GSH and SOD2 protein expression were minimally increased in the IC_{50}-treated cells. This study showed that the RNS levels in the treated cells also approximated those of the control group. Increased ROS levels prompted a surge in pro-apoptotic Bax expression with a concurrent reduction in anti-apoptotic Bcl2 expression which is a precondition for mitochondrial membrane pore formation and the release of cytochrome c. This results in caspase 9 activation in the apoptosome and the subsequent initiation of intrinsic apoptosis, which confirms that A. *afra* indeed has pro-apoptotic properties. Intriguingly, the levels of activated caspase 9 and, though not significant, activated caspase 8 were reduced in treated cells, implying the role of an anti-apoptotic constituent in the phytochemical profile of *A. afra*. The initiation of apoptosis does not mean that it will be executed. Flavonoids in *A. afra* and increased oxidative stress are known activators of the transcription factor Nrf2. Activated Nrf2 upregulates stress response proteins including HSP27 and HSP90. These two potent anti-apoptotic HSPs together with Nrf2 were increased in the treated cells and were possibly involved in inhibition of apoptosis as they correlated with reduced caspase activation. The findings of low levels of activated executor caspases 3/7 and lower levels of PS externalisation in the treated cells compared to the control further supported this notion showing that apoptosis was not the mode of cytotoxicity carried out by *A. afra* in the lung cancer cells, rather that it was instead being inhibited. The results of tests for necrosis also excluded necrosis as the mode

of cytotoxicity. Therefore, given that the MTT assay does not distinguish between modes of cytotoxicity, these results suggest an alternative mode of cell death.

Taken together, the current study has successfully demonstrated the cytotoxicity of the crude extract of *A. afra* through induction of oxidative stress. The inhibition of apoptosis through upregulation of heat shock proteins was not expected, and suggests an alternate mode of cell death in A549 lung cancer cells. More studies on the mode of *A. afra* crude extract cytotoxicity in A549 cells and the mechanisms thereof are needed. Further investigations are also needed to explore the bioactive individual phytochemical constituents of the medicinal plant and their synergistic and antagonistic roles in cancer cell cytotoxicity. There is also impetus for studies that will characterise the different cell signalling pathways it affects in different cell lines. *In vivo* studies in the context of cancer would also be beneficial to growing the body of knowledge in anti-cancer efforts.

REFERENCES

- Adams, L., Franco, M.C., and Esteves, A.G. 2015. Reactive nitrogen species in cellular signalling. Experimental Biology and Medicine; 240(6): 711-717. PMC4935209.
- Ahmad, M., Wolberg, A., and Chadi, 2023. Electron transport chain. K. Biochemistry. StatPearls.
- Ali, D., Tripathi, A., Al Ali, H., Shahi, Y., Mishra, K.K., Alarifi, S., Alkahtane, A.A., and Manohardas, S. 2018. ROS-dependant Bax/Bcl2 and caspase 3 pathway-mediated apoptosis induced by zineb in human keratinocyte cells. *OncoTargaets and Therapy.* 11: 489-497. Doi:10.2147/OTT.S140358.
- : Allkin, B., 2017. At least 28,187 plant species are currently recorded as being of medicinal use. Useful plants–Medicines.
- Antoniou, C., Savvides, A., Georgiadou, E.C. and Fotopoulos, V., 2018. Spectrophotometric quantification of reactive oxygen, nitrogen and sulfur species in plant samples. Polyamines: Methods and Protocols, pp.155-161.
- Arfin, S., Jha, N.K., Jha, S.K., Kesari, K.K., Ruokolainen, J., Roychoudhury, S., Rathi, B. and Kumar, D., 2021. Oxidative stress in cancer cell metabolism. Antioxidants, 10(5), p.642.
- Aziz, M.A., Diab, A.S. and Mohammed, A.A., 2019. Antioxidant categories and mode of action (pp. 3-22). London, UK: IntechOpen.
- Bade, B.C. and Cruz, C.S.D., 2020. Lung cancer 2020: epidemiology, etiology, and prevention. Clinics in chest medicine, 41(1), pp.1-24.
- Bray, F., Ferlay, J., Soerjomataram, I., Siegel, R.L., Torre, L.A. and Jemal, A., 2018. Global cancer statistics 2018: GLOBOCAN estimates of incidence and mortality worldwide for 36 cancers in 185 countries. CA: a cancer journal for clinicians, 68(6), pp.394-424.
- Brenner, D.R., Brennan, P., Boffetta, P., Amos, C.I., Spitz, M.R., Chen, C., Goodman, G., Heinrich, J., Bickeböller, H., Rosenberger, A. and Risch, A., 2013. Hierarchical modeling identifies novel lung cancer susceptibility variants in inflammation pathways among 10,140 cases and 11,012 controls. Human genetics, 132(5), pp.579-589.
- Brentnall, M., Rodriguez-Menocal, L., De Guevara, R.L., Cepero, E. and Boise, L.H., 2013. Caspase-9, caspase-3 and caspase-7 have distinct roles during intrinsic apoptosis. BMC Cell Biology, 14, pp.1-9.

- Brieger, K., Schiavone, S., Miller, F.J. and Krause, K.H., 2012. Reactive oxygen species: from health to disease. Swiss medical weekly, 142, p.w13659.
- Burton, G.J. and Jauniaux, E., 2011. Oxidative stress. Best practice and research Clinical obstetrics and gynaecology, 25(3), pp.287-299.
- Cadenas, S. 2018. Mitochondrial uncoupling, ROS generation and cardioprotection. Biochimica et BIophysica Acta (BBA) – Bioenergetics. Volume 1859, Issue 9, Pages 940-950.
- Cai, H., Meng, X., Li, Y., Yang, C. and Liu, Y., 2014. Growth inhibition effects of isoalantolactone on K562/A02 cells: Caspase-dependent apoptotic pathways, S phase arrest, and downregulation of Bcr/Abl. Phytotherapy Research, 28(11), pp.1679-1686.
- Chen, W., Li, P., Liu, Y., Yang, Y., Ye, X., Zhang, F. and Huang, H., 2018. Isoalantolactone induces apoptosis through ROS-mediated ER stress and inhibition of STAT3 in prostate cancer cells. Journal of Experimental and Clinical Cancer Research, 37, pp.1-12.
- Chen, Y., Azad, M.B. and Gibson, S.B., 2009. Superoxide is the major reactive oxygen species regulating autophagy. Cell Death and Differentiation, 16(7), pp.1040-1052.
- Chen, Y., Azad, M.B. and Gibson, S.B., 2009. Superoxide is the major reactive oxygen species regulating autophagy. Cell Death and Differentiation, 16(7), pp.1040-1052.
  Cooper GM. The Cell: A Molecular Approach. 2nd edition. Sunderland (MA): Sinauer Associates; 2000. The Development and Causes of Cancer. [accessed @]: https://www.ncbi.nlm.nih.gov/books/NBK9963/ 03/03/2023.
- Cragg, G.M. and Newman, D.J., 2013. Natural products: a continuing source of novel drug leads. Biochimica et Biophysica Acta (BBA)-General Subjects, 1830(6), pp.3670-3695.
- D'arcy, M.S., 2019. Cell death: a review of the major forms of apoptosis, necrosis and autophagy. Cell Biology International., 43(6), pp.582-592.
- De Leon, J.A.D. and Borges, C.R., 2020. Evaluation of oxidative stress in biological samples using the thiobarbituric acid reactive substances assay. JoVE (Journal of Visualized Experiments), (159), p.e61122.
- Di, W., Khan, M., Rasul, A., Sun, M., Sui, Y., Zhong, L., Yang, L., Zhu, Q., Feng, L. and Ma, T., 2014. Isoalantolactone inhibits constitutive NF-κB activation and induces reactive oxygen species-mediated apoptosis in osteosarcoma U2OS cells through mitochondrial dysfunction. Oncology Reports, 32(4), pp.1585-1593.

- Dube, A., 2006. The design, preparation and evaluation of Artemisia afra and placebos in tea bag dosage form suitable for use in clinical trials (Doctoral dissertation, University of the Western Cape).
- Eckelman, B., Salvesen, G.S., and Scott, F.L. 2006. Human Inhibitor of apoptosis protein: Why XIAP is the black sheep of the family. EMBO reports. 7(10): 988-994. Doi: 10.1038/sj.embor.7400795.
- Ekor, M., 2014. The growing use of herbal medicines: issues relating to adverse reactions and challenges in monitoring safety. Frontiers in Pharmacology, 4, p.177.
- Elmore, S., 2007. Apoptosis: a review of programmed cell death. Toxicologic Pathology, 35(4), pp.495-516.
- Ferreira, L.L., Coelho, A.R., Oliveira, P.J., and Cunha-Oliveira, T. 2018. Mitochondrial Toxicity Induced by Chemotherapeutic Drugs. Wiley Online Library. Chapter 40.
- Forest, V., Figarol, A., Boudard, D., Cottier, M., Grosseau, P. and Pourchez, J., 2015. Adsorption of lactate dehydrogenase enzyme on carbon nanotubes: How to get accurate results for the cytotoxicity of these nanomaterials. Langmuir, 31(12), pp.3635-3643.
- Garibyan, L. and Avashia, N., 2013. Research Techniques Made Simple: Polymerase Chain Reaction (PCR). Journal of Investigative Dermatology. 133(3): e6.
- Garnero, J., 1977. Huile essentielle de lanyana. Parfums, Cosmetiques, Aromes, 16, 45-47.
- Ghambiri, N., 2019. Exploiting the Cellular Redox Control System for Activatable Photodynamic Therapy Msc. Thesis. University of Toronto.
- Ghasemi, M., Turnbull, T., Sebastian, S. and Kempson, I., 2021. The MTT assay: utility, limitations, pitfalls, and interpretation in bulk and single-cell analysis. International Journal of Molecular Sciences, 22(23), p.12827.
- Glorieux, C., Enriquez, C., Gonzalez, C., Aguirre-Martinez, G., and Buc Calderon, P. The Multifaceted Roles of NRF2 in Cancer: Friend or Foe. 2024. Antioxidants. 13(1):70. https://doi.org/10.3390/antiox13010070.
- Hanahan, D., 2022. Hallmarks of cancer: new dimensions. Cancer discovery, 12(1), pp.31-46.
- Harvey, C.J., Thimmulappa, R.K., Singh, A., Blacke, D.J., Ling, G., Wakabayashi, N., Fujii, J., Myers, A., and Biswal, S. 2008. Nrf2-ewgulated glutathione recycling independent of biosynthesis is critical for cell survival during oxidative stress. Free Radic Biol Med. 10.1016/j.freeadbiomed.2008.10.040.

- Hirano, S., Yang, L., Juul, M., Purdie, C.A., O'Neill, B.P., Kabbe, R., Papaemmanuil, E., Fan, Y., Hayes, D.N., Raeder, B. and Stunnenberg, H.G., 2020. Pan-cancer analysis of whole genomes. Nature, 578(DKFZ-2020-01051), pp.82-93.
- Holanda Pinto, S.A., Pinto, L.M.S., Cunha, G.M.A., Chaves, M.H., Santos, F.A. and Rao, V.S., 2008. Anti-inflammatory effect of α, β-Amyrin, a pentacyclic triterpene from Protium heptaphyllum in rat model of acute periodontitis. Inflammopharmacology, 16(1), pp.48-52.
- Hughes, M.A., Harper, N., Butterworth, M., Cain, K., Cohen, G.M. and MacFarlane, M., 2009. Reconstitution of the death-inducing signaling complex reveals a substrate switch that determines CD95-mediated death or survival. Molecular Cell, 35(3), pp.265-279.
- Imyanitov, E.N., Kuligina, E.S., Belogubova, E.V., Togo, A.V. and Hanson, K.P., 2005. Mechanisms of lung cancer. Drug Discovery Today: Disease Mechanisms, 2(2), pp.213-223.
- Jemal, A., Miller, K.D., Ma, J., Siegel, R.L., Fedewa, S.A., Islami, F., Devesa, S.S. and Thun, M.J., 2018. Higher lung cancer incidence in young women than young men in the United States. New England Journal of Medicine, 378(21), pp.1999-2009.
- Jeong, S.H., Kim, J., and Min, H., 2018. *In vitro* anti-inflammatory activity of the Artemesia montana leaf ethanol extract in macrophage RAW 264.7 cells, Food and Agricultural Immunology, 29:1, 688-698.
- Jones, G.S. and Baldwin, D.R., 2018. Recent advances in the management of lung cancer. Clinical Medicine, 18(Suppl 2), p.s41.
- Kamiloglu, S., Sari, G., Ozdal, T. and Capanoglu, E., 2020. Guidelines for cell viability assays. Food Frontiers, 1(3), pp.332-349.
- Katiyar, C., Gupta, A., Kanjilal, S. and Katiyar, S., 2012. Drug discovery from plant sources: An integrated approach. Ayu, 33(1), p.10.
- Khan, M., Ding, C., Rasul, A., Yi, F., Li, T., Gao, H., Gao, R., Zhong, L., Zhang, K., Fang, X. and Ma, T., 2012. Isoalantolactone induces reactive oxygen species mediated apoptosis in pancreatic carcinoma PANC-1 cells. International Journal of Biological Sciences, 8(4), p.533.
- Koegelenberg, C.F., Dorfman, S., Schewitz, I., Richards, G.A., Maasdorp, S., Smith, C. and Dheda, K., 2019. Recommendations for lung cancer screening in Southern Africa. Journal of Thoracic Disease, 11(9), p.3696.
- Kumar, P., Nagarajan, A. and Uchil, P.D., 2018. Analysis of cell viability by the lactate dehydrogenase assay. Cold Spring Harbor Protocols, 2018(6), pp.pdb-prot095497.

- Kupcho, K., Shultz, J., Hurst, R., Hartnett, J., Zhou, W., Machleidt, T., Grailer, J., Worzella, T., Riss, T., Lazar, D. and Cali, J.J., 2019. A real-time, bioluminescent annexin V assay for the assessment of apoptosis. Apoptosis, 24, pp.184-197.
- Lee, S.Y., Ju, M.K., Jeon, H.M., Jeong, E.K., Lee, Y.J., Kim, C.H., Park, H.G., Han, S.I., & Kang, H.S. 2018. Regulation of Tumor progression by Programmed Necrosis. Oxidative Medicine and Cellular Longevity. Doi: 10.115/2018/3537471. PMID: 29636841.
- Liberti, M.V. and Locasale, J.W., 2016. The Warburg effect: how does it benefit cancer cells?. Trends in Biochemical Sciences, 41(3), pp.211-218.
- Liu, B., Chen, Y. and Clair, D.K.S., 2008. ROS and p53: a versatile partnership. Free Radical Biology and Medicine, 44(8), pp.1529-1535.
- Lortet-Tieulent, J., Renteria, E., Sharp, L., Weiderpass, E., Comber, H., Baas, P., Bray et al., F., Coebergh, J.W. and Soerjomataram, I., 2015. Convergence of decreasing male and increasing female incidence rates in major tobacco-related cancers in Europe in 1988–2010. European Journal of Cancer, 51(9), pp.1144-1163.
- Lu, Z., Zhang, G., Zhang, Y., Hua, P., Fang, M., Wu, M. and Liu, T., 2018. Isoalantolactone induces apoptosis through reactive oxygen species-dependent upregulation of death receptor 5 in human esophageal cancer cells. Toxicology and Applied Pharmacology, 352, pp.46-58.
- Luff, S.A., Kao, C.Y. and Papoutsakis, E.T., 2018. Role of p53 and transcription-independent p53-induced apoptosis in shear-stimulated megakaryocytic maturation, particle generation, and platelet biogenesis. PLoS One, 13(9), p.e0203991.
- Mahmood, T. and Yang, P.C., 2012. Western blot: technique, theory, and trouble shooting. North American Journal of Medical Sciences, 4(9), p.429.
- Malhotra, J., Malvezzi, M., Negri, E., La Vecchia, C. and Boffetta, P., 2016. Risk factors for lung cancer worldwide. European Respiratory Journal, 48(3), pp.889-902.
- Matés, J.M., Segura, J.A., Alonso, F.J. and Márquez, J., 2012. Oxidative stress in apoptosis and cancer: an update. Archives of Toxicology, 86, pp.1649-1665.
- McKay, J.D., Hung, R.J., Gaborieau, V., Boffetta, P., Chabrier, A., Byrnes, G., Zaridze, D., Mukeria, A., Szeszenia-Dabrowska, N., Lissowska, J. and Rudnai, P., 2008. Lung cancer susceptibility locus at 5p15. 33. Nature Genetics, 40(12), pp.1404-1406.
- Morgan, M.J. and Liu, Z.G., 2011. Crosstalk of reactive oxygen species and NF-κB signaling. Cell Research, 21(1), pp.103-115.

- Narasimhan, T. Kim. H., and Safe, S. 1988. Effects of sesquiterpene lactones on mitochondrial oxidative phosphorylation. General Pharmacology: The Vascular System. Volume 20. Pages 681-687.
- Nishida, T., Naguro, I., & Ichijo, H. 2022. NAMPT-dependant NAD+ salvage is crucial for the decision between apoptotic and necrotic cell death under oxidative stress. Cell Death Discovery. Article number 195.
- Nuhu, F., Gordon, A., Sturmey, R., Seymour, A. M., and Bhandari, S. 2020. Measurement of Glutathione as a tool for oxidative stress studies by high performance liquid chromatography. Molecules (Basel, Switzerland), 25(18), 4196.
- Panomarev, A., Gilazeva, Z., Solovyeva, V., Allegrucci, C., Rizvanov., A. intrinsic and extrinsic factors impacting cancer stemness and tumour progression. 2022. Cancers 14(4).
- Patil, G.V., Dass, S.K. and Chandra, R., 2011. Artemisia afra and Modern Diseases. J Pharmacogenom Pharmacoproteomics, 2(105), pp.2153-0645.
- Peng, C., Zhao, F., Li, H., Yang, Y., and Liu, F. 2022. HSP 90 mediates the connection of multiple programmed cell death in diseases. *Cell Death and Disease.* Article number: 929
- Personalised Medicine Coalition. 2017. The personalised medicine report. Opportunity, challenges and, the future. PubMed Central.
- Phytoalchemy., 2023. [accessed @] http://phytoalchemy.co.za/2020/05/17/artemisia-afra-umhlonyane-african-wormwood/ . 14/02/2023
- Pizzino, G., Irrera, N., Cucinotta, M., Pallio, G., Mannino, F., Arcoraci, V., Squadrito, F., Altavilla, D. and Bitto, A., 2017. Oxidative stress: harms and benefits for human health. Oxidative Medicine and Cellular Longevity.
- Raghunath, A., Sundarraj, K., Nagarajan, R., Arfuso, F., Bian, J., Kumar, A.P., Sethi, G. and Perumal, E., 2018. Antioxidant response elements: Discovery, classes, regulation and potential applications. Redox Biology, 17, pp.297-314.
- Rasul, A., Khan, M., Yu, B., Ali, M., Bo, Y.J., Yang, H. and Ma, T., 2013. Isoalantolactone, a sesquiterpene lactone, induces apoptosis in SGC-7901 cells via mitochondrial and phosphatidylinositol 3-kinase/Akt signaling pathways. Archives of pharmacal research, 36, pp.1262-1269.
- Riley, J.S., Quarato, G., Cloix, C., Lopez, J., O'Prey, J., Pearson, M., Chapman, J., Sesaki, H., Carlin, L.M., Passos, J.F. and Wheeler, A.P., 2018. Mitochondrial inner membrane permeabilisation enables mt DNA release during apoptosis. The EMBO Journal, 37(17), p.e99238.

- Riss, L., Moravec, R., Niles, A., Duellman, S., Benink, H., Worxella T., and Minor, L. Cell Viability Assays. 2016 Assay Guidance Manual.
- Riudavets, M., Garcia de Herreros, M., Besse, B. and Mezquita, L., 2022. Radon and lung cancer: current trends and future perspectives. Cancers, 14(13), p.3142.
- Rubio, V., Garcia-Perez, A., Harraez, A., and Diez, J. Different roles of Nrf2 and NFKB in the antioxidant imbalance produced by esculetin or querticine on NB4 leukemia cells. 2018 Chemico-Biological Interactions. Volume 294, pages 158-166.
- Saelens, X., Festjens, N., Walle, L.V., Gurp, M.V., Loo, G.V. and Vandenabeele, P., 2004. Toxic proteins released from mitochondria in cell death. Oncogene, 23(16), pp.2861-2874.
- Schabath, M.B. and Cote, M.L., 2019. Cancer progress and priorities: lung cancer. Cancer Epidemiology, Biomarkers and Prevention, 28(10), pp.1563-1579.
- Siddiqui F, Vaqar S, Siddiqui AH. Lung Cancer., 2022. In: StatPearls. Treasure Island (FL): StatPearls Publishing; Available from: https://www.ncbi.nlm.nih.gov/books/NBK482357/
- Sies, H., 2014. Role of metabolic H2O2 generation: redox signaling and oxidative stress. Journal of Biological Chemistry, 289(13), pp.8735-8741.
- Silbernagel, E. Spreitzer, H. Buchbauer, G. 1990. Nichtflüchtige Inhaltsstoffe von Artemisia afra. Monatshefte für Chemie, 121, 433-436.
- Son, Y., Cheong, Y.K., Kim, N.H., Chung, H.T., Kang, D.G. and Pae, H.O., 2011. Mitogen-activated protein kinases and reactive oxygen species: how can ROS activate MAPK pathways?. Journal of Signal Transduction, 2011.
- Sonnenschein, C., Davis, B. and Soto, A.M., 2014. A novel pathogenic classification of cancers. Cancer Cell International, 14(1), pp.1-5.
- Soumyadip, P., Suvranil, G., Sukhendu, M., Subrata, S., and Mahadeb, P. NRF2 transcriptionally activates the heat shock factor 1 promoter under oxidative stress and affects survival and migration potential of MCF7 cells. 201. Journal of Biological Chemistry. DOI 10.1074/jbc.RA118.003376.
- Środa-Pomianek, K., Michalak, K., Świątek, P., Poła, A., Palko-Łabuz, A. and Wesołowska, O., 2018. Increased lipid peroxidation, apoptosis and selective cytotoxicity in colon cancer cell line LoVo and its doxorubicin-resistant subline LoVo/Dx in the presence of newly synthesized phenothiazine derivatives. Biomedicine and Pharmacotherapy, 106, pp.624-636.

- Su, L.J., Zhang, J.H., Gomez, H., Murugan, R., Hong, X., Xu, D., Jiang, F. and Peng, Z.Y., 2019. Reactive oxygen species-induced lipid peroxidation in apoptosis, autophagy, and ferroptosis. Oxidative medicine and cellular longevity, 2019.
- Sung, H., Ferlay, J., Siegel, R.L., Laversanne, M., Soerjomataram, I., Jemal, A. and Bray et al., F., 2021. Global cancer statistics 2020: GLOBOCAN estimates of incidence and mortality worldwide for 36 cancers in 185 countries. CA: A Cancer Journal for Clinicians, 71(3), pp.209-249.
- Suraweera, T.L., Rupasinghe, H.P.V., Delaire, G., and Xu, Z. 2020. Regulation of Nrf2/ARE pathway by Dietary Flavonoids: A Friend or Foe for Cancer Management. Antioxidants. Doi: 10.3390/antiox9100973.
- Szyller, J., and Bil-Lula, I. 2021. Heat Shock Proteins in Oxidative Stress and Ischemia/Reperfusion Injury and Benefits from Physical Exercise: A Review of Current Knowledge. Oxidative Medicine and Cellular Longevity. 6678457. Doi: 10.115/2021/6678457.
- Taha, Z.H., 2003. Nitric oxide measurements in biological samples. Talanta, 61(1), pp.3-10.
- Theil, E.C., 2010. Ferritin iron minerals are chelator targets, antioxidants, and coated, dietary iron. Annals of the New York Academy of Sciences, 1202(1), pp.197-204.
- Thomford, N.E., Senthebane, D.A., Rowe, A., Munro, D., Seele, P., Maroyi, A. and Dzobo, K., 2018. Natural products for drug discovery in the 21st century: innovations for novel drug discovery. International Journal of Molecular Sciences, 19(6), p.1578.
- Thuye le, T.T., Thuy, T.T.V., Hai, H., and Kawada, N. 2017. Chapter 16 – Roloe of Oxidative and Nitrative stress in Hepatic Fibrosis. Liver Pathophysiology. Pages 213-224.
- Timoshnikov, V.A., Selyutina, O.Y., Polyakov, N.E., Didichenko, V. and Kontoghiorghes, G.J., 2022. Mechanistic insights of chelator complexes with essential transition metals: antioxidant/pro-oxidant activity and applications in medicine. International Journal of Molecular Sciences, 23(3), p.1247.
- Tomasetti, C., Li, L. and Vogelstein, B., 2017. Stem cell divisions, somatic mutations, cancer etiology, and cancer prevention. Science 355(6331), pp.1330-1334.
- van Loggenberg, S., Willers, C., van der Kooy, F., Gouws, C., Hamman, J.H., & Steyn, J.D. 2022. Evaluating in vitro cytotoxic effects of Artemisia afra and Artemisia annua infusions against selected lung cancer cell lines, South African Journal of Botany 150, 404-411

- Wang, C. and Youle, R.J., 2009. The role of mitochondria in apoptosis. Annual Review of Genetics, 43, pp.95-118.
- Wang, F., Yuan, Q., Chen, F., Pang, J., Pan, C., Xu, F., & Chen, Y. 2022. Fundamental Mechanisms of the Cell Death by Nitrosative Stress. Frontiers in Cell and Developmental Biology. https://doi.org/10.3389/fcell.2021.742483.
- Wang, X., Chen, M., Zhou, J., and Zhang, X. 2014. HSP27, 70 and 90, anti-apoptotic proteins in clinical cancer therapy (Review)
- Wang, Y., Zhang, R., Shen, Y., Su, L., Dong, B., and Hao, Q. Prediction of chemotherapy adverse reactions and mortality in older patients with primary lung cancer through frailty index based on routine laboratory data. 2019. Dovepress. Volume 14.
- Wong, M.L. and Juan, J.F. 2018. Real-time PCR for mRNA quantification. BioTechniques, vol. 39, No. 1.
- Wu, F., Shao, R., Zheng, P., Zhang, T., Qiu, C., Sui, H., Li, S., Jin, L., Pan, H., Jin, X. and Zou, P., 2022. Isoalantolactone Enhances the Antitumor Activity of Doxorubicin by Inducing Reactive Oxygen Species and DNA Damage. Frontiers in Oncology, p.81.
- Wu, S., Lu, H. and Bai, Y., 2019. Nrf2 in cancers: A double-edged sword. Cancer Medicine, 8(5), pp.2252-2267.
- Wu, S., Zhu, W., Thompson, P. et al. 2018 Evaluating intrinsic and non-intrinsic cancer risk factors Nature Communications 9, 3490. https://doi.org/10.1038/s41467-018-05467-z
- Xia, Z.B., Meng, F.R., Fang, Y.X., Wu, X., Zhang, C.W., Liu, Y., Liu, D., Li, G.Q., Feng, F.B. and Qiu, H.Y., 2018. Inhibition of NF-κB signaling pathway induces apoptosis and suppresses proliferation and angiogenesis of human fibroblast-like synovial cells in rheumatoid arthritis. Medicine, 97(23).
- Yabal, M., Muller, N., Adler, M., Knies, N., Grob, C.J., Damgaard, R.B., Kanegane, H., Ringelhan, M., Kaufmann, T., Heikenwalder, M., Strasser, A., Grob, O., Ruland, J., Peschel, C., Gyrd-Hansen, M., and Jost, P.J. 2014. XIAP Restricts TNF- amd RIP3-Dependent Cell Death and Inflammasome Activation. CellPress. http://dx.doi.org/10.1016/j.celrep.2014.05.008
- Yang, H.Y. and Lee, T.H., 2015. Antioxidant enzymes as redox-based biomarkers: a brief review. BMB Reports, 48(4), p.200.
- Younes, N., Alsahan, B.S., Al-Mesaifri, A.J., Da'as, S.I., Pintus, G., Majdalawieh, A.F. and Nasrallah, G.K., 2022. JC-10 probe as a novel method for analyzing the mitochondrial membrane potential and cell stress in whole zebrafish embryos. Toxicology Research, 11(1), pp.77-87.

- Younus, H., 2018. Therapeutic potentials of superoxide dismutase. International Journal of Health Sciences, 12(3), p.88.
- Zhao, R., Jiang, S., Zhang, L., and Yu, Z., 2019. Mitochondrial electron transport chain, ROS generation and uncoupling (Review). International Journal of Molecular Medicine; 44(1): 3-5.

APPENDIX

APPENDIX A

The MTT assay raw data and analysis.

Table A1:

Concentration	Log concentration	24 hours	48 hours
0	0	100	100
50	1,69897	100	100
100	2	101	83
200	2,30103	86	58
300	2,477121	54	43
400	2,60206	42	36
500	2,69897	43	26
1000	3	16	12
2000	3,30103	9	4
3000	3,477121	9	4
4000	3,60206	8	4
5000	3,69897	7	5

APPENDIX B

The nitrates assay standard curve.

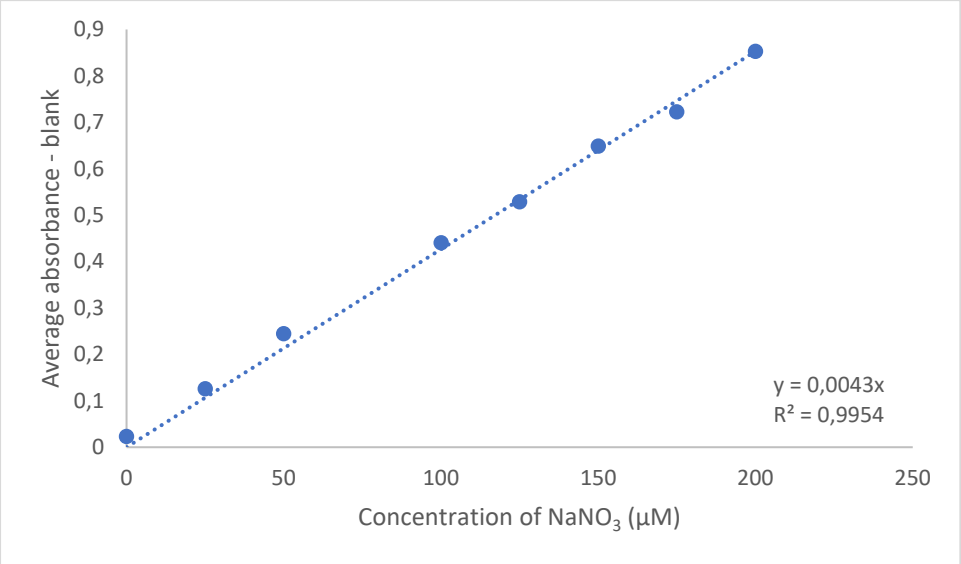

Figure A1:

APPENDIX C

The Bovine serum albumin (BSA) standard curve used to quantify and standardise protein for western blotting.

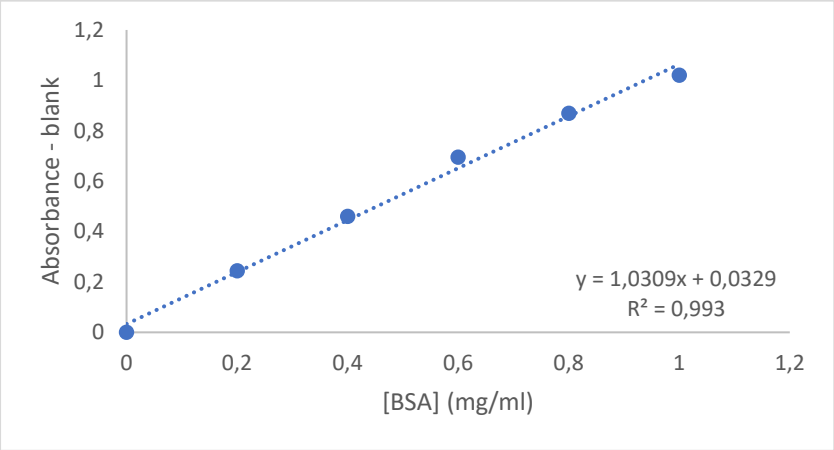

Figure A2:

APPENDIX D

The melt curves generated for the amplification of catalase and Nrf2.

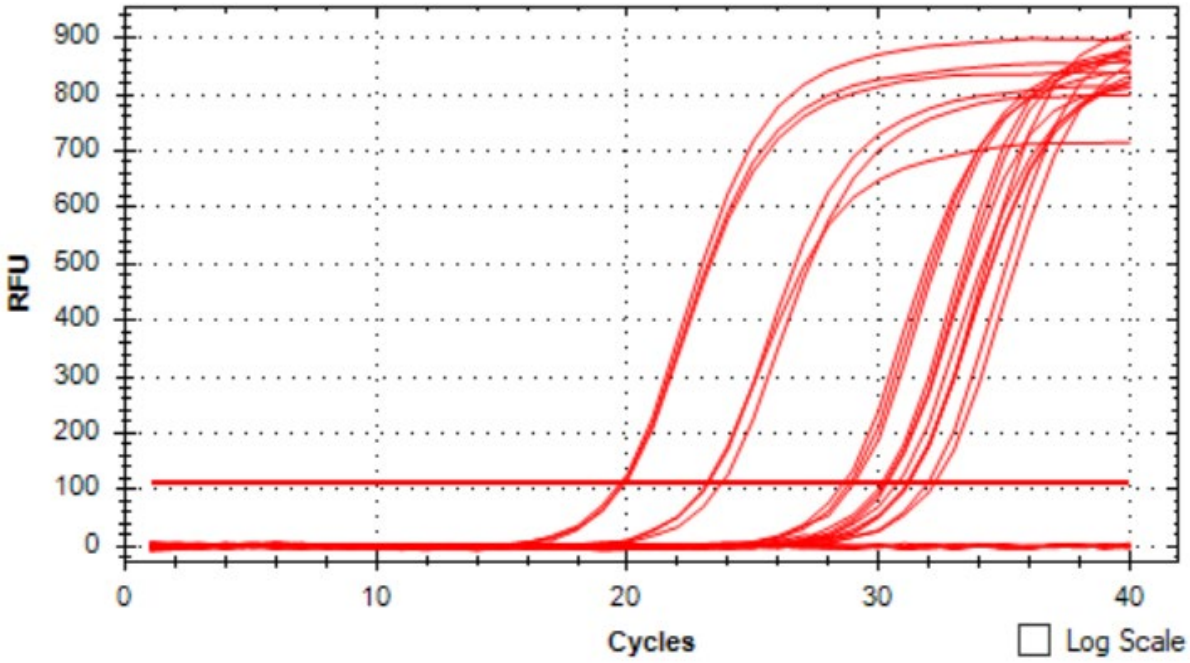

Figure A3:

APPENDIX E

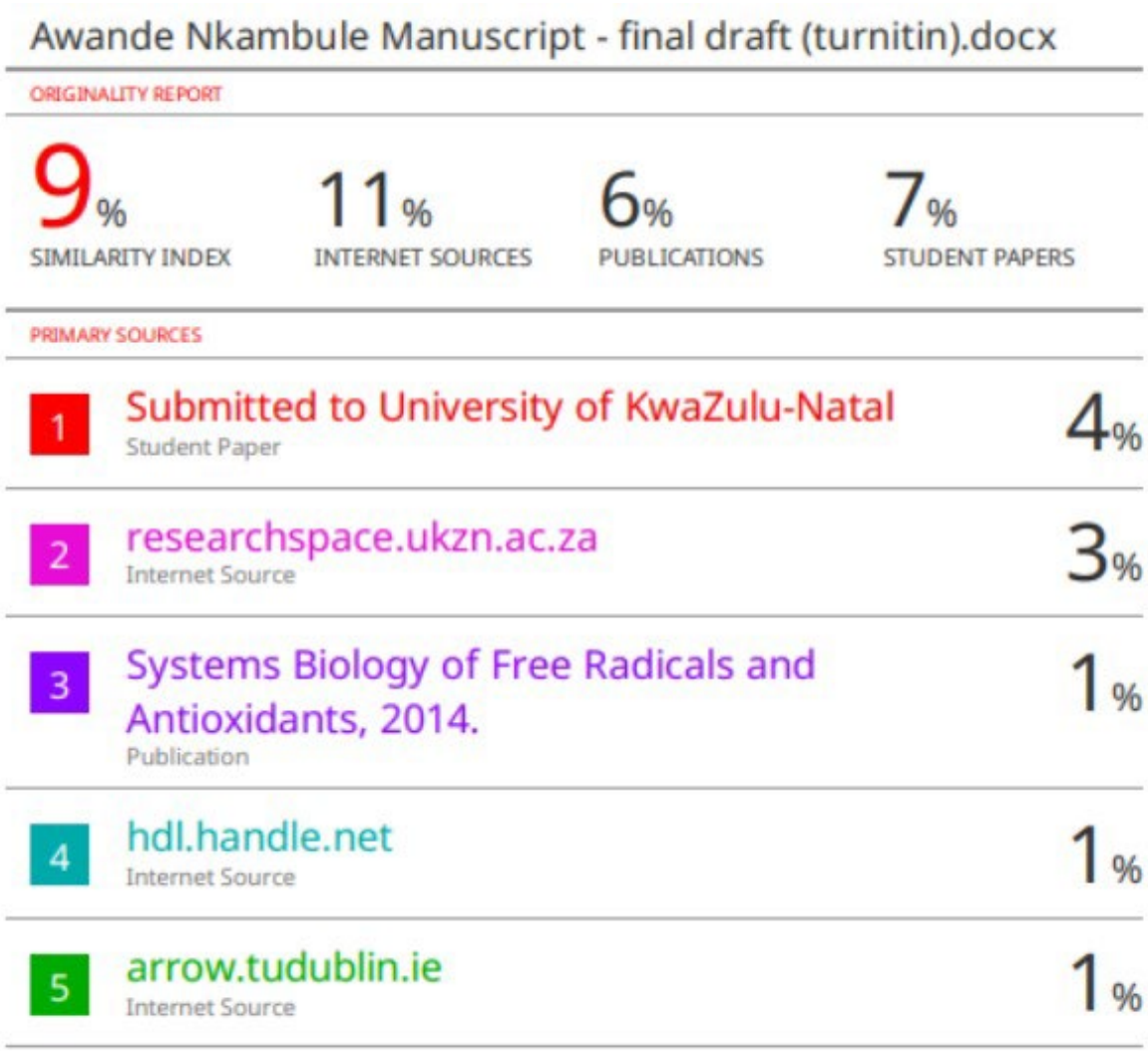

Awande Nkambule Manuscript - final draft (turnitin).docx

ORIGINALITY REPORT

9%	11%	6%	7%
SIMILARITY INDEX	INTERNET SOURCES	PUBLICATIONS	STUDENT PAPERS

PRIMARY SOURCES

1	Submitted to University of KwaZulu-Natal Student Paper	4%
2	researchspace.ukzn.ac.za Internet Source	3%
3	Systems Biology of Free Radicals and Antioxidants, 2014. Publication	1%
4	hdl.handle.net Internet Source	1%
5	arrow.tudublin.ie Internet Source	1%